The Official Journal of the Chinese Stomatological Association (CSA)

Chinese Journal of Dental Research

CJDR

VOLUME 28 2025 NUMBER 1

Join us in celebration and explore our special anniversary offers

These and many other anniversary offers:
www.quint.link/anniversary

QUINTESSENCE PUBLISHING

Chinese Journal of Dental Research

The Official Journal of the Chinese Stomatological Association (CSA)

Chinese Journal of Dental Research

The Official Journal of the Chinese Stomatological Association (CSA)

Review

Original article

Chinese Journal of Dental Research

CN 10-1194/R • ISSN 1462-6446 • eISSN 1867-5646 • Quarterly

The Official Journal of the Chinese Stomatological Association
Co-sponsor: Peking University School of Stomatology, Quintessenz Verlag

Publication Department

Production Manager: Megan Platt (London, UK)
Managing Editor: Xiao Xia ZHANG (Beijing, P.R. China)

Address: 4F, Tower C, Jia 18#, Zhongguancun South Avenue, HaiDian District, 100081, Beijing, P.R. China.
Tel: 86 10 82195785, **Fax:** 86 10 62173402
Email: editor@cjdrcsa.com

Manuscript submission: Information can be found on the Guidelines for Authors page in this issue. To submit your outstanding research results more quickly, please visit: http://mc03.manuscriptcentral.com/cjdr

Administrated by: China Association for Science and Technology
Sponsored by: Chinese Stomatological Association and Popular Science Press
Published by: Popular Science Press
Printed by: Beijing ARTRON Colour Printing Co Ltd
Subscription (domestically) by Post Office

Chinese Journal of Dental Research is indexed in MEDLINE.

For more information and to download the free full text of the issue, please visit
www.quint.link/cjdr
http://www.cjdrcsa.com

Acknowledgements

We would like to express our gratitude to the peer reviewers for their great support to the journal in 2024.

Abdulmajeed, Aous (USA)
Afify, Ahmed (Egypt)
Ahmad, Basaruddin (Malaysia)
Akbarizadeh, Fatemeh (Iran)
Aly, Yousra (Egypt)
An, Na (China)
Arpornmaeklong, Premjit (Thailand)
Asaumi, Rieko (Japan)
Aslan, Tugrul (Turkey)
Attard, N (Malta)
Ayan, Gizem (Turkey)
Ayna, Emrah (Turkey)
Aytaç Bal, Fatma (Turkey)
Bacci, Christian (Italy)
Ballal, Nidambur (India)
Ballal, Vasudev (USA)
Bayoumi, Amr (Egypt)
Belli, Sema (Turkey)
Boffano, Paolo (Italy)
Buldur, Burak (Turkey)
Cao, Ye (China)
Caplin, Jennifer (USA)
Chabbra, Dr Ajay (India)
Chen, Chen (China)
Chen, Feng (China)
Chen, Jian Huan (China)
Chen, Jiang (China)
Chen, Jing (China)
Chen, Li Li (China)
Chen, Peng (China)
Chen, Zhi (China)
Dalben, Gisele da Silva (Brazil)
de Oliveira-Neto, O B (Brazil)
de-Jesus-Soares, Adriana (Brazil)
Dede, Dogu Omur (Turkey)
Dedeoğlu, Numan (Turkey)
Delaney, Eliza (France)
Deng, Ke (China)
Ding, Chun Mei (China)
Doğan Çankaya, Tülin (Turkey)
Dong, Yan Mei (China)
Duman, Şuayip Burak (Turkey)
EKINCI, Merve Sena (Turkey)
Fan, Zhi Peng (China)
Flores-Mir, Carlos (Canada)
Fu, Bai Ping (China)
Gao, Xue Mei (China)
Garoushi, Sufyan (Finland)
Gaur, Sumit (India)
Gautam, Chandkiram (India)
GÖK, Tuba (Turkey)
Gruber, Reinhard (Austria)
Gu, Li Sha (China)
Gundala, Rupasree (India)
Guo, Jie (China)
HafeziMotlagh, Kimia (Iran)
Hajeer, Mohammad Y (Syria)
Hamdy, Tamer (Egypt)
Han, Dong (China)
Han, Xiang Long (China)
Hasan, Arshad (Pakistan)
He, Jing Wei (China)
He, Miao (China)
Hourfar, Jan (Germany)
Hua, Cheng Ge (China)
Huang, Xin (China)
Huang, Yi Ping (China)
Huang, Zheng Wei (China)
Hür Şahin, Özge (Turkey)
Hussein, Ahmed (Egypt)
Hussein, Seenaa (Iraq)
Ismail, Hadi (Iraq)
Jakovljevic, Aleksandar (Syria)
Jamilian, Abdolreza (Iran)
JE, LeÃ³n (Brazil)
Jepsen, Soren (Germany)
Jia, Ling Fei (China)
Jiang, Hong Bing (China)
Jiang, Shao Yun (China)
Jotikasthira, Dhirawat (Thailand)
Katbeh, Imad (Russia)
Kinzinger, Gero (Germany)
Korucu, Hulde (Turkey)
Kuwata, Hirotaka (Japan)
Lagravere, Manuel O (Canada)
Li, Gang (China)
Li, Xiaodong (China)
Li, Zehan (China)
Liu, Jian Zhang (China)
Liu, Li Bing (China)
Liu, Ou Sheng (China)
Liu, Xue Nan (China)
Liu, Yan (China)
Long, Anna E (UK)
Long, Hu (China)
Ma, Ning (China)
Magan-Fernandez, Antonio (Spain)
Mancini, Manuele (Italy)
Markande, Dr Archana (India)
Mavragani, Maria (Norway)
Miron, Richard J (Switzerland)
Motgi, Anagha A (India)
Nagarajappa, Ramesh (India)
Ngeow, Wei Cheong (Malysia)
Nuvvula, Sivakumar (India)
Okutan, Alev (Turkey)
Osman, Ranjdar (Iraq)
Özdemir, Burcu (Turkey)
Pan, Ya Ping (China)
Park, Joo-Cheol (Korea)
Ramalingam, Karthikeyan (India)
Ramesan, Manammel Thankappan (India)
Rezaeifar, Kosar (Iran)
Rodrigues, Renata Cristina Silveira (Brazil)
Rong, Wen Sheng (China)
Sadrzadeh-Afshar, Maryam-Sadat (Iran)
Saul, Pavle (Ukraine)
Scribante, Andrea (Italy)
Shetty, Shishir Ram (United Arab Emirates)
Si, Yan (China)
Song, Jiang Yuan (China)
Srilatha, Adepu (India)
Su, Jia Zeng (China)
Sui, Lei (China)
Sun, Yu Chun (China)
Sun, Zhi Jun (China)
Sun, Zhi Peng (China)
Tagg, John R (New Zealand)
Tang, Xiao Lin (China)
Tao, Ren Chuan (China)
Tatakis, Dimitris (USA)
Tian, Fu Cong (China)
Trophimos, Akeem (Switzerland)
Uctasli, Sadullah (Turkey)
Valente, Nicola Alberto (Italy)
Viana Casarin, Renato Correa (Brazil)
Viktar, Muthoni (Algeria)
Wang, Fu (China)
Wang, Jing (China)
Wang, Peng Fei (China)
Wang, Wei Qi (China)
Wang, Wen Mei (China)
Wang, Yi Xiang (China)
Wang, Zuo Min (China)
Wu, Xiao Shan (China)
Xi, Tong (China)
Xia, Bin (China)
Xia, Lun Guo (China)
Xing, Hai Xia (China)
Yang, Bo (China)
Yang, Jing (China)
Yang, Yan Qi (China)
Yu, Jin Hua (China)
Yuan, Xue (China)
Zhang, Cheng Fei (China)
Zhang, Ran (China)
Zhang, Xu (China)
Zhang, Yu Feng (China)
Zhang, Zhi Hui (China)
Zhao, Yu Ming (China)
Zhao, Zhong Fang (China)
Zheng, Shu Guo (China)
Zheng, Yun Fei (China)
Zhong, Lai Ping (China)
Zhou, Bo (China)
Zhou, Xuan (China)
Zhu, Gui Quan (China)
Zhuang, Zi Yao (China)
Zong, Chen (China)
Zou, Jing (China)

Editorial Office
Chinese Journal of Dental Research

Dynamic Balance of Non-collagenous Proteins in Dentine Mineralisation

Min Juan SHEN[1,#], Yang Yang ZHANG[1,#], Meng Qi ZHU[1,#], Chun Yan ZHANG[1], Zhi Yong WANG[1], Qian Ming CHEN[1]

Dentine, the predominant structural element of the tooth, exhibits varying structural components, properties and mineralisation patterns across different regions. During dentinogenesis, diverse non-collagenous proteins (NCPs) play essential and varied roles in the mineralisation process. This paper systematically reviews the spatial distribution of NCPs across different dentine substructures and highlights their multifarious functions and collaborative interplay in governing the intricate mineralisation process. Specifically focusing on phosphorylated and glycosylated proteins, this review underscores their precisely programmed dynamic balance in orchestrating a series of distinct morphological patterns of dentinal substructures with varying degrees of mineralisation. By discussing the collaboration and balance of NCPs in dentine mineralisation, this paper also aims to advance the understanding of biomineralisation and provide valuable insights into developing highly biomimetic remineralisation strategies for dental applications.

Keywords: *biomineralisation, collagen matrix, dentine, hydroxyapatite, non-collagenous proteins*

Chin J Dent Res 2025;28(1):9–18; doi: 10.3290/j.cjdr.b6097589

Dentine, which constitutes the major portion of the tooth, is deemed one of nature's masterpieces that comprises highly hierarchical inorganic-organic components. It is a mineralised collagen-based hard tissue encompassing 20% organic matrix and 70% inorganic hydroxyapatite (HAP) crystals. Unlike the highly uniform arrangement of HAP rods in enamel, the internal mineralisation of dentine is uneven, and distinct substructures are observable under the microscope due to varying degrees of mineralisation.[1] From the interior pulp chamber to the exterior dentinoenamel junction (DEJ), these structures include predentine, a translucent narrow band adjacent to the pulp consisting of unmineralised collagen matrix; dentinal tubules, minute channels extending from the pulp to the DEJ, traversing almost the entirety of the dentine; peritubular dentine (PTD), a concentric layer around the tubules that appears relatively darker under the microscope due to its higher mineral content; intertubular dentine (ITD), the substance between PTD with lower mineral density; globular dentine, a peripheral layer characterised by void nonmineralised spaces between globular mineralised masses; and mantle dentine, the outermost layer adjacent to enamel (Fig 1). Due to its hierarchical architecture, dentine emerges as a multifaceted entity with a unique combination of strength, flexibility and resistance to fracture, ensuring its vital role in supporting tooth structure and function.[2]

Within the well-organised architecture of the dentine matrix, a small yet significant amount (~ 10%) of non-collagenous proteins (NCPs) is present alongside the

1 Stomatology Hospital, School of Stomatology, Zhejiang University School of Medicine, Zhejiang Provincial Clinical Research Center for Oral Diseases, Key Laboratory of Oral Biomedical Research of Zhejiang Province, Engineering Research Center of Oral Biomaterials and Devices of Zhejiang Province, Hangzhou, P.R. China

# These authors contributed equally to this work.

Corresponding author: Prof Qian Ming CHEN, Stomatology Hospital, School of Stomatology, Zhejiang University School of Medicine, #166 Qiutao North Road, Shangcheng District, Hangzhou 310003, P.R. China. Tel: 86-571-88208020. Email: qmchen@zju.edu.cn

The present work was funded by the National Key R&D Program of China (2022YFC2402900), the National Natural Science Foundation of China (81991502, 82301138) and the Young Elite Scientists Sponsorship Program by CAST (2022QNRC001).

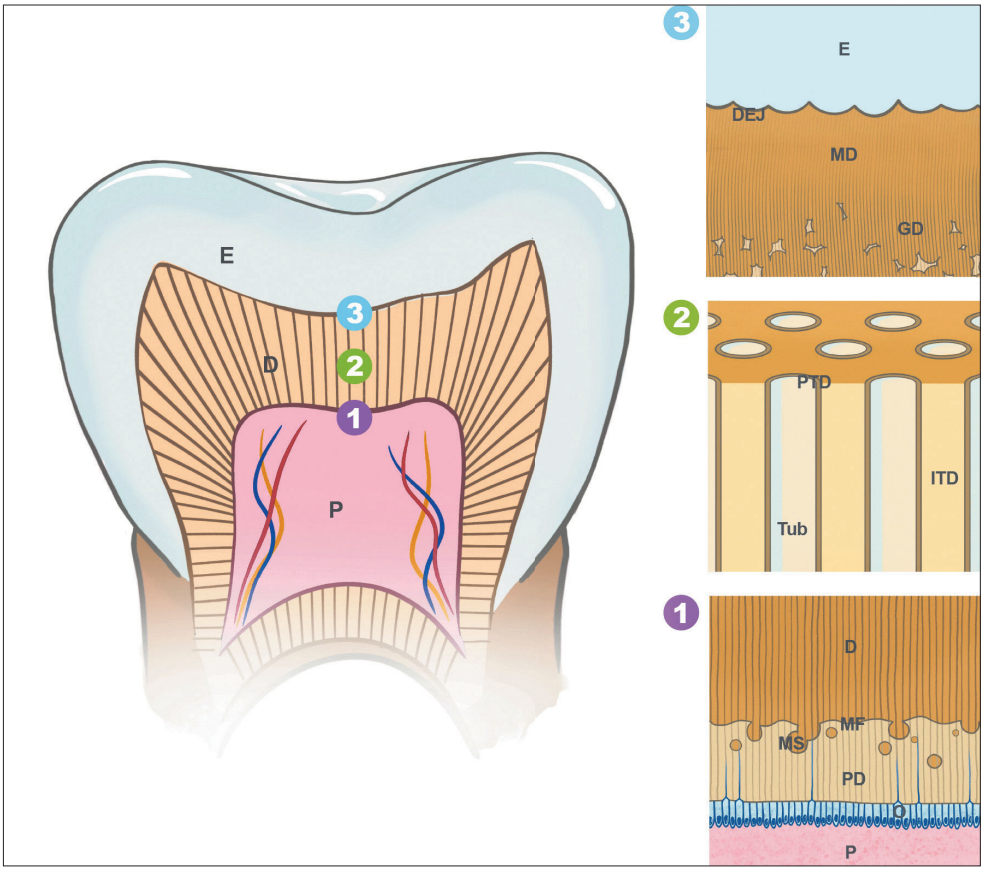

Fig 1 Schematic representation of the structure of dentine. Three typical subregions marked by numbers on the left are magnified on the right. From the interior pulp chamber to the exterior DEJ, these typical subregions include the predentine and mineralisation front (marked as 1); circumpulpal dentine, including PTD and ITD (marked as 2) and mantle dentine and globular dentine (marked as 3). D, dentine; DEJ, dentinoenamel junction; E, enamel; GD, globular dentine; ITD, intertubular dentine; MD, mantle dentine; MF, mineralisation front; MS, mineralised spherules; O, odontoblasts; P, pulp; PD, predentine; PTD, peritubular dentin; Tub, tubules.

predominant type I collagen matrix (~ 90%).[3] Previous studies have underscored the crucial and indispensable role played by various NCPs in governing dentinogenesis, such as dentine sialophosphoprotein (DSPP) and dentine matrix protein 1 (DMP1).[4] These NCPs, which can be divided into the phosphorylated group and the glycosylated group according to their post-translational modifications and molecular structures, are actively engaged in dentine matrix synthesis and mineralisation. Once the expression of these NCPs in dentine is disturbed, mineralisation-related disorders such as dentinogenesis imperfecta and dentine dysplasia emerge.[5] A crucial but as yet unanswered question pertains to how these proteins function collaboratively to precisely control the mineralisation of the collagen matrix to varying degrees. It is therefore imperative to investigate the spatial distribution, molecular structure and expression patterns of these NCPs, as well as the molecular regulation of the biosynthetic and proteolytic events accompanying the mineralisation processes. This is vital in order to comprehend the mechanisms involved in hard tissue formation.

Considering temporal and spatial distribution, this article systematically reviews the roles and interactions of NCPs in dentine mineralisation and draws a distribution map of their configuration patterns. By unravelling the intricate interplay between NCPs and mineral deposition, it aims to provide a comprehensive understanding of the balance and collaboration of NCPs in the dentine formation and maturation processes. Deciphering the intricacies of dentine hierarchical mineralisation and its well-programmed regulatory molecular components offers valuable insights for developing highly biomimetic strategies in hard tissue regeneration.

Predentine and mineralisation front

Dentine continues to grow throughout the entire lifespan of a tooth. Between the bulk of mineralised dentine and the central pulp chamber lies a narrow layer of nonmineralised collagen matrix, which is termed predentine.[1] Predentine is visible in all stages of tooth development, arising from a subtle time delay between the initial collagen matrix secretion and subsequent mineral deposition. Structurally, predentine is predominantly composed of randomly scattered collagen fibres, primarily type I collagen. Its thickness is approximately 20 to 60 µm, depending on age, site and systemic

conditions.[6] On the interior side, collagenous and noncollagenous proteins are secreted by odontoblasts and transported along the odontoblast processes to form the dentine matrix. On the exterior side, collagen fibres become more tightly packed, and minerals are deposited as calcified globules (also termed mineralised spherules[7]) under the regulation of NCPs. Numerous mineralised spherules assemble and construct the distinct continuous wavy line, termed the mineralisation front, indicating the border between nonmineralised predentine and mineralised dentine.

Decorin (DCN) and biglycan (BGN)

Predentine, interacting dynamically with odontoblasts, serves as an active interaction site for various NCPs during the continuous processes of collagen synthesis and mineral deposition. Proteoglycans, including DCN and BGN, are secreted into the sub-odontoblastic layer, accompanying collagen fibrils. DCN consists of a protein core with leucine repeats and a glycosaminoglycan chain, which may be either chondroitin sulphate or dermatan sulphate. BGN has a homologous structure and features two glycosaminoglycan chains.[8] Both BGN and DCN interact with type I collagen and serve as structural components in connective tissues, regulating the fibrillogenesis process during dentinogenesis.

In situ immunohistochemistry analysis revealed a significantly higher density of both DCN and BGN in predentine compared to mineralised dentine.[9] While BGN is uniformly distributed in the predentine layer, DCN content is increased in the distal region near the mineralisation front, where collagen fibres become more compact and minerals begin to deposit. In circumpulpal dentine, both DCN and BGN can be found in the dentinal tubules and ITD in relatively low amounts, which is supposed to be vital in maintaining the mechanical properties and homeostasis of the mature collagen matrix of the mineralised dentine.[10]

Analysis of the phenotype of *Dspp/Dcn* and *Dspp/Bgn* double knockout mice[11] indicated that DCN expression contributed to the exacerbation of enlarged predentine and hypomineralisation in *Dspp*-knockout mice, and BGN expression reduced the defect in the coalescence of mineralised spherules. With a high affinity for apatite that is facilitated by the glycosaminoglycan chains, BGN is able to initiate HAP nucleation and regulate crystal proliferation at a low concentration in vitro.[12,13] It is suggested that BGN can promote dentinogenesis from both fibrillogenesis and mineralisation.

In dentinogenesis, DCN is believed to be primarily associated with the fibrillogenesis process, predominantly regulating collagen fibril diameter and orientation.[14,15] Upregulation of DCN accelerates the assembly of collagen fibrils into hierarchical fibre-like structures both in vitro and in vivo. DCN possesses a higher affinity for type I collagen than other mineralisation regulators, such as DMP1, bone sialoprotein (BSP) and osteopontin (OPN).[16] It can easily crosslink with fibrils, possibly contributing to the prevention of intrafibrillar mineral deposition. Analysis based on the knockout mice revealed that DCN inhibits mineral deposition, hindering the conversion from predentine into dentine. The temporal expression pattern of DCN in osteoblastic cells shows a significant downregulation at the onset of mineralised spherule deposits, with content level remaining relatively low throughout the mineralisation process.[14] In vitro, the intrafibrillar mineralisation and mineralised spherule formation are severely delayed by DCN.[15,16] Based on the aforementioned evidence, DCN primarily acts as a promoter in collagen maturation and potentially serves as an inhibitor in mineral deposition. Given the partially collaborative promoting effect in fibrillogenesis and potential opposite effect in mineralisation, it is reasonable to speculate that there is a dynamic balance of DCN and BGN in regulating fibril assembly and maintaining the unmineralised status of predentine, as well as governing the predentine-dentine transformation.

Interestingly, in *Bgn*-knockout mice, the hypomineralisation in dentine was evident in the newborn mice, but no significance was detected in adult mice. In the absence of BGN, glycosylated proteins, such as dentin sialoprotein (DSP), BSP and OPN, exhibited overexpression.[17] Accordingly, a potential compensatory effect among these structurally assembled proteins is suggested in dentinogenesis.

DMP1

DMP1 is an osteo- and dentinogenesis-related protein that is widely distributed in hard tissues like bone and teeth.[18] In dentine, it presents primarily in predentine, dentinal tubules, PTD and mantle dentine.[18,19] DMP1 has an intrinsically highly acidic nature, with a large number of glutamic acid (Glu) and aspartic acid (Asp) residues interspersed in its amino acid sequence. It undergoes various post-translational modifications, including phosphorylation and glycosylation to different extents.

DMP1 primarily functions as fragments: a 37 kDa fragment from the N-terminal region, a 57 kDa fragment from the C-terminal region and a chondroitin-sulphate-linked N-terminal fragment, which is also known

as the proteoglycan form of DMP1 (DMP1-PG). In situ immunolocalisation[20] showed that the N-terminal fragment and DMP1-PG are mainly distributed in the nonmineralised predentine, whereas the C-terminal fragment localised at the mineralisation front and in mineralised circumpulpal dentine. The C-terminal fragment contains 41 phosphorylated serine (Ser) residues, which endow the fragment with a high affinity for calcium ions. It is suggested that the 57 kDa C-terminal fragment acts as a mineralisation promoter, which can initiate de novo HAP formation in vitro.[21] Meanwhile, DMP1-PG not only contains 12 phosphate groups but also a chondroitin 4-sulphate glycosaminoglycan chain. Based on in vitro and in situ evidence, it is supposed to be a mineralisation inhibitor.[22] Although the function of 57 kDa C-terminal fragment and DMP1-PG is relatively clear, the role of 37 kDa N-terminal fragment remains poorly understood. There is speculation that DMP1-PG is the functional form of this 37 kDa fragment after glycosylation, or the 37 kDa fragment is the remnant after DMP1-PG proteolytical degradation.[20] This may offer a reasonable explanation of the different outcomes of in vitro mineralisation experiments that do not take post-translational modification into consideration.

In addition to these fragments, a small amount of full-length isoform of DMP1 is identified in dentine,[23] yet whether it has a certain biological function or merely exists as a precursor to the functional fragments remains to be established. In vitro studies have shown that the full-length DMP1 regulates mineral deposition in a phosphorylation- and concentration-dependent manner.[24,25] *Dmp1*-knockout mice exhibited notable dental phenotypic alterations during the postnatal period, including increasing predentine width, failed maturation from nonmineralised predentine to mineralised dentine, and hypomineralisation of circumpulpal dentine.[26] In situ hybridisation analysis revealed that DMP1 mRNA could be detected as early as E20 in the preodontoblasts of rats, and continues to be expressed during dentinogenesis in polarised secretory odontoblasts.[27] The coincidence of the initial expression of DMP1 with the onset of mineral deposition in the dentine matrix indicates that DMP1 is the promoter of dentine mineralisation.[28]

DSPP and dentine phosphoprotein (DPP)

DSPP-derived proteins are dominant among all the NCPs in dentine. In contrast to DMP1, they are highly tooth-specific, with their presence in bone being approximately one-four hundredth of their concentration in dentine.[29] After being secreted by odontoblasts, DSPP is immediately proteolytically cleaved by metalloproteinases (MMPs) into three segments: DPP, located in the C-terminal region of DSPP, which is a highly phosphorylated intrinsically disordered protein (IDP) with genetic polymorphisms; DSP, found in the N-terminal region of DSPP, which is richly glycosylated with N-linked asparagine; and dentine glycoprotein (DGP), which is a phosphorylated and glycosylated segment in the middle region of DSPP in pigs that lacks reported occurrences in other species, and the function of which in dentinogenesis has remained unexplored.[30]

DPP constitutes over 50% of dentine NCPs in most species and is notably prevalent in the mineralisation front and mineralised circumpulpal dentine, yet absent in nonmineralised predentine.[31] It is a highly phosphorylated protein containing multiple Ser, Asp and threonine (Thr) residues, conferring hydrophilicity and capability to interact with calcium ions.[32] Among toothed mammalian species, although the general molecular weight of DPP differs dramatically among species, the repetition of the elemental SerSerAsp (SSD) motifs is highly conserved.[33] The phosphorylation status of the SSD motif serves as a mediator for DPP's function in dentine mineralisation. Dephosphorylation leads to the loss of its effectiveness in guiding mineralisation.[34] In *Dspp*-knockout mice, the transgenic expression of DPP partially restored the reduced dentine volume and mineral density.[35] The mineralisation process was actively promoted by DPP, accelerating the transformation and maturation from nonmineralised predentine to mineralised dentine. In vitro, DPP induces mineral nucleation at low concentrations and inhibits crystal growth at elevated concentrations.[36] Within the collagen matrix, DPP primarily binds to the gap zone of the collagen fibrils, initiating the mineralisation process.[37]

Interestingly, recent studies have reported that the DPP domain of DSPP is mutated in truly toothless mammals, such as the anteater, while DSP is normally expressed.[38] This indicates the physiological significance of DPP in dentine mineralisation and tooth development, suggesting that it plays a more indispensable role compared to DSP. However, DSP is not redundant, as it contributes to the regulation of HAP morphology,[39] facilitating the coalescence of mineralised spherules at the mineralisation front. The balance and synergy of DPP and DSP drive the serial key events of dentine mineralisation, including mineral nucleation, mineralised spherule growth and coalescence, as well as HAP morphology regulation and alignment. Further details about DSP will be discussed in the following section.

PTD and ITD

Circumpulpal dentine can be divided into two types: PTD and ITD. Gilding the inner surface of dentinal tubules, PTD forms a protective sheath that envelops the odontoblast processes, clearly delineating the boundary between dentinal tubules and interstitial dentine, whereas ITD, the rest of the tissue between the tubules, constitutes the majority of the dentinal volume. These two types of dentine exhibit distinct differences in composition and structure. ITD consists of approximately 90% type I collagen, whereas PTD is nearly devoid of fibrils.[40] In ITD, needle-like HAP crystals deposit intra- and extra-fibrillarly within the dense network of collagen matrix. In PTD, mineral content is approximately 40% higher than in ITD, and the crystals exhibit a more ordered and compact arrangement.[41] Recent studies have revealed the porous nature of PTD, demonstrating a transient or even homogeneous state in the arrangement of HAP crystals and collagen fibrils between PTD and ITD.[42] Thus, these two structures should be regarded as a communicable and successive entity rather than separate motifs.

DSP

DSP constitutes approximately 5% to 8% of NCPs in dentine, predominantly situated in PTD, with minor expression in predentine.[43] The primary structure of DSP is rich in Asp and Ser, with fewer phosphorylated sites but more glycosylated residues in comparison with DPP.

In vitro, Boskey et al[39] observed that DSP at low concentrations modestly enhanced HAP formation, whereas at higher concentrations, it exhibited a slight inhibition of HAP accumulation. Compared to other mineralisation-related glycosylated proteins, such as OPN or BSP, DSP shows a relatively lower calcium binding affinity, suggesting its limited impact on mineral nucleation. Ex vivo, Jaha et al[44] reported that DSP induces type I collagen production, highlighting its potential role in dentine fibrillogenesis.

In vivo, Fang et al[45] observed that a large portion of the circumpulpal dentine matrix of *Dspp*-knockout mice remained nonmineralised, featuring numerous spherulitic mineralised inclusions. Further, based on the conditional *Dpp*-knockout mice that only express DSP in a DSPP null background, Suzuki et al[46] demonstrated that DSP expression can partially mitigate the decreased dentine matrix volume and irregular mineral deposition resulting from the absence of DSPP. DSP expression restored the dentinal collagen matrix volume to levels equivalent to the wild type and eliminated the abnormal sporadic mineralisation phenomenon, with an absence of irregular unmineralised areas in the circumpulpal dentine; however, the width of predentine and mineral density remained abnormal. In this situation, it is postulated that following the initial mineral deposition guided by alternative NCPs like DMP1, DSP plays a pivotal role in regulating HAP alignment and mineralised spherule coalescence within the collagen matrix. In comparison, transgenic expression of DPP in *Dspp*-knockout mice accelerated the transformation from nonmineralised predentine to mineralised dentine, by which the width of predentine and the mineral density of circumpulpal dentine were restored.[35]

In dentine, some NCPs like DPP exhibit high affinities for calcium and promote mineral nucleation, and some NCPs like DSP preferentially bind to HAP and collagen fibrils, regulating crystal morphology and alignment. Besides, a certain NCP can perform different functions depending on its varying post-translational modifications and concentrations. Such cooperation and balance of NCPs are fundamental in dentinogenesis, where every up- or downregulation of each molecule can influence the dynamic equilibrium between the nonmineralised and mineralised states, or alter the degree and pattern of mineralisation of specific regions.

BSP

BSP is a sulphated, glycosylated and phosphorylated protein with high affinities for selectively binding to both HAP and collagen fibrils.[47] In dentine, BSP is primarily distributed in the PTD and mantle dentine.[48] Building on the work of Hunter et al[49] and Baht et al,[50] BSP is considered a potential HAP crystal nucleator; however, its exact function in tooth development remains up for debate. Studies on *Bsp*-knockout mice showed that BSP deficiency impairs new bone formation, leading to hypomineralisation of cementum and alveolar bone.[47] However, no evident defects were observed in dentinogenesis when compared to the wild type.[51] Accordingly, though capable of regulating mineral deposition, BSP has a limited effect in dentine mineralisation. Considering its relatively low content (approximately 1% of the total NCPs in dentine),[52] BSP may serve as a subordinate regulator in dentinogenesis.

BSP belongs to the small integrin-binding ligand N-linked glycoprotein (SIBLING) family, which also includes DSPP, DMP1 and OPN. These proteins are genomically related, showing similarity in amino acid sequences and biochemical features that are crucial for their functions, such as calcium ion binding.[3] It is rational to speculate a

possible compensatory effect among these structurally resembled proteins, in which the overexpression of one protein can partially compensate for the absence of another. Gene expression studies of *Opn*-knockout mice revealed an increased expression of BSP transcripts, providing validation for this speculation.[53]

DMP1

In situ immunohistochemistry studies also localised DMP1 in PTD,[18] but further validation is required to determine whether it is present in the fragment or full-length form. It is reasonable to speculate that phosphorylated and glycosylated DMP1 plays a vital role in PTD formation, as it can not only initiate mineral deposition but also guide HAP crystals into ordered alignment in extrafibrillar spaces.

In vitro experiments have shown that recombinant DMP1 (rDMP1) can initiate HAP nucleation and mediate crystallisation in a sequential and stepwise process with or without collagen fibrils.[54] After chelating supersaturated calcium and phosphorous ions, rDMP1 nucleated the minerals in an amorphous shape, then restructured into a porous structure, and gradually transformed into highly ordered plate-like HAP aggregates. The mature form of HAP guided by rDMP1 in vitro resembles the physiological structure of PTD in vivo,[18,54] which offers evidence for the aforementioned speculation; however, further exploration is required for a comprehensive understanding of the specific role of DMP1 in PTD.

Studies indicate that DMP1, DSPP and other SIBLING family proteins closely interact with each other in dentinogenesis. DMP1 can directly induce DSPP gene expression.[55] Both DSPP and DMP1 contribute to hard tissue mineralisation, but the tissues affected by DSPP and DMP1 are different, presumably due to variations in their expression levels and distinct biochemical properties.[56] Accordingly, DMP1 and DSPP may serve complementary roles in mineralisation.

Interglobular dentine and mantle dentine

Globular dentine, located at the peripheral outer layer of the circumpulpal dentine, features shallow void spaces (known as interglobular dentine) within dense globular masses (coalescing mineralised spherules) when observed under a microscope.[3] This is a physiological developmental phenomenon resulting from deficient mineralisation during the final maturation of odontoblasts; however, the function of this layer has not been well demonstrated. It is widely acknowledged that the microstructure and development of dentine resemble the lamellar bone. Inspired by the crossfibrillar mineral tessellation pattern of bones, it is suggested that the globular dentine layer has similar physical functions of resistance to compression and bending at the globular-interglobular interfaces[57]; however, this presumption needs further validation.

Between the globular dentine and the DEJ lies the mantle dentine. Compared to the inner bulk of circumpulpal dentine, the mantle dentine features a relatively irregular arrangement of collagen fibrils and an atubular structure with fewer, thinner and more curved dentinal tubules.[58] The matrix primarily comprises type III collagen fibrils extending from enamel. Although thinner in diameter, these fibrils weave into a more stable network that offers potential binding sites. The mineral content of mantle dentine shows a gradual increment from the outer DEJ to the inner circumpulpal dentine.[59] Based on the features of collagen alignment and mineralisation gradient, mantle dentine is proposed to act as a resilience zone capable of transforming stress and dissipating tensile forces from oral physiological activities, which would otherwise induce enamel fissuration and detachment from the outer DEJ.

Immunolabelling reveals an absence of the highly phosphorylated DPP in mantle dentine,[60] indicating the limited influence and significance of protein phosphorylation in the formation and function of mantle dentine. It is further supported by the dentinal phenotype of *Dspp*-knockout mice[44] and patients with hypophosphatemic vitamin D-resistant rickets,[61] in which the mantle dentine remains unaffected whereas the interstitial dentine is hypomineralised with an abundance of calcified globules that fail to coalesce. Instead, OPN, an NCP characterised by both glycosylation and phosphorylation, was found to be prominent in mantle dentine.[62]

OPN

OPN is a phosphorylated and glycosylated protein widely distributed in mineralised tissues.[63] In teeth, OPN primarily abounds in the cementum lining root surfaces and at the junction of periodontal ligament fibre attachment. In dentine, the majority of OPN resides at the mantle dentine,[62] with a small amount present in the PTD, possibly originating from the odontoblast processes in dentinal tubules.[64]

Though OPN has been widely found to be involved in modulating mineralised tissue formation, its function in dentinogenesis still remains a matter of debate. Rittling et al[65] reported that the dental phenotype of *Opn*-

knockout mice was hardly affected, indicating that OPN plays a trivial role in primary dentine growth; however, Foster et al[66] found that the lack of OPN promoted the increment of dentine volume and mineral density at an early age; simultaneously, the volume of unmineralised periodontal ligament decreased due to ectopic calcification of cellular cementum and alveolar bone. In vitro, Boskey et al[67] evaluated the mineral binding affinity of OPN using a gel diffusion system. OPN showed a dose- and phosphate-dependent inhibitory effect on HAP formation and crystal proliferation. These observations suggest that the distribution of OPN in mantle dentine contributes to its unique gradient of mineral density. Again, this speculation reflects the core of this review; that is, that the intricate distributions of NCPs precisely regulate the mineralisation patterns of different substructures in dentine, which endow the entity with excellent mechanical properties and multifarious functions. Nevertheless, this still requires further validation.

In addition, OPN is significant in reparative dentine formation. In situ hybridisation analysis demonstrated that OPN participates in the reparative dentinogenesis process, as an elevated expression level of OPN can be detected at the boundary between the tertiary and preexisting dentine.[68] In contrast, the process of reparative dentinogenesis cannot be detected in *Opn*-null mice. The administration of recombinant OPN partially recovered the secretion of type I collagen for reparative dentine formation.[68] In conclusion, OPN plays a nonredundant role in dentinogenesis, but its exact regulating mechanism needs further exploration.

Conclusion and prospects

This review delves into the sophisticated landscape of dentine mineralisation, highlighting the synergy of multiple NCPs as well as their individual roles in controlling the formation and governing the function of multifaceted dentine substructures. The intricate organisation and mineralisation of dentinal substructures are precisely governed by a dynamic collaboration and balance of these NCPs, particularly phosphorylated and glycosylated proteins. Any subtle alterations in the content or post-translational modification of these NCPs can impact dentinogenesis significantly.

At the predentine layer, glycosylated DMP1-PG, DCN and BGN are secreted at relatively higher concentrations to promote fibrillogenesis. These glycosylated proteins bind to collagen fibrils, maintaining the nonmineralised state of predentine and preserving the matrix flexibility. At the mineralisation front, these glycosylated proteins undergo metabolism, proteolysis or removal; simultaneously, the secretion of DPP and other phosphorylated proteins promotes mineral deposition and nucleation, initiating the mineralisation process of the dentinal matrix. The dynamic balance between these glycosylated and phosphorylated proteins elaborately orchestrates the transformation from nonmineralised predentine to mineralised dentin. In the circumpulpal dentine, DSP, BSP and other NCPs distributed in specific locations further participate in the HAP maturation and alignment, endowing dentine with intricate and well-defined substructures. These observations suggest that in dentine mineralisation, each NCP with diverse molecular structures and post-translational modification patterns is distributed in specific places with varying concentrations, playing various functions. Together, they maintain a dynamic balance and synergistically orchestrate the sophisticated process of dentinogenesis. Having a comprehensive understanding of the spatial and temporal distribution of NCPs and their synergetic roles in precisely regulating mineralisation, as highlighted in this study (Table 1), sheds light on their crucial involvement in dentine formation and maturation.

This review not only enhances understanding of dentine mineralisation but also opens up avenues for clinical applications. The potential utilisation of the dynamic balance of NCPs serves as an innovative strategy for the effective treatment of dentinal caries and dental hypersensitivity. By biomimetic remineralisation of demineralised regions, such a strategy may hold promise for restoring damaged dentine with high biocompatibility and ideal mechanical properties.

Conflicts of interest

The authors declare no conflicts of interest related to this study.

Author contribution

Drs Min Juan SHEN, Yang Yang ZHANG and Meng Qi ZHU drafted the manuscript; Drs Chun Yan ZHANG and Zhi Yong WANG made the figure and the table; Prof. Qian Ming CHEN contributed to the conceptualization and revision of the manuscript. All authors read and approved the final manuscript.

(Received June 26, 2024; accepted Dec 03, 2024)

Table 1 Distribution map of NCPs across dentine.

Region	Main NCPs	Molecular characteristics	Relative concentrations	Functions	Studies
Predentine	DCN	Contains one glycosaminoglycan chain	+++	Promotes fibrillogenesis, potentially inhibits mineral deposition	8-11,14-16
	BGN	Contains two glycosaminoglycan chains	+++	Promotes fibrillogenesis, potentially promotes mineral deposition	8-13,17
	DMP1-PG	Contains a chondroitin 4-sulphate glycosaminoglycan chain	++	HAP nucleation inhibitor	18-22
	DSP	Both glycosylated and phosphorylated	+	Promotes fibrillogenesis, possibly serves as a compensatory reservoir	29,39,43
Mineralisation front	DPP	Highly phosphorylated, contains abundant SSD motifs	+++++	Initiates nucleation, promotes HAP maturation	31-37
	57 kDa DMP1 C-terminal fragment	Multiple phosphorylated Ser residues	++	HAP nucleation promoter	24-28
	DSP	Both glycosylated and phosphorylated	+	Promotes fibrillogenesis, regulates the coalescence and morphology of mineralised spherules	29,39,42-46
PTD and ITD	DPP	Highly phosphorylated, contains abundant SSD motifs	++++	Initiates nucleation, promotes HAP maturation	31-37
	DSP	Both glycosylated and phosphorylated	+++	Regulates HAP alignment, promotes mineralised spherule coalescence	39,43-46
	BSP	Sulphated, glycosylated, and phosphorylated	++	Potential HAP nucleator, possibly serves as a compensation of the SIBLING family	47-53
	DMP1	Exact functional form needs further validation	+	Potentially promotes HAP nucleation and regulates HAP alignment	18,54-56
	DCN	Contains one glycosaminoglycan chain	+	Promotes fibrillogenesis	8-11,14-16
	BGN	Contains two glycosaminoglycan chains	+	Promotes fibrillogenesis, promotes coalescence of mineralised spherules	8-13,17
Globular dentine and mantle dentine	OPN	Both glycosylated and phosphorylated	+++	Inhibits mineralisation, possibly helps maintaining the gradient mineral density of mantle dentine	63-68

References

1. Moradian-Oldak J, George A. Biomineralization of enamel and dentin mediated by matrix proteins. J Dent Res 2021;100:1020–1029.
2. Zhang H, Ma Y, Wang Y, et al. Rational design of soft-hard interfaces through bioinspired engineering. Small 2023;19:e2204498.
3. Goldberg M, Kulkarni AB, Young M, Boskey A. Dentin: Structure, composition and mineralization. Front Biosci (Elite Ed) 2011;3:711–735.
4. de La Dure-Molla M, Philippe Fournier B, Berdal A. Isolated dentinogenesis imperfecta and dentin dysplasia: Revision of the classification. Eur J Hum Genet 2015;23:445–451.
5. Jia J, Bian Z, Song Y. The role of DSPP in dentine formation and hereditary dentine defects. Chin J Dent Res 2024;27:17–28.
6. Basandi PS, Madammal RM, Adi RP, Donoghue M, Nayak S, Manickam S. Predentin thickness analysis in developing and developed permanent teeth. J Nat Sci Biol Med 2015;6:310–313.
7. Kashiwa HK, Komorous J. Mineralized spherules in the cells and matrix of calcifying cartilage from developing bone. Anat Rec 1971;170:119–127.
8. Chen J, Sun T, Lin B, Wu B, Wu J. The essential role of proteoglycans and glycosaminoglycans in odontogenesis. J Dent Res 2024;103:345–358.
9. Orsini G, Ruggeri A, Mazzoni A, et al. Immunohistochemical identification of decorin and biglycan in human dentin: A correlative field emission scanning electron microscopy/transmission electron microscopy study. Calcif Tissue Int 2007;81:39–45.
10. Robinson KA, Sun M, Barnum CE, et al. Decorin and biglycan are necessary for maintaining collagen fibril structure, fiber realignment, and mechanical properties of mature tendons. Matrix Biol 2017;64:81–93.
11. Haruyama N, Sreenath TL, Suzuki S, et al. Genetic evidence for key roles of decorin and biglycan in dentin mineralization. Matrix Biol 2009;28:129–136.
12. Hao JX, Shen MJ, Wang CY, et al. Regulation of biomineralization by proteoglycans: From mechanisms to application. Carbohydr Polym 2022;294:119773.
13. Boskey AL, Spevak L, Doty SB, Rosenberg L. Effects of bone cs-proteoglycans, ds-decorin, and ds-biglycan on hydroxyapatite formation in a gelatin gel. Calcif Tissue Int 1997;61:298–305.

14. Li Q, Han B, Wang C, et al. Mediation of cartilage matrix degeneration and fibrillation by decorin in post-traumatic osteoarthritis. Arthritis Rheumatol 2020;72:1266–1277.
15. Mochida Y, Parisuthiman D, Pornprasertsuk-Damrongsri S, et al. Decorin modulates collagen matrix assembly and mineralization. Matrix Biol 2009;28:44–52.
16. Bai Y, Wu P, Zhang Q, et al. Decorin in the spatial control of collagen mineralization. Mater Horiz 2024;11:3396–3407.
17. Goldberg M, Septier D, Rapoport O, Iozzo RV, Young MF, Ameye LG. Targeted disruption of two small leucine-rich proteoglycans, biglycan and decorin, excerpts divergent effects on enamel and dentin formation. Calcif Tissue Int 2005;77:297–310.
18. Beniash E, Deshpande AS, Fang PA, Lieb NS, Zhang X, Sfeir CS. Possible role of DMP1 in dentin mineralization. J Struct Biol 2011;174:100–106.
19. Machla F, Sokolova V, Platania V, et al. Tissue engineering at the dentin-pulp interface using human treated dentin scaffolds conditioned with DMP1 or BMP2 plasmid DNA-carrying calcium phosphate nanoparticles. Acta Biomater 2023;159:156–172.
20. Maciejewska I, Cowan C, Svoboda K, Butler WT, D'Souza R, Qin C. The NH2-terminal and COOH-terminal fragments of dentin matrix protein 1 (DMP1) localize differently in the compartments of dentin and growth plate of bone. J Histochem Cytochem 2009;57:155–166.
21. Gericke A, Qin C, Sun Y, et al. Different forms of DMP1 play distinct roles in mineralization. J Dent Res 2010;89:355–359.
22. Cai M, Li J, Yue R, Wang Z, Sun Y. Glycosylation of DMP1 maintains cranial sutures in mice. J Oral Rehabil 2020;47(suppl 1):19–28.
23. Huang B, Maciejewska I, Sun Y, et al. Identification of full-length dentin matrix protein 1 in dentin and bone. Calcif Tissue Int 2008;82:401–410.
24. Tartaix PH, Doulaverakis M, George A, et al. In vitro effects of dentin matrix protein-1 on hydroxyapatite formation provide insights into in vivo functions. J Biol Chem 2004;279:18115–18120.
25. Tsuji T, Onuma K, Yamamoto A, Iijima M, Shiba K. Direct transformation from amorphous to crystalline calcium phosphate facilitated by motif-programmed artificial proteins. Proc Natl Acad Sci U S A 2008;105:16866–16870.
26. Ye L, MacDougall M, Zhang S, et al. Deletion of dentin matrix protein-1 leads to a partial failure of maturation of predentin into dentin, hypomineralization, and expanded cavities of pulp and root canal during postnatal tooth development. J Biol Chem 2004;279:19141–19148.
27. George A, Silberstein R, Veis A. In situ hybridization shows Dmp1 (AG1) to be a developmentally regulated dentin-specific protein produced by mature odontoblasts. Connect Tissue Res 1995;33:67–72.
28. Whyte MP, Amalnath SD, McAlister WH, et al. Hypophosphatemic osteosclerosis, hyperostosis, and enthesopathy associated with novel homozygous mutations of DMP1 encoding dentin matrix protein 1 and SPP1 encoding osteopontin: The first digenic SIBLING protein osteopathy? Bone 2020;132:115190.
29. Ritchie H. The functional significance of dentin sialoprotein-phosphophoryn and dentin sialoprotein. Int J Oral Sci 2018;10:31.
30. Yamakoshi Y, Hu JC, Fukae M, Zhang H, Simmer JP. Dentin glycoprotein: The protein in the middle of the dentin sialophosphoprotein chimera. J Biol Chem 2005;280:17472–17479.
31. MacDougall M, Zeichner-David M, Slavkin HC. Production and characterization of antibodies against murine dentine phosphoprotein. Biochem J 1985;232:493–500.
32. Gulseren G, Tansik G, Garifullin R, Tekinay AB, Guler MO. Dentin phosphoprotein mimetic peptide nanofibers promote biomineralization. Macromol Biosci 2019;19:e1800080.
33. He G, Ramachandran A, Dahl T, et al. Phosphorylation of phosphophoryn is crucial for its function as a mediator of biomineralization. J Biol Chem 2005;280:33109–33114.
34. Villarreal-Ramirez E, Eliezer D, Garduño-Juarez R, Gericke A, Perez-Aguilar JM, Boskey A. Phosphorylation regulates the secondary structure and function of dentin phosphoprotein peptides. Bone 2017;95:65–75.
35. Zhang H, Xie X, Liu P, Liang T, Lu Y, Qin C. Transgenic expression of dentin phosphoprotein (DPP) partially rescued the dentin defects of DSPP-null mice. PLoS One 2018;13:e0195854.
36. Lussi A, Crenshaw MA, Linde A. Induction and inhibition of hydroxyapatite formation by rat dentine phosphoprotein in vitro. Arch Oral Biol 1988;33:685–691.
37. Saito T, Yamauchi M, Abiko Y, Matsuda K, Crenshaw MA. In vitro apatite induction by phosphophoryn immobilized on modified collagen fibrils. J Bone Miner Res 2000;15:1615–1619.
38. McKnight DA, Fisher LW. Molecular evolution of dentin phosphoprotein among toothed and toothless animals. BMC Evol Biol 2009;9:299.
39. Boskey A, Spevak L, Tan M, Doty SB, Butler WT. Dentin sialoprotein (DSP) has limited effects on in vitro apatite formation and growth. Calcif Tissue Int 2000;67:472–478.
40. Dorvee JR, Deymier-Black A, Gerkowicz L, Veis A. Peritubular dentin, a highly mineralized, non-collagenous, component of dentin: Isolation and capture by laser microdissection. Connect Tissue Res 2014;55(suppl 1):9–14.
41. Xu C, Wang Y. Chemical composition and structure of peritubular and intertubular human dentin revisited. Arch Oral Biol 2012;57:383–391.
42. Wang R, Li Q, Niu L, Yang B, Liu G, Zuo H. Fracture toughening of peritubular microstructure in biological porous dentine. J Mech Behav Biomed Mater 2019;93:194–203.
43. Prasad M, Butler WT, Qin C. Dentin sialophosphoprotein (DSPP) in biomineralization. Connect Tissue Res 2010;51:404–417.
44. Jaha H, Husein D, Ohyama Y, et al. N-terminal dentin sialoprotein fragment induces type I collagen production and upregulates dentinogenesis marker expression in osteoblasts. Biochem Biophys Rep 2016;6:190–196.
45. Fang PA, Verdelis K, Yang X, Lukashova L, Boskey AL, Beniash E. Ultrastructural organization of dentin in mice lacking dentin sialo-phosphoprotein. Connect Tissue Res 2014;55(suppl 1):92–96.
46. Suzuki S, Sreenath T, Haruyama N, et al. Dentin sialoprotein and dentin phosphoprotein have distinct roles in dentin mineralization. Matrix Biol 2009;28:221–229.
47. Chavez MB, Tan MH, Kolli TN, et al. Bone sialoprotein is critical for alveolar bone healing in mice. J Dent Res 2023;102:187–196.
48. Chen J, McCulloch CA, Sodek J. Bone sialoprotein in developing porcine dental tissues: Cellular expression and comparison of tissue localization with osteopontin and osteonectin. Arch Oral Biol 1993;38:241–249.
49. Hunter GK, Poitras MS, Underhill TM, Grynpas MD, Goldberg HA. Induction of collagen mineralization by a bone sialoprotein–decorin chimeric protein. J Biomed Mater Res 2001;55:496–502.

50. Baht GS, O'Young J, Borovina A, et al. Phosphorylation of Ser136 is critical for potent bone sialoprotein-mediated nucleation of hydroxyapatite crystals. Biochem J 2010;428:385–395.
51. Foster BL, Ao M, Willoughby C, et al. Mineralization defects in cementum and craniofacial bone from loss of bone sialoprotein. Bone 2015;78:150–164.
52. Ganss B, Kim RH, Sodek J. Bone sialoprotein. Crit Rev Oral Biol Med 1999;10:79–98.
53. Monfoulet L, Malaval L, Aubin JE, et al. Bone sialoprotein, but not osteopontin, deficiency impairs the mineralization of regenerating bone during cortical defect healing. Bone 2010;46:447–452.
54. He G, Dahl T, Veis A, George A. Nucleation of apatite crystals in vitro by self-assembled dentin matrix protein 1. Nat Mater 2003;2:552–558.
55. Narayanan K, Gajjeraman S, Ramachandran A, Hao J, George A. Dentin matrix protein 1 regulates dentin sialophosphoprotein gene transcription during early odontoblast differentiation. J Biol Chem 2006;281:19064–19071.
56. Suzuki S, Haruyama N, Nishimura F, Kulkarni AB. Dentin sialophosphoprotein and dentin matrix protein-1: Two highly phosphorylated proteins in mineralized tissues. Arch Oral Biol 2012;57:1165–1175.
57. Buss DJ, Reznikov N, McKee MD. Crossfibrillar mineral tessellation in normal and Hyp mouse bone as revealed by 3D FIB-SEM microscopy. J Struct Biol 2020;212:107603.
58. Dechichi P, Biffi JC, Moura CC, de Ameida AW. A model of the early mineralization process of mantle dentin. Micron 2007;38:486–491.
59. Wang RZ, Weiner S. Strain-structure relations in human teeth using Moiré fringes. J Biomech 1998;31:135–141.
60. MacDougall M, Slavkin HC, Zeichner-David M. Characteristics of phosphorylated and non-phosphorylated dentine phosphoprotein. Biochem J 1992;287:651–655.
61. Jin X, Xu Y, Liu W, et al. Dental manifestations and treatment of hypophosphatemic rickets: A case report and review of literature. BDJ Open 2023;9:2.
62. McKee MD, Zalzal S, Nanci A. Extracellular matrix in tooth cementum and mantle dentin: Localization of osteopontin and other noncollagenous proteins, plasma proteins, and glycoconjugates by electron microscopy. Anat Rec 1996;245:293–312.
63. Icer MA, Gezmen-Karadag M. The multiple functions and mechanisms of osteopontin. Clin Biochem 2018;59:17–24.
64. Sodek J, Ganss B, McKee MD. Osteopontin. Crit Rev Oral Biol Med 2000;11:279–303.
65. Rittling SR, Matsumoto HN, McKee MD, et al. Mice lacking osteopontin show normal development and bone structure but display altered osteoclast formation in vitro. J Bone Miner Res 1998;13:1101–1111.
66. Foster BL, Ao M, Salmon CR, et al. Osteopontin regulates dentin and alveolar bone development and mineralization. Bone 2018;107:196–207.
67. Boskey AL, Maresca M, Ullrich W, Doty SB, Butler WT, Prince CW. Osteopontin-hydroxyapatite interactions in vitro: Inhibition of hydroxyapatite formation and growth in a gelatin-gel. Bone Miner 1993;22:147–159.
68. Saito K, Nakatomi M, Ida-Yonemochi H, Ohshima H. Osteopontin is essential for type I collagen secretion in reparative dentin. J Dent Res 2016;95:1034–1041.

Comprehensive Management of Impacted Teeth in Cystic Lesions of the Jaws

Yan Fang SUN[1], Qian Ling WANG[2], Zhuo Yue SHI[2], Yi ZHAO[2]

Cystic lesions in the jaws are frequently associated with impacted teeth, and include dentigerous cysts, odontogenic keratocysts, unicystic ameloblastoma and adenoid odontogenic tumours. The most common treatment modality is enucleation of cysts with removal of the impacted tooth. Marsupialisation is a more conservative treatment modality than enucleation and is considered the first-line treatment, especially in the initial management of benign cystic lesions during the mixed dentition period. Depending on the size of the lesion, the position of the impacted tooth and the available space, the majority of teeth can erupt spontaneously after marsupialisation. A multidisciplinary approach has been used in recent years for management of these lesions. Orthodontic traction is sometimes performed on the impacted tooth to guide tooth eruption postoperatively. When an impacted tooth or teeth within cystic lesions are preserved and functional occlusion is obtained, the patient's quality of life can improve significantly. Prospective clinical trials with a larger patient cohort are necessary to determine the clinical benefit of the conservative approach with marsupialisation or surgical-orthodontic treatment of impacted teeth in cystic lesions since only studies of small groups of patients or case reports have been published to date.

Keywords: *cystic lesions, enucleation, impacted tooth, marsupialisation, orthodontic traction*
Chin J Dent Res 2025;28(1):19–30; doi: 10.3290/j.cjdr.b6097603

A cystic lesion is a pathological cavity that contains fluid or a semisolid material and is lined by epithelium.[1] Most cysts in the jaw are lined by epithelium that is derived from odontogenic epithelium and are referred to as odontogenic cysts.[2] Odontogenic keratocysts (OKCs) and unicystic ameloblastomas (UAs) can share a similar clinical and radiographic presentation to dentigerous cysts (DCs).[3] Cystic lesions in the jaws are usually asymptomatic, and may be detected incidentally via routine radiographic examinations or when they are large enough to cause facial asymmetry.[4,5] The expansion of cystic lesions may impinge on surrounding structures, such as the inferior alveolar nerve or roots of adjacent teeth, resulting in paraesthesia, tooth displacement or root resorption. They may displace or obliterate the maxillary sinus, nasal cavity and orbital cavity, which leads to diplopia.[6,7]

Cystic lesions in the jaws have been commonly found to be associated with unerupted teeth. A vast majority of DCs are associated with impacted mandibular third molars, followed by permanent maxillary canines and maxillary third molars[8]; however, in a literature review about DCs in children, Tuwirqi et al[5] found that the substantial majority of DCs involve the mandibular second premolars and second molars followed by the maxillary permanent canines, but rarely the mandibular incisors. Mandibular OKCs and UAs are often associated with impacted third molars, with some reports indicating that up to 80% of these lesions occur around an unerupted mandibular third molar.[9,10] It is commonly found that adenoid odontogenic tumours (AOTs) and calcifying odontogenic cysts (COCs) are associated with impacted teeth.[11]

The standard treatment for cystic lesions involves enucleation and extraction of the affected teeth. During

1 Department of Oral and Maxillofacial Surgery, School and Hospital of Stomatology, Wuhan University, Wuhan, P.R. China.
2 Department of Prosthodontics, School and Hospital of Stomatology, Wuhan University, Wuhan, P.R. China.

Corresponding author: Dr Yi ZHAO, Department of Prosthodontics, School and Hospital of Stomatology, Wuhan University, Wuhan 430079, P.R. China. Tel: 86-27-87686221. Email: zhao_yi@whu.edu.cn

removal of the lesion, extraction of the unerupted permanent third molar, inverted or severely dislocated impacted tooth or supernumerary tooth is usually carried out.[6,12,13] When preservation of the impacted teeth is planned, marsupialisation is a rather conservative treatment option, and has the advantage of promoting spontaneous eruption of the affected tooth within the cyst.[4,14] In preadolescents, a permanent tooth in a DC often erupts successfully after having undergone marsupialisation and resolution of the cyst.[14,15] Combined orthodontic-surgical techniques may help promote cyst-related tooth eruption, but treatment plans are difficult to carry out for huge cystic lesions with deeply impacted teeth. In these circumstances, enucleation and simultaneous removal of the impacted teeth may cause nerve injury or pathological mandibular fracture during surgery. DCs with deeply impacted mandibular third molars can be treated by means of marsupialisation with orthodontic traction.[16] This orthodontic-surgical procedure may reduce the risk of nerve damage and pathological fracture of the mandible. In these cases, coronectomy is an elective procedure that poses decreased risk of nerve injury or mandibular fracture.[17]

Marsupialisation or surgical-orthodontic treatment for cystic lesions has been widely recommended in order to preserve the impacted teeth and create favourable conditions for the further development and function in the oral-maxillary structures. Preservation of cyst-associated teeth requires a reliable and intuitive protocol, thus the present authors systemically reviewed the types of cystic lesions of the jaws and various methods of managing these lesions based on recent publications in the literature.

Types of cystic lesions of the jaws associated with impacted teeth

DCs are developmental cysts associated with impacted teeth, but other odontogenic cystic lesions, including OKCs, orthokeratinised odontogenic cysts (OOCs) and UAs, sometimes share a similar presentation to DCs.[3] Clinical, radiographic and histological evidence is often required to make appropriate diagnoses and manage these lesions.

DCs

DCs are the second most commonly observed type of odontogenic cyst after radicular cysts, and are the most common developmental cyst found in the jaws.[8,18] They occur most frequently in the posterior mandible and maxilla, and are most often associated with an impacted third molar.[19-21] The second most prevalent location for them is the maxillary canines, but some cysts occur around premolars or very rarely, around incisors and supernumerary teeth.[8,22] Benn and Altini[23] were the first to propose the classification of DCs based on their aetiology by dividing them into two separate groups: DCs of developmental and inflammatory origin. Inflammatory DCs are most commonly located in the premolar region, with the non-vital primary tooth still present in the dental arch.

DCs are more commonly found in patients in their second and third decades of life than in older age groups.[19,20] It was reported that the mean age of children with DCs was between 11.05 and 11.60 years.[1,24] The late mixed dentition period corresponds to the time at which the crowns of permanent teeth have developed completely and have started to erupt. Thus, DCs in paediatric populations may occur more frequently in the late mixed dentition stage because during this time, there is a higher probability of impaction of the maxillary canines, as well as of periapical inflammation spreading from a non-vital primary tooth to involve the follicle of the unerupted permanent tooth.[24]

OKCs and OOCs

OKCs represent 4% to 11% of odontogenic cysts.[25,26] They frequently occur in patients aged between 10 and 40 years, and approximately 70% are located in the mandible.[26,27] OKCs have less of a tendency to expand buccolingually. Radiologically, OKCs present unilocular or multilocular radiolucency. Multiple OKCs are observed in association with nevoid basal cell carcinoma syndrome (NBCCS). An unerupted tooth is associated with the lesion in 25% to 40% of cases.[28] Importantly, OKCs exhibit a high recurrence rate, varying from 20% to 80%.[28,29] PTCH1 inactivating mutations were demonstrated in 93% of sporadic OKCs.[30]

The term OOC was first coined by Wright[31] in 1981 as a variant of OKC. Subsequent studies have demonstrated that OOCs do not share the same clinical behaviour, histological characteristics, PTCH1 gene mutation or association with NBCCS as seen in OKC.[32,33] There is a male predominance and the mean age of presentation is in the third to fourth decade of life.[34] The posterior mandible is the most common location for OOCs and up to two-thirds of reported cases are associated with an unerupted tooth.[35] Up to 50% of OOCs are asymptomatic and > 90% of cases present as a well-demarcated unilocular lesion.[33,34]

UAs

Ameloblastomas account for around 13% to 50% of all odontogenic tumours.[36] Of these, 5% to 22% of all ameloblastomas are of the unicystic type.[37] Conventional ameloblastomas and UAs may be associated with impacted teeth, particularly mandibular third molars; however, the majority of UAs have this clinical presentation.[38,39] UA presents in a younger age group, with 50% of cases reported in patients in the second decade of life in contrast to conventional ameloblastomas, which have a peak incidence in the fourth and fifth decades.[38,39]

AOTs

AOTs are a relatively rare benign lesion and account for < 5% of odontogenic tumours[37] and occur twice as frequently in female patients as in male patients. Canines are the most common unerupted teeth associated with AOTs. Lesions are unilocular in 91% of cases.[40] Generally, the disease occurs in the second decade of life.[40,41] Clinically, an AOT resembles a DC or an ameloblastoma. It is completely radiolucent and mimics a DC in terms of growth pattern and appearance; however, it often appears to envelop both the crown and roots of a tooth, and is seen as a corticated radiolucency with small radiopacities.

COCs

COC mostly affect the anterior region of the jaw and are most common during the second and third decades of life.[37,42] Radiographically, they appear as a well-circumscribed unilocular radiolucency containing flecks of indistinct radiopacities. The lesion encompassing the crown is attached to the cementoenamel junction.[11] In around one-third of cases, an impacted tooth is associated with the lesion.

Imaging evaluation and histology of cystic lesions

Imaging examinations

Imaging modalities used to evaluate cystic lesions of the jaws include intraoral radiography, panoramic tomography, CBCT, computed tomography (CT), MRI and ultrasound. Radiographs are a routine part of the diagnostic process and treatment planning. The classic radiological appearance of an odontogenic cyst in the jaws is a well-defined, round or oval area of radiolucency, circumscribed by a sharp radiopaque margin.[6,43]

Panoramic radiography and periapical films are the backbone of diagnostic imaging; however, plain radiography has several limitations, such as the superimposition of anatomical structures, and the inability to observe small changes in bone density. CT, especially CBCT, is a commonly used technique for evaluating the topography of cystic lesions of the jaws.[44-46] The integrity/discontinuity of the bony margins, dimensions, exact anatomical site of lesions, internal calcifications, proximity to vital structures and displacement and root resorption of teeth are well documented on radiographs. CBCT images are not distorted or enlarged, and have a margin of error of < 0.1 mm. In contrast, one multislice CT scan has a margin of error of 1.0 to 1.5 mm.[47] CBCT has a usual exposure dose that is 40 to 60 times lower than that of multislice CT.[48] The main advantages of CBCT over conventional CT are its very high spatial resolution, which introduces a 3D image in one rotation only with a lower dose and simpler technique.[45,49] Application of the technique can enhance the quality of the diagnosis and preoperative assessment of cystic lesions in the jaw and determine the optimal surgical treatment plan.[44,50,51]

DCs appear as a well-defined unilocular radiolucency associated with the crown of an unerupted tooth.[8,21,22] Often, the radiolucent area surrounds the crown, but sometimes it lies mainly or entirely to one side. The central type has been found to be the most common (60.6%), followed by the lateral type (29.2%) and the circumferential type (10.2%).[21] Unilocular lesions with the crown of an impacted third molar in the mandible may be DCs, OKCs or UAs, and it is impossible to distinguish these lesions through clinical or radiographic examinations.

A unilocular radiolucency with opacities and tooth displacement in the anterior region of the jaws is the radiological feature most characteristic of the majority of AOTs.[40] The follicular (pericoronal) type is associated with the crown of the impacted tooth. AOTs can be radiographically indistinguishable from DCs, but in around two-thirds of cases, small foci of radiopacity can be detected.[37,50] COCs are rare, accounting for < 1% of all odontogenic cysts. Radiographs of COCs reveal a well-defined radiolucent lesion, which is usually unilocular. Around half of all cases have amounts of calcified tissue.[37] A complex odontoma in its intermediate stage may mimic an AOT.

Histopathological examination

Clinical and radiographic examination alone cannot differentiate between the abovementioned cystic lesions

associated with an unerupted tooth, so a histopathological examination should be performed for all cystic lesions. A specimen of the cyst membrane is routinely sent for histological examination and diagnosis. The intraoperative frozen specimen can also detect an occult pathological condition.

Recognising the key histological features of the various odontogenic cystic lesions associated with the crown of an impacted tooth will aid in arriving at the correct diagnosis and ensuring appropriate clinical management.[3]

DCs

DCs are lined with nonkeratinising epithelium of uniform thickness of two to four layers of cuboidal/squamous cells, overlying fibrous or fibromyxoid stroma.[8,20,37] Small islands or cords of inactive-appearing odontogenic epithelial rests are usually present within the connective tissue. Scattered mucous cells, cilia, hyaline bodies and calcifications can be encountered in the cyst lining. If secondarily inflamed, the epithelium can become hyperplastic.

It may be more likely to encounter inflammatory DCs in paediatric populations.[23,24] Inflammatory DCs in paediatric patients may occur due to periapical inflammation of a primary tooth that spreads to involve the underlying follicle of the unerupted permanent tooth.[24]

OKCs and OOCs

The OKC shows corrugated parakeratinised epithelium without a granular cell layer, with a basal layer containing prominent palisaded and hyperchromatic nuclei.[8,37] Other histological findings in OKCs include budding of the basal layer. The dense fibrous connective tissue wall usually lacks inflammation unless it is secondarily inflamed. The satellite or daughter cysts of OKCs are more commonly seen in syndromic OKCs. Most OKCs are sporadic, but up to 5% of cases are associated with NBCCS. PTCH1 gene inactivation has been identified in around 90% of OKCs.[30]

OOCs are characterised by a thin, uniform epithelium of five to nine cell layers, lacking rete ridges. Thick, lamellated orthokeratin is present on the surface and a prominent granular cell layer is seen. The basal cells lack palisading and hyperchromatic nuclei.[3,37] The absence of PTCH1 mutations is confirmed by sequencing epithelial lining samples from 14 OOCs.[52]

UAs

Three histological growth patterns of UAs are recognised: luminal, intraluminal and mural.[38] The epithelium has the characteristic peripheral palisading and nuclear polarisation (reverse polarity) seen in ameloblastomas. Overlying the basal cells may be the vacuolated cells and loosely arranged epithelium, reminiscent of the stellate reticulum. The purely luminal variant is mostly associated with an impacted tooth, and is considered less aggressive.[37,38]

AOTs

AOT are benign epithelial tumours that have a duct-like structure.[37,53] They produce a variety of architectural patterns, most notably multiple, variably sized nodules of nondescript to spindled epithelial cells with minimal stroma. Within these nodules are variably sized rosette-like or duct-like spaces. These spaces are lined by a columnar or cuboidal epithelium, with the nuclei tending to be displaced away from the lumen.[37] Small foci of calcification are frequently seen within the tumour.

COCs

Histopathology in COCs is unicystic and is lined by epithelium of variable thickness with a wide range of histological characteristics. The key diagnostic feature is the presence of a well-defined basal layer of palisading columnar cells and a thick overlying layer resembling the stellate reticulum of the enamel organ, with focal accumulations of ghost cells, which may calcify.[37,42] A variable amount of dentinoid is sometimes laid down adjacent to the epithelial lining.

Marsupialisation or decompression of cystic lesions

Marsupialisation procedures

The standard treatment for cystic lesions is enucleation of the cyst with extraction of the teeth associated with it, particularly the third molar or supernumerary or malformed teeth.[54] In large lesions that pose a real risk of damaging important anatomical structures during enucleation, marsupialisation or decompression, coronectomy in conjunction with cystectomy may be considered. The first treatment option for DCs in children and preadolescents is marsupialisation or decompression as minimally invasive surgical procedures.[55,56] This

enables progressive reduction of the cystic lesion with minimal risk of injury to the adjacent structures, and promotes spontaneous eruption of the teeth involved.[1,57]

Marsupialisation and decompression are very similar surgical procedures aimed at decreasing the cystic size by reducing the pressure of the cystic fluid and inducing bony apposition to the bony surface in the void created by the shrinking cystic walls.[58-60] However, technically they have different meanings. Marsupialisation of cysts in the jaws with retention of part of the lining[6] creates a larger communication or pouch connecting the oral and cystic cavities after unroofing the outer wall of the cyst and suturing the cyst wall to the oral mucosa.[61,62] An obturator (cyst plug or acrylic stent) is fabricated and placed into the cavity to maintain patency after surgery.[63-65] Decompression, proposed by Thoma,[66] creates a smaller opening or connection between the cyst and the oral environment, which is maintained via a small-diameter polyethylene or rubber drainage tube until an epithelial slit forms.[67-69] Excised tissue (biopsy sample) from the epithelial lining is sent for histological examination during marsupialisation.

When preservation of the impacted teeth is planned, marsupialisation is a rather conservative treatment option,[4] and has the advantage of promoting spontaneous eruption of the involved teeth within the cyst.[14] Two studies found that between 71.4% and 72.4% of the individuals who participated presented with natural eruption of teeth enclosed in the cyst after marsupialisation was carried out.[14,15] Nahajowski et al[70] determined that almost 62% of premolars associated with DCs erupted spontaneously after marsupialisation of the cyst. The key factors involved in the eruption of the tooth in the arch are the status of root development and the angle and depth of the tooth in the jaw. The impacted teeth, together with incomplete root development, show potential for eruption if the angle was less than 25 degrees and the space between adjacent teeth was greater than the size of the teeth.[71] It is very well established that the mean amount of time it takes teeth to erupt without carrying out orthodontic traction is approximately 3 months.[14,15]

The impacted teeth without complete root formation or with an open apex have considerable potential to erupt after marsupialisation.[72] If the dental roots have been matured, the teeth might not erupt to the normal position after marsupialisation.[15,57,73] Patients aged over 10 years old would not be expected to experience spontaneous eruption of an impacted tooth, indicating the need for orthodontic treatment to guide occlusion or surgical removal of the entire cyst with impacted teeth.[71]

When large cystic lesions of the mandible are associated with deeply impacted teeth, enucleation and simultaneous removal of the impacted tooth may cause nerve injury or pathological mandibular fracture during surgery. Sun et al[74] found that after marsupialisation, all the cystic lesions shrunk and all impacted teeth with or without mature roots moved towards the bony windows, and the distance of tooth movement ranged from 8.3 to 12.1 mm, which facilitated tooth extraction during stage-two surgery (enucleation). After the second surgery, there were no occurrences of numbness in the ipsilateral lower lip or mandibular fracture, or indeed any other complications.[74] When the third molar is deeply impacted within the cyst cavity, a combined orthodontic-surgical procedure may further facilitate tooth extraction and reduce the risk of damage to the inferior alveolar nerve and the possibility of pathological fractures.[16,75]

Cyst plug or obturator

A cyst plug or obturator must be used to maintain patency of fenestration when marsupialisation of a cystic lesion in the jaw is performed. The cyst plug is usually inserted between 10 days and 2 weeks after marsupialisation. These obturators are designed and inserted, taking into consideration the missing tooth, the anteroposterior position of the lesion and the direction of marsupialisation. The obturator design is determined by the prosthodontist. Three types of obturator prosthesis have been designed,[76-79] namely the clasp type, consisting of a retainer and obturator; the denture type, consisting of a retainer, artificial tooth, denture base and obturator; and the plug type, consisting only of an obturator.[78] Significant differences among the three obturator groups were found for age, number of remaining teeth, location, direction of marsupialisation (labial, buccal or occlusal surface) and pattern of missing teeth (free-end, bounded or none missing). Clasp- and denture-type obturators, which use retainers, require invasive rest seat preparation on the abutment teeth. When the loss of an anterior tooth or premolar occurs after marsupialisation, the device used is an obturator in acrylic resin incorporated in a removable partial denture,[79] and a denture-like obturator can be provided for space maintenance and masticatory function.[56,79] Because obturator design has a minimal effect on the ability of the appliance to maintain the surgical opening, it is preferable to use the least invasive design (plug-type obturator).

A one-piece cast appliance is fabricated to maintain patency of the cyst fenestration when marsupialisation of a cyst in the jaw is performed.[80] The appliance con-

sists of a clasp, a connector and an insert, formed as a one-piece casting of chromium alloy and attached to a tooth or teeth adjacent to the surgical site. A one-piece cast appliance has several advantages: positive retention, stability and comfort; minimum irritation of the wound margins; positive maintenance of the orifice diameter; no irritation of the periodontal attachment of the ligated tooth; ease of removal for cleaning and irrigation; and radiopacity of the appliance.[80] However, postoperative modification of the appliance is not easy to perform compared with acrylic resin.

The clasp and base of the traditional cyst plug play the main role for retention[78,79]; however, because of the anatomical shape and arrangement of the teeth in teenagers in the mixed dentition stage, the retention force of the cyst plug is often insufficient, which may lead to accidental swallowing. Therefore, a vacuum-formed cyst plug is designed,[81] whose retainer, the vacuum-formed part, covers the entire dentition and plays an important role in retention. The plug body is responsible for maintaining drainage. This vacuum-formed cyst plug may replace the classic one, and provides a more comfortable experience for children in the mixed dentition stage.

After insertion, all patients are advised of the importance of wearing the prosthesis continuously and are recalled to the hospital every 1 to 2 months for radiological and prosthetic review. When bone regeneration occurs, the cavity reduces in size and the tooth continues to erupt, the prosthodontist carefully reduces the intra-cystic length of the obturator, but the diameter at the opening is fully maintained.[76,79] The ultimate decision to terminate the use of the obturator is made by an oral surgeon based on assessment of radiographic images.[78]

Factors associated with effects of marsupialisation

Factors potentially influencing the effects of marsupialisation

There are various factors to consider when performing marsupialisation, such as patient age, size and location of cystic lesions, and patient cooperation.[70] The factors influencing the eruption of the DC-associated tooth after marsupialisation include cusp depth, angulation, eruption space, root formation and patient age.[14,15,57] A tooth with completely formed roots, that is severely displaced or that has insufficient eruption space cannot erupt spontaneously, and requires orthodontic traction if the impacted tooth is to be preserved.

Two-stage surgery

Marsupialisation can be performed alone or in combination with subsequent enucleation based on types of and postoperative changes in cystic lesions. Tomomatsu et al[82] evaluated the 3D changes that occurred in cystic lesions of the mandible after marsupialisation, and found that the effect of marsupialisation on cystic lesions with a major axis of 3 cm or more showed a significant difference between 3.0 and 4.5 months; however, the difference was not significant between 4.5 and 6.0 months. An indication for the timing of enucleation after marsupialisation would be 4.5 months when the rate of decrease of the cysts after fenestration slows down. However, Bodner et al[63] recommended that cysts be enucleated at 3.0 months after marsupialisation based on CT with multiplanar reconstruction in 23 patients treated with marsupialisation.

Two-stage surgery is often carried out in the cases of OKCs and UAs in order to eliminate the residual lesion because of their aggressive character and high recurrence rate.[64,83-85] Sano et al[73] performed marsupialisation followed by enucleation, without extracting the involved second molar in UA of the mandible in a 13-year-old girl, with the intention to improve the patient's oral function. As a result, spontaneous eruption of the involved second molar and excellent occlusion were obtained without orthodontic treatment, and no tumour recurrence was documented over a follow-up period of 51 months.[73]

Eliminating the disadvantages of marsupialisation

The disadvantage of marsupialisation is the very long healing process and the necessity of regular follow-up appointments. Cooperation of patients and their parents is essential and plays a major role in clinical success.[55,58] The most serious disadvantage is that pathological tissue is left in place and the entire lesion is not examined histopathologically. This runs the risk of unrecognised benign or malignant neoplastic processes being left behind, or malignant transformation of the remaining cyst lining.[56] All these drawbacks may be eliminated when DCs in children and preadolescents are managed with enucleation (cystectomy) but with preservation of associated teeth and adjacent tooth buds as a single surgical procedure. Hauer et al[54] presented a retrospective case series of seven patients with 15 unerupted teeth associated with or adjacent to DCs treated using the uniform surgical protocol (cystectomy, preservation of cyst-associated teeth, without use of orthodontic traction,

primary wound closure). The mean age of patients was 9.0 ± 2.1 years. All teeth erupted spontaneously. They suggested that the cystectomy of DCs with preservation of associated teeth may be considered an alternative to marsupialisation in children and preadolescents; however, enucleation carries a risk of possible loss of developing tooth buds when the dental crown is sharply separated from the cystic wall.

Cyst enucleation with coronectomy of impacted teeth

There are different treatment options for cystic lesions associated with an impacted tooth, and cyst enucleation with the removal of the unerupted tooth is a common one. These lesions have the potential to grow to a significant size, resulting in displacement of the unerupted tooth and weakening of the jaw. If the extensive cyst is associated with mandibular teeth, this can complicate surgery, with the risk of inferior alveolar nerve injury from removal of either the cyst or the unerupted tooth where proximity to the inferior alveolar nerve is present. Removal of the intracystic impacted tooth is sometimes difficult due to limited access, increased risk of damage to vital structures or jaw fracture. In such cases, coronectomy is likely to reduce these risks due to its conservative nature.[17]

Coronectomy is an alternative procedure for extraction of an entire wisdom tooth to minimise the risk of temporary or permanent inferior alveolar nerve (IAN) neuropathy. It involves careful removal of the crown of the tooth while maintaining its roots.[86,87] The most common complication of coronectomy is root mobilisation. Cosola et al[87] reported the data and follow-up radiographs of 130 patients who underwent coronectomy of mandibular third molars. The roots migrated in a mesial or coronal direction in 31 patients; in four cases, they were removed because of patient preference.[87] The placement of a bone graft material in the coronectomy socket could significantly decrease the incidence of root migration requiring reoperation of the exposed roots and reduce the preexisting pocket depth distal to the second molar, especially in patients with mesioangularly or horizontally impacted wisdom teeth.[88]

Despite the increase in popularity of coronectomy as an adequate preventative technique for IAN protection, its use in conjunction with the management of DCs has not been widely reported in the literature. O'Riordan[89] described a Gorlin-Goltz patient who had undergone coronectomy and removal of an OKC of the mandibular left second premolar. Malden and D'Costa[90] first reported the use of coronectomy with removal of DCs. Performance of coronectomy for DCs is based on the principle that the cyst originates from the enamel-dentine junction. Therefore, removing the crown below the enamel-dentine junction completely removes the cyst at its origin.[90,91] Patel et al[91] presented a case series of 21 patients with DCs treated by coronectomy. One patient had permanent injury to the inferior dental nerve, but no mandibular fracture or recurrence of cyst was reported.[91]

A retrospective review of 68 patients was undertaken by Henien et al[17] in a single department where 73 teeth with associated DCs were treated by coronectomy, and found that one patient experienced permanent injury of the IAN, and no intraoperative mandibular fractures occurred. Four coronectomy roots required retrieval at 2, 4 and 20 months and 10 years after the initial surgery due to persistent surgical site infection and incomplete coronectomy with retained enamel and associated cystic tissue leading to symptoms.[17] The authors suggested coronectomy in conjunction with enucleation of DCs is an effective treatment when there is concern regarding IAN injury or jaw fracture from extraction, with minimal morbidity seen in both short- and long-term periods.[17]

Orthodontic eruption of impacted teeth

Indications for surgical-orthodontic treatment of impacted teeth

The two most recommended conservative options are marsupialisation and decompression, which offer the possibility of preserving the impacted tooth associated with cystic lesions of the jaws. The major advantages of marsupialisation are limitation of the extent of surgery, gradual shrinkage of the cystic volume, stimulation of osteogenesis and promotion of the eruption of lesion-associated teeth. It has been well established that the mean amount of time it takes teeth to erupt without carrying out orthodontic traction is approximately 3 months. Tooth eruption does not always occur spontaneously after marsupialisation or decompression, especially when there is not enough space to allow eruption or no favourable axis is available.[70,71,92] The factors influencing the eruption of the DC-associated tooth include cusp depth, angulation, eruption space, root formation and patient age.[14,15,57,74] The impacted tooth without complete root formation or with an open apex has considerable potential to erupt spontaneously in the normal position in the dental arch after marsupialisation.[60]

A tooth with completely formed roots, that is severely displaced or has insufficient eruption space cannot erupt spontaneously. The combined approach of marsupialisation and orthodontic traction is considered the best option for patients with cystic lesions if the impacted tooth is to be preserved.[93-95] Combined orthodontic-surgical techniques may help promote tooth eruption related to cysts. The goals of this combination are to achieve traction of the tooth associated to cysts, open or maintain space, and correct the tooth position after marsupialisation or decompression.[16] Complete eruption and alignment of impacted teeth by means of orthodontic appliances may take more than 3 years after marsupialisation in some complicated cases.[1,93]

Marsupialisation with orthodontic traction of impacted teeth

A multidisciplinary approach proved to be an effective modality in treating a large cyst associated with a deeply impacted tooth. Tsironi et al[96] presented a case of a DC with a deeply impacted mandibular first molar in an 11-year-old girl that was treated with combined surgical and orthodontic procedures. The roots of the impacted molar were completely developed with closed apices.[96] After clinical and radiographic evaluation, marsupialisation of the cyst was performed, and a molar attachment was bonded onto the buccal side of the impacted molar as part of a full orthodontic treatment with fixed appliances.[96] After 18 months of orthodontic traction, the molar was moved to a more advantageous position, and new bone apposition was observed at the site of the cystic lesion, then the molar was left to erupt spontaneously for 14 more months and a functional occlusion was finally achieved.[96] When a third molar is deeply impacted within the cyst cavity, a combined orthodontic-surgical procedure may reduce the risk of damage to the IAN.[16] This approach may facilitate extraction and also reduce the possibility of nerve damage and pathological fractures of the mandible.

Comprehensive orthodontic treatment combined with marsupialisation can also be used to treat patients with OKCs and AOTs, especially young, growing patients with impacted anterior teeth or premolars.[97,98] Baik et al[98] described successful orthodontic treatment combined with marsupialisation of a cyst in a 10-year-old girl who exhibited a mandibular OKC with an impacted left canine and first premolar, as well as congenitally missing bilateral mandibular second premolars. After marsupialisation of the OKC, the positions of the impacted teeth showed spontaneous improvement, along with a reduction in the size of the cyst.[98] Orthodontic traction of the impacted teeth was easily achieved by using a removable appliance.[98] After treatment, the affected teeth showed normal vitality and fully developed roots.[98] The sequential use of removable and fixed appliances enabled orthodontic traction of the impacted teeth.[98] The treatment outcome was stable 2.5 years after the end of treatment.[98] Erdur et al[97] reported the uneventful eruption of an impacted canine in an AOT treated with combined orthodontics and marsupialisation, with no evidence of recurrence 3 years after treatment.

Enucleation with orthodontic traction of impacted teeth

Cyst enucleation in combination with orthodontics has been successfully used to treat cystic lesions with impacted teeth. Francisquini et al[99] reported a rare case of bilateral DCs associated with impacted maxillary canines treated by enucleation in association with orthodontic traction in an 11-year-old girl. Cystic lesions were enucleated by dissection and curettage of the tissue capsule surrounding the impacted teeth. Concomitantly, two orthodontic brackets were bonded to the surface of the crowns of the impacted canines for traction. Surgical enucleation, traction and orthodontic treatment enabled positioning of the impacted canines in the dental arches, thus ensuring maintenance of the functional and aesthetic characteristics, and no recurrence of the cyst was confirmed over the 5-year follow-up period.

Currently, there is an absence of quantitative data on orthodontic eruption of impacted teeth in cystic lesions due to the limited number of reported cases (only case reports are available). The success rate of surgical-orthodontic treatment of impacted teeth for cystic lesions of the jaws and long-term function of the preserved teeth should be further investigated.

Summary and conclusion

Cystic lesions of the jaws may be either symptomatic or asymptomatic and can be found in routine clinical and radiological investigations. Early identification and management are important, as this may avoid potential negative sequelae including failure of eruption, impaction of associated and surrounding teeth, displacement of teeth, resorption of adjacent roots, destruction of bone, encroachment on vital structures and occasionally pathological fracture. Surgical treatment for cystic lesions depends on the size, location, patient age and perforation of the cortical layer, as well as proximity

to vital structures such as teeth, the inferior alveolar canal and the maxillary sinus. The standard treatment for cystic lesions is enucleation of the cyst with extraction of the impacted tooth, particularly the third molar, supernumerary or malformed tooth. Marsupialisation and decompression are widely accepted conservative surgical procedures for the primary treatment of certain cystic lesions of the jaw. These techniques can be used either as a single therapy or in combination with other treatment modalities to eliminate the residual lesion. In children and preadolescents, this form of therapy is considered the first option with the main goal of preserving lesion-associated teeth. A multidisciplinary approach, such as orthodontic treatment combined with marsupialisation, can be an effective treatment strategy for DCs, especially in growing patients with impacted teeth that are severely displaced or that have insufficient eruption space, where spontaneous eruption is not possible. Marsupialisation followed by enucleation, without tooth removal, can be undertaken as a treatment option to obtain functional occlusion in some cases of OKCs, UAs or AOTs with impacted teeth; however, strict follow-up is necessary due to the possibility of recurrence. When unerupted third molars are involved, cyst enucleation with coronectomy can be a solution if the lesion is extensive and teeth are deeply impacted.

In conclusion, it is suggested that the management of impacted teeth associated with cystic lesions of the jaws should involve individualised treatment based on the characteristics of impacted teeth (position, root formation stage, angulation and depth of inclusion), type and size of the lesion, and the age of the patient.

Conflicts of interest

The authors declare no conflicts of interest related to this study.

Author contribution

Dr Yan Fang SUN contributed to the data collection and manuscript draft and revision; Drs Qian Ling WANG and Zhuo Yue SHI contributed to the data collection; Dr Yi ZHAO supervised the study and contributed to the manuscript revision.

(Received Apr 09, 2024; accepted Sep 19, 2024)

References

1. Allon DM, Allon I, Anavi Y, Kaplan I, Chaushu G. Decompression as a treatment of odontogenic cystic lesions in children. J Oral Maxillofac Surg 2015;73:649–654.
2. Anavi Y, Gal G, Miron H, Calderon S, Allon DM. Decompression of odontogenic cystic lesions: clinical long-term study of 73 cases. Oral Surg Oral Med Oral Pathol Oral Radiol Endod 2011;112:164–169.
3. Müller S. Developmental odontogenic lesions associated with the crown of an impacted tooth: A guide to the distinct histologic features required for classification. Head Neck Pathol 2021;15:107–112.
4. Motamedi MHK, Talesh KT. Management of extensive dentigerous cysts. Br Dent J 2005;198:203–206.
5. Tuwirqi AA, Khzam N. What do we know about dentigerous cysts in children: A review of literature. J Res Med Dent Sci 2017;5:67–79.
6. Killey HC, Kay LW, Seward GR. Benign Cystic Lesions of the Jaws, Their Diagnosis and Treatment, ed 3. Edinburgh: Churchill Livingstone, 1977.
7. Kara MI, Yanik S, Altan A, Oznalcin O, Ay S. Large dentigerous cyst in the maxillary sinus leading to diplopia and nasal obstruction: case Report. J Istanb Univ Fac Dent 2015;49:46–50.
8. Shear M, Speight PM. Cysts of the oral and maxillofacial regions, ed 4. Oxford: Blackwell Munksgaard, 2007.
9. Lee JH, Kim SM, Kim HJ, Jeon KJ, Park KH, Huh JK. Characteristics of bony changes and tooth displacement in the mandibular cystic lesion involving the impacted third molar. J Korean Assoc Oral Maxillofac Surg 2014;40:225–232.
10. Roos RE, Raubenheimer EJ, van Heerden WF. Clinico-pathological study of 30 unicystic ameloblastomas. J Dent Assoc S Afr 1994;49:559–562.
11. Okura S, Igarashi C, Wakae-Morita S, et al. Differential diagnosis between calcifying odontogenic cyst and adenomatoid odontogenic tumor by computed tomography images. Oral Radiol 2022;38:99–104.
12. Ikarashi T, Fujimori Y, Ohshiro K, et al. Dentigerous cyst associated with a supernumerary malformed tooth: Report of a case and a clinicopathologic review. Oral Medicine Pathol 2003;8:55–59.
13. Shashikiran ND, Kumar NC, Reddy VV. Unusual presentation of inverted impacted premolars as a result of dentigerous cyst: A case report. J Indian Soc Pedod Prev Dent 2006;24:97–99.
14. Hyomoto M, Kawakami M, Inoue M, Kirita T. Clinical conditions for eruption of maxillary canines and mandibular premolars associated with dentigerous cysts. Am J Orthod Dentofac Orthop 2003;124:515–520.
15. Yahara Y, Kubota Y, Yamashiro T, Shirasuna K. Eruption prediction of mandibular premolars associated with dentigerous cysts. Oral Surg Oral Med Oral Pathol Oral Radiol Endod 2009;108:28–31.
16. Celebi N, Canakci GY, Sakin C, Kurt G, Alkan A. Combined orthodontic and surgical therapy for a deeply impacted third molar related with a dentigerous cyst. J Maxillofac Oral Surg 2015;14:93–95.
17. Henien M, Sproat C, Kwok J, Beneng K, Patel V. Coronectomy and dentigerous cysts: A review of 68 patients. Oral Surg Oral Med Oral Pathol Oral Radiol 2017;123:670–674.
18. Daley TD, Wysocki GP, Pringle GA. Relative incidence of odontogenic tumors and oral and jaw cysts in a Canadian population. Oral Surg Oral Med Oral Pathol 1994;77:276–280.

19. Zhang LL, Yang R, Zhang L, Li W, MacDonald-Jankowski D, Poh CF. Dentigerous cyst: a retrospective clinicopathological analysis of 2082 dentigerous cysts in British Columbia, Canada. Int J Oral Maxillofac Surg 2010;39:878–882.
20. Lin HP, Wang YP, Chen HM, Cheng SJ, Sun A, Chiang CP. A clinicopathological study of 338 dentigerous cysts. J Oral Pathol Med 2013;42:462–467.
21. Noujeim Z, Nasr L. The prevalence, distribution, and radiological evaluation of dentigerous cysts in a Lebanese sample. Imaging Sci Dent 2021;51:291–297.
22. Rajendra Santosh AB. Odontogenic cysts. Dent Clin North Am 2020;64:105–119.
23. Benn A, Altini M. Dentigerous cysts of inflammatory origin. A clinicopathologic study. Oral Surg Oral Med Oral Pathol Oral Radiol Endod 1996;81:203–209.
24. Huang G, Moore L, Logan RM, Gue S. Histological analysis of 41 dentigerous cysts in a paediatric population. J Oral Pathol Med 2019;48:74–78.
25. Johnson NR, Gannon OM, Savage NW, Batstone MD. Frequency of odontogenic cysts and tumors: A systematic review. J Investig Clin Dent 2014;5:9–14.
26. Boffano P, Cavarra F, Agnone AM, et al. The epidemiology and management of odontogenic keratocysts (OKCs): A European multicenter study. J Craniomaxillofac Surg 2022;50:1–6.
27. Chirapathomsakul D, Sastravaha P, Jansisyanont P. A review of odontogenic keratocysts and the behavior of recurrences. Oral Surg Oral Med Oral Pathol Oral Radiol Endod 2006;101: 5–9.
28. Neville BW, Damm DD, Allen CM, Bouquot JE (eds). Oral and Maxillofacial Pathology, ed 2. Philadelphia, PA: WB Saunders Co, 2002.
29. Blanas N, Freund B, Schwartz M, Furst IM. Systematic review of the treatment and prognosis of the odontogenic keratocyst. Oral Surg Oral Med Oral Pathol Oral Radiol Endod 2000;90:553–558.
30. Stojanov IJ, Schaefer IM, Menon RS, et al. Biallelic PTCH1 Inactivation is a dominant genomic change in sporadic keratocystic odontogenic tumors. Am J Surg Pathol 2020;44:553–560.
31. Wright JM. The odontogenic keratocyst: Orthokeratinized variant. Oral Surg Oral Med Oral Pathol 1981;51:609–618.
32. Wright JM, Vered M. Update from the 4th Edition of the World Health Organization Classification of Head and Neck Tumours Odontogenic and Maxillofacial Bone Tumors. Head Neck Pathol 2017;11:68–77.
33. Crane H, Forno PD, Kyriakidou E, Speight PM, Hunter KD. Multiple orthokeratinized odontogenic cysts: A report of two cases and review of the literature. Head Neck Pathol 2020;14:381–385.
34. Dong Q, Pan S, Sun LS, Li TJ. Orthokeratinized odontogenic cyst: A clinicopathologic study of 61 cases. Arch Pathol Lab Med 2010;134:271–275.
35. Uddin N, Zubair M, Abdul-Ghafar J, Khan ZU, Ahmad Z. Orthokeratinized odontogenic cyst (OOC): Clinicopathological and radiological features of a series of 10 cases. Diagn Pathol 2019;14:28.
36. Boffano P, Cavarra F, Tricarico G, et al. The epidemiology and management of ameloblastomas: A European multicenter study. J Craniomaxillofac Surg 2021;49:1107–1112.
37. EI-Naggar AK, Chan JKC, Grandis JR, Takata T, Slootweg PJ (eds). WHO Classification of Head and Neck Tumours, ed 4. Lyon: IARC Press, 2017.
38. Philipsen HP, Reichart PA. Unicystic ameloblastoma. A review of 193 cases from the literature. Oral Oncol 1998;34:317–325.
39. Seintou A, Martinelli-Kläy CP, Lombardi T. Unicystic ameloblastoma in children: Systematic review of clinicopathological features and treatment outcomes. Int J Oral Maxillofac Surg 2014;43:405–412.
40. Becker T, Buchner A, Kaffe I. Critical evaluation of the radiological and clinical features of adenomatoid odontogenic tumour. Dentomaxillofac Radiol 2012;41:533–540.
41. Philipsen HP, Reichart PA. Adenomatoid odontogenic tumour: Facts and figures. Oral Oncol 1999;35:125–131.
42. Moreno-Rodríguez P, Guerrero LM, Gómez-Delgado A, Castro-Núñez J. Active decompression and distraction sugosteogenesis for the treatment of calcifying odontogenic cyst. Oral Maxillofac Surg 2021;25:89–97.
43. Bodner L, Woldengerg Y, Bar-Ziv J. Radiographic features of large cystic lesions of the jaws in children. Pediatr Radiol 2003;33:3–6.
44. MacDonald D. Lesions of the jaws presenting as radiolucencies on cone-beam CT. Clin Radiol 2016;71:972–985.
45. Boeddinghaus R, Whyte A. Trends in maxillofacial imaging. Clin Radiol 2018;73:4–18.
46. Cardoso LB, Lopes IA, Ikuta CRS, Capelozza ALA. Study between panoramic radiography and cone beam-computed tomography in the diagnosis of ameloblastoma, odontogenic keratocyst, and dentigerous cyst. J Craniofac Surg 2020;31:1747–1752.
47. Nakamura N, Mitsuyasu T, Mitsuyasu Y, Taketomi T, Higuchi Y, Ohishi M. Marsupialization for odontogenic keratocysts: Long-term follow-up analysis of the effects and changes in growth characteristics. Oral Surg Oral Med Oral Pathol Oral Radiol Endod 2002;94:543–553.
48. Lizio G, Tomaselli L, Landini L, Marchetti C. Dentigerous cysts associated with impacted third molars in adults after decompression: A prospective survey of reduction in volume using computerised analysis of cone-beam computed tomographic images. Brit J Oral Maxillofac Surg 2017;55:691–696.
49. Nakagawa Y, Kobayashi K, Ishii H, et al. Preoperative application of limited cone beam computerized tomography as an assessment tool before minor oral surgery. Int J Oral Maxillofac Surg 2002;31:322–326.
50. Jiang M, You M, Wang H, Xu L. Characteristic features of the adenomatoid odontogenic tumour on cone beam CT. Dentomaxillofac Radiol 2014;43:20140016.
51. Shujaat S, Tijskens E, De Grauwe AMR, EzEldeenc M, Jacobs R. Inflammatory dentigerous cyst following unresolved endodontic infection of deciduous teeth: A report of three cases with CBCT imaging. Pediatr Dent J 2022;32:50–55.
52. Wang YJ, Zhang JY, Dong G, Li TJ. Orthokeratinized odontogenic cysts: A clinicopathologic study of 159 cases and molecular evidence for the absence of PTCH1 mutations. J Oral Pathol Med 2022;51:659–665.
53. Budakoti A, Khanna KS, Choudhary A. Adenomatoid odontogenic tumor- A rare case report of "two third tumor". J Pharm Res Int 2021;33:117–124.
54. Hauer L, Seidlová P, Merglová V, et al. Complete removal of dentigerous cysts with preservation of associated teeth as an alternative to marsupialization in children and preadolescents. J Craniomaxillofac Surg 2020;48:808–814.
55. Akay MC, Kaya E, Zeytinoğlu M. Treatment of nonsyndromic dentigerous cysts in primary dentition. Clin Cosmet Investig Dent 2011;3:17–23.
56. Hu YH, Chang YL, Tsai A. Conservative treatment of dentigerous cyst associated with primary teeth. Oral Surg Oral Med Oral Pathol Oral Radiol Endod 2011;112:e5–e7.

57. Qian WT, Ma ZG, Xie QY, Cai XY, Zhang Y, Yang C. Marsupialization facilitates eruption of dentigerous cyst-associated mandibular premolars in preadolescent patients. J Oral Maxillofac Surg 2013;71:1825–1832.
58. Gurler G, Yilmaz S, Delilbasi C, Dilaver E, Yuzbasioglu E, Patir-Munevveroglu A. Conservative surgical treatment of the jaw cysts in children: Case study of five patients. Niger J Clin Pract 2017;20:1216–1220.
59. Hu X, Zhao Y, Man QW, Li RF, Liu B, Zhao YF. The effects of marsupialization on bone regeneration adjacent to keratocystic odontogenic tumors, and the mechanisms involved. J Oral Sci 2017;59:475–481.
60. Zhao Y, Liu B, Zhao YF. Controversies regarding the management of teeth associated with cystic lesions of the jaws. Chin J Dent Res 2019;22:81–92.
61. Pogrel MA. Treatment of keratocysts: The case for decompression and marsupialization. J Oral Maxillofac Surg 2005;63:1667–1673 [erratum 2007;65:362–363].
62. Giuliani M, Grossi GB, Lajolo C. Conservative management of a large odontogenic keratocyst: Report of a case and review of the literature. J Oral Maxillofac Surg 2006;64:308–316.
63. Bodner L, Bar-Ziv J. Characteristics of bone formation following marsupialization of jaw cysts. Dentomaxillofacial Radio 1998;27:166–171.
64. Zhao YF, Wei JX, Wang SP. Treatment of odontogenic keratocysts: A follow-up of 255 Chinese patients. Oral Surg Oral Med Oral Pathol Oral Radiol Endod 2002;94:151–156.
65. Huang IY, Lai ST, Chen CH, Chen CM, Wu CW, Shen YH. Surgical management of ameloblastoma in children. Oral Surg Oral Med Oral Pathol Oral Radiol Endod 2007;104:478–485.
66. Thoma KH, Oral Surgery, ed 3. St. Louis: Mosby, 1958.
67. Enislidis G, Fock N, Sulzbacher I, Ewers R. Conservative treatment of large cystic lesions of the mandible: A prospective study of the effect of decompression. Br J Oral Maxillofac Surg 2004;42:546–550.
68. Lizio G, Sterrantino AF, Ragazzini S, Marchetti C. Volume reduction of cystic lesions after surgical decompression: A computerized three-dimensional computed tomographic evaluation. Clin Oral Investig 2013;17:1701–1708.
69. Zhu F, Huang S, Chen Z, Li W, Zhang D. New method to secure cyst decompression tube in tooth-bearing areas. Br J Oral Maxillofac Surg 2017;55:200–201.
70. Nahajowski M, Hnitecka S, Antoszewska-Smith J, Rumin K, Dubowik M, Sarul M. Factors influencing an eruption of teeth associated with a dentigerous cyst: A systematic review and meta- analysis. BMC Oral Health 2021;23:180.
71. Fujii R, Kawakami M, Hyomoto M, Ishida J, Kirita J. Panoramic findings for predicting eruption of mandibular premolars associated with dentigerous cyst after marsupialization. J Oral Maxillofac Surg 2008;66:272–276.
72. Kokich VG, Mathews DP. Surgical and orthodontic management of impacted teeth. Dent Clin North Am 1993;37:181–204.
73. Sano K, Yoshimura H, Tobita T, Kimura S, Imamura Y. Spontaneous eruption of involved second molar in unicystic ameloblastoma of the mandible after marsupialization followed by enucleation: a case report. J Oral Maxillofac Surg 2013;71:66–71.
74. Sun R, Cai Y, Wu Y, Zhao JH. Marsupialization facilitates movement of the cystic lesion-associated deeply impacted mandibular third molar in spite of its mature roots. Med Oral Patol Oral Cir Bucal 2017;22:e625–e629.
75. Checchi L, Alessandri Bonetti G, Pelliccioni GA. Removing high-risk impacted mandibular third molars: A surgical-orthodontic approach. J Am Dent Assoc 1996;127:1214–1217.
76. Moore JR. Surgery of the Mouth and Jaws. Oxford: Blackwell, 1985.
77. Taicher S, Steinberg H, Lewin-Epstein J, Sela M. Acrylic resin stents for marsupialization. J Prosthet Dent 1985;54:818–819.
78. Murakami M, Nishi Y, Nishio M, Minemoto Y, Shimizu T, Nishimura M. A retrospective cohort study of the cumulative survival rate of obturator prostheses for marsupialization. J Prosthodont 2019;28:e811–e816.
79. Zhao Y, Liu B. Drainage devices in marsupialization/decompression for odontogenic cysts of the jaws: the design and clinical application [in Chinese]. Zhongguo Shi Yong Kou Qiang Ke Za Zhi 2020;13:577–581.
80. Ramsey WO, Denegri RF, King WF. Clasp retained devices for drainage of marsupialized cysts. J Oral Maxillofac Surg 1982;40:759–761.
81. Zhao Q, Du S, Wang J, Zhao Y. Application of vacuum-formed cyst plug-in conservative treatment of jaw cyst in children. J Craniofac Surg 2023;34:e366–e368.
82. Tomomatsu N, Takahara N, Kurasawa Y, Terauchi M, Iwasaki T, Yoda T. Three-dimensional changes in cystic lesions of the mandible after marsupialization. J Oral Maxillofacl Surg Med Pathol 2022;34:126–130.
83. Hou R, Zhou HZ. Articles of marsupialization and decompression on cystic lesions of the jaws: A literature review. J Oral Maxillofacl Surg Med Pathol 2013;25:299–304.
84. Wushou A, Zhao YJ, Shao ZM. Marsupialization is the optimal treatment approach for keratocystic odontogenic tumour. J Craniomaxillofac Surg 2014;42:1540–1544.
85. Castro-Núñez J. Decompression of odontogenic cystic lesions: past, present, and future. J Oral Maxillofac Surg 2016;74:104.e1-104.e9.
86. Patel V, Moore IS, Sproat C. Coronectomy - Oral surgery's answer to modern day conservative dentistry. Br Dent J 2010;209:111–114.
87. Cosola S, Kim YS, Park YM, Giammarinaro E, Covani U. Coronectomy of mandibular third molar: Four years of follow-up of 130 cases. Medicina (Kaunas) 2020;56:654.
88. Almontashri SM, Aldossary NM, Assyria AA. Comparing the outcomes of conventional coronectomy and graft coronectomy: A systematic review. Open Dentistry Journal 2023;17:e230111.
89. O'Riordan BC. Coronectomy (intentional partial odontectomy of lower third molars). Oral Surg Oral Med Oral Pathol Oral Radiol Endod 2004;98:274–280.
90. Malden N, D'Costa e Rego A. Coronectomy of a third molar with cyst lining enucleation in the management of a dentigerous cyst. Dent Update 2010;37:622–624.
91. Patel V, Sproat C, Samani M, Kwok J, McGurk M. Unerupted teeth associated with dentigerous cysts and treated with coronectomy: Mini case series. Br J Oral Maxillofac Surg 2013;51:644–649.
92. Nawrocka A, Szelkowska P, Kossakowska P, Małkiewicz K. The interdisciplinary orthodontic-surgical diagnostic and treatment protocol for odontogenic cyst-like lesions in growing patients-A literature review and case report. Appl Sci 2022;12:7146.
93. Abu-Mostafa N, Abbasi A. Marsupialization of a large dentigerous cyst in the mandible with orthodontic extrusion of three impacted teeth. A case report. J Clin Exp Dent 2017;9:e1162–e1166.
94. Aoki N, Ise K, Inoue A, et al. Multidisciplinary approach for treatment of a dentigerous cyst-marsupialization, orthodontic treatment, and implant placement: A case report. J Med Case Rep 2018;12:305.

95. Maltoni I, Maltoni M, Santucci G, Ramina F, Lombardo L, Siciliani G. Marsupialization of a dentigerous cyst followed by orthodontic traction of two retained teeth: A case report. Int Orthod 2019;17:365–374.
96. Tsironi K, Inglezos E, Vardas E, Mitsea A. Uprighting an impacted permanent mandibular first molar associated with a dentigerous cyst and a missing second mandibular molar-A case report. Dent J (Basel) 2019;7:63.
97. Erdur EA, Ileri Z, Ugurluoglu C, Cakir M, Dolanmaz D. Eruption of an impacted canine in an adenomatid odontogenic tumor treated with combined orthodontic and surgical therapy. Am J Orthod Dentofacial Orthop 2016;149:923–927.
98. Baik WK, Baik HS, Choi SH. Comprehensive orthodontic treatment of a young girl with an odontogenic keratocyst and impacted teeth in the mandible. Korean J Orthod 2020;50:63–71.
99. Francisquini IDA, Medeiros YDL, Campos HN, Marlière DAA, Assis NMSP. Orthosurgical treatment of impacted canines with the presence of bilateral dentigerous cysts: A case report with five-year follow-up. J Maxillofac Oral Surg 2022 (Early Access). doi: https://doi.org/10.1007/s12663-022-01811-5.

Analysis of Differential Translation Profiles of Human Bone Marrow Mesenchymal Stem Cells during Osteogenic Differentiation

Hua LIU[1], Zhi Peng FAN[2,3,4], Qiu Bo YANG[1], Hui Na LIU[2,5]

Objective: *To explore the differential translation profiles and coding products of human jaw bone marrow mesenchymal stem cells (h-JBMMSCs) during osteogenic differentiation.*

Methods: *Ribo-seq was used to examine the differential translated genes (DEGs), open reading frames (ORFs) and genes associated with the osteogenic differentiation phase of h-JBMMSCs. Western blotting (WB) was performed to detect the expression of osteocalcin (OCN) and bone sialoprotein (BSP). Alkaline phosphatase (ALP) activity and alizarin red staining (ARS) were used to detect osteogenic differentiation. A lentivirus containing 5'UTR-ORF-GFPmut was designed to transfect h-JBMMSCs, and fluorescence and green fluorescent protein (GFP) expression were analysed. The SNHG1 peptide was synthesised for osteogenic induction and to detect osteogenic markers.*

Results: *A total of 53,432 ORFs were detected and 199 candidate translation sORFs, including lncRNA SNHG1, were identified after removing the annotated protein-coding genes. In addition, the 5'UTR-ORF-GFPmut showed green fluorescence and expressed GFP. Knockdown of the lncRNA SNHG1 increased the ALP activity of h-JBMMSCs, promoted the expression of OCN and BSP, and enhanced the intensity of ARS and calcium ion content. However, overexpression of lncRNA SNHG1 and the SNHG1 polypeptide inhibited the osteogenic differentiation of h-JBMMSCs.*

Conclusion: *LncRNA SNHG1 inhibited the osteogenic differentiation of h-JBMMSCs. LncRNA SNHG1 can encode a peptide of 19-amino acid and inhibit the osteogenic differentiation of h-JBMMSCs.*

Keywords: *h-JBMMSCs, lncRNA SNHG1, osteogenic differentiation, peptide, ribosome profiling*

Chin J Dent Res 2025;28(1):31–43; doi: 10.3290/j.cjdr.b6097608

1 Beijing Stomatological Hospital, School of Stomatology, Capital Medical University, Beijing, P.R. China.
2 Beijing Key Laboratory of Tooth Regeneration and Function Reconstruction, Beijing Stomatological Hospital, School of Stomatology, Capital Medical University, Beijing, P.R. China.
3 Beijing Laboratory of Oral Health, Capital Medical University, Beijing, P.R. China.
4 Research Unit of Tooth Development and Regeneration, Chinese Academy of Medical Sciences, Beijing, P.R. China.
5 Department of General Dentistry and Integrated Emergency Dental Care, Capital Medical University School of Stomatology, Beijing, P.R. China.

Corresponding authors: Dr Qiu Bo YANG, Beijing Stomatological Hospital, School of Stomatology, Capital Medical University, Beijing 100050, P.R. China. Tel: 86-10-57099114. Email: qiuboyang2003@163.com

Dr Hui Na LIU, Beijing Key Laboratory of Tooth Regeneration and Function Reconstruction, Beijing Stomatological Hospital, School of Stomatology, Capital Medical University, Beijing 100050, P.R. China. Tel: 86-10-57099114. Email: 948581537@qq.com

Bone marrow mesenchymal stem cells (BMMSCs) are generally derived from the jaws, long bones (the femur and tibia) and ilium, and BMMSCs from different bone sites have different characteristics.[1,2] Their multipotency allows them to differentiate into osteoblasts, adipocytes and chondrocytes, which can be used to treat bone defects or cartilage injuries.[3,4] Jaw BMMSCs have stronger odontogenic and osteogenic abilities, and are considered more suitable for maxillofacial stem cell therapy.[5,6] Therefore, JBMMSCs are more suitable for jaw defect reconstruction, periodontal tissue regeneration and dentine regeneration.[7] However, osteopet-

This study was supported by grants from the National Natural Science Foundation of China (82130028), National Key Research and Development Program (2022YFA1104401, 2022YFC2504201) and the National Natural Science Foundation of China (82100970).

rosis is a bone developmental disorder characterised by extremely dense bones and easy fracture. It often causes delayed or failed tooth eruption, root deformity and mandibular osteomyelitis in the maxillofacial region. Thus, the osteogenic differentiation of JBMMSCs has been explored to provide ideas for treating osteopetrosis.

At present, many studies have shown that the multidirectional differentiation of BMMSCs, especially osteogenic differentiation, is regulated by noncoding RNAs (ncRNAs).[8-10] Long ncRNAs (lncRNAs) are more than 200 nucleotides (nt) in length and can regulate osteogenic differentiation by regulating transcription and translation.[8,9] For example, heterogeneous ribonucleoprotein K regulates lncRNA-OG to promote the osteogenic differentiation of BMMSCs.[10] lncRNA-H19 can enhance the osteogenic differentiation of postmenopausal osteoporosis patients by regulating forkhead box C2 (Foxc2).[11] The lncRNA HOTAIR inhibits the osteogenic differentiation of BMMSCs by negatively regulating miR-378g.[12] Apart from being therapeutic targets, a few studies have indicated that lncRNAs have the potential to serve as biomarkers for bone-related diseases. For example, the lncRNA DANCR can be a diagnostic biomarker for postmenopausal osteoporosis, and the lncRNA HOTAIR may be used for the clinical diagnosis of rheumatoid arthritis.[13-15] However, clinical translation based on RNA therapy is impeded by delivery, tolerance and specificity issues.[16] Polypeptide drugs can effectively circumvent these problems, possess strong penetration and low immunogenicity, and are easier to chemically synthesise and modify.

As understanding of lncRNAs has increased, it has been discovered that they can also encode peptides and play a biological role.[17,18] Ribosome profiling sequencing (Ribo-seq) has been used to detect RNA translation levels.[19] Ribo-seq can shield mRNA fragments of 20 to 30 nucleotides in length from nuclease digestion by translating ribosomes and can be used to identify small open reading frames (sORFs) with translation potential.[20] An ORF is defined as a potential translation sequence, starting from the start codon to the end of the stop codon.[21] The length of an sORF differs from that of an ORF, theoretically ranging from 2 to 100 codons.[22] Initially considered noncoding due to its extremely short length, it has been found that the molecular sequence of ncRNA contains an sORF capable of encoding micropeptides with fewer than 100-amino acid (aa).[23-27] Prediction analysis of sORFs includes the prediction of the start codon, the sORF position and the translation potential of ncRNAs. In addition to three-nucleotide (3-nt) periodicity and RPF distribution, the ribosome P site is also used as a discriminant condition.[28,29] During the initial stage of peptide chain synthesis, the ribosome subunit, mRNA and initial aminoacyl-tRNA with a priming function are assembled into the initial complex. Once the initial complex is formed, the P position is occupied by the initial tRNA, which binds to the initial codon. Subsequently, based on the codon sequence on mRNA, various aminoacyl-tRNAs bind to ribosomes in sequence, leading to the gradual extension of the peptide chain is gradually extended from the N-terminus to the C-terminus. Some studies have indicated that these micropeptides can interact with other proteins or RNAs after processing and modification, playing a role in various physiological and pathophysiological processes.[30,31] For example, the 90-amino-acid (aa) polypeptide SPAR, encoded by the lncRNA LINC00961, inhibits mTORC1 activity via lysosomes. This action modulates the regenerative response of skeletal muscle.[31] Additionally, these micropeptides regulate mitochondrial metabolism and embryonic development and influence the onset and progression of cancer. However, research on lncRNAs related to the osteogenic differentiation of JBMMSCs remains limited.

The lncRNA small nucleolar RNA host gene 1 (SNHG1), situated on chromosome 11, consists of 11 exons.[32,33] Some studies have confirmed that SNHG1 significantly influences osteogenic differentiation, osteoclast differentiation and angiogenesis. It regulates osteogenic differentiation by regulating the p38 MAPK signalling pathway,[34] a key trigger of BMSCs.[35] In periodontal ligament stem cells, SNHG1 inhibits osteogenic differentiation through EZH2-mediated methylation of the KLF2 promoter H3K27me3.[36] SNHG1 also promotes osteoclast differentiation of BMMSCs[37] and angiogenesis of endothelial cells.[38,39] However, the regulatory effects of SNHG1 on human JBMMSCs (h-JBMMSCs) require further investigation. The presence of a sORF within SNHG1 and its potential to encode an endogenous peptide are still unclear.

To investigate the translation of h-JBMMSCs during osteogenic differentiation, Ribo-seq of h-JBMMSCs was conducted at 0 and 7 days after osteogenic differentiation. Through the screening of sORFs and differentially translational efficiency genes (DTEGs), the SNHG1 gene was chosen for further study. To explore the role of SNHG1 in the osteogenic differentiation of h-JBMMSCs, the present authors preliminarily verified its coding potential.

Materials and methods

Cells and cell culture

All the experimental procedures were approved by the Ethics Committee of Beijing Stomatological Hospital of Capital Medical University (license no: CMUSH-IRB-KJ-PJ-2023-50). Bone samples extracted from patients after orthognathic surgery were washed with phosphate-buffered saline (PBS) (HyClone, Logan, UT, USA) and cut into small fragments (< 1 mm^3). The fragments were cultured using mesenchymal stem cell medium (MSCM; ScienCell, Carlsbad, CA, USA). Osteogenic differentiation induction by h-JBMMSCs for 0 and 7 days was assessed via Ribo-seq.

Library preparation and sequencing

In sample selection, we established the criteria to include healthy individuals aged 18 to 35 years, excluding those with oral infections (acute or chronic), a family history of genetic disorders, diabetes, hypertension, heart disease or jaw bone diseases. One type of h-JBMMSCs was selected for osteogenic differentiation at 0 and 7 days, with three replicates in each group (n = 3). Translation inhibitors were applied to halt translation. The ribosome-peptide complex underwent treatment with a low concentration of RNase, allowing degradation of RNA fragments not shielded by ribosomes. Then, ribosomes were removed, and the RNA fragments protected by the ribosome, termed ribosome protect frame (RPF), were identified. The raw sequencing data acquired were compressed and stored in fastq format. To avoid affecting the subsequent data analysis, the original data were partitioned and quality controlled to produce clean data for subsequent data analysis. FastQC analysed the quality of the sequencing data. To confirm biological reproducibility among the groups, Pearson correlation analysis was executed on FPKM values.

Triplet periodicity analysis

Three-nucleotide (3-nt) periodicity reflects the distribution pattern of ribosome reading density and serves as an intrinsic characteristic of translation, proceeding three nucleotides at a time. Ribosomes display a pause after every three bases (one codon) during transcript translation. By assigning the ribosome P site to each base position of each codon, distribution counts were determined and the RPF distribution graph was created. Given that ribosomes reside longest at the first base of the codon, the ratio of RPFs at this position typically peaks.[40]

Differential gene expression analysis

Differentially translated genes (DTGs) were evaluated by using DESeq2 R, and the genes with different translations were screened using $P < 0.05$ and $Log_2FC > 2$. Pathway annotation of the identified differentially translated genes was conducted using the KEGG database. Significant pathway terms were determined for differentially translated genes through *P* value calculation via a Fisher test.

Estimation of translational efficiency

Translational efficiency (TE) refers to the ratio of the total RNA molecules of each gene in the sample to the ribosome for translation. The calculation formula was TE = (FPKM in Ribo-seq) / (FPKM in RNA-seq). TE represents RNA utilisation rather than a direct measure of protein output.[29] DESeq2 R was used to analyse the differential TEs, and the DTEGs were screened for $P < 0.05$ and $log_2FC > 2$. The DESeq2 R package was used to calculate the log_2FoldChange, *P* value and padj values of the translation efficiency difference multiple for subsequent analysis, and KEGG analysis was subsequently performed on the DEGs.

Detection of actively translated open reading frames (ORFs)

Open reading frame (ORF) analysis can be used to examine small peptides encoded by ncRNAs. Translated ORFs are identified based on the 3-nt periodicity, ribosome P site and RPF distribution.[28,29] To more accurately identify ORFs with coding potential, RPF readings need to be analysed using various indicators and methods. Annotated protein-coding genes were excluded from the ORF prediction table to isolate the ORF of ncRNA and extract the amino acid sequence. Logistic regression analysis determines the likelihood of finding the start codon.

Lentiviral transduction

After excluding annotated coding genes, we screened the remaining ORFs, prioritising genes showing significant expression differences between h-JBMMSCs on day 0 and day 7 of osteogenic differentiation. Additionally, the ORF's start codon frequency is relatively high, and the predicted peptide chain length exceeds two amino acids. Finally, drawing upon previous re-

search, we selected lncRNA SNHG1 for further study. The cDNA of the human lncRNA SNHG1 and short hairpin RNAs (shRNAs) were inserted into the LV6 lentiviral vector (Genepharma, Suzhou, China) and GV112 lentiviral vector (Genechem, Shanghai, China) respectively. The culture medium was changed 12 hours after lentivirus infection, and puromycin (2 μg/ml) was used for screening 48 hours after infection. The target sequences were as follows: lncRNA SNHG1 shRNA (sh-SNHG1), 5′-GGTTTCAAGGCCATAGCTTTA-3′; and control shRNA (sh-Control), 5′-TTCTCCGAACGTGTCACGT-3′. To generate GFP fusion protein constructs with the lncRNA SNHG1 5' untranslated region (UTR)-ORF (5'UTR-ORF-GFPmut), the 5'UTR-ORF sequence was cloned and inserted into the GV348 vector, in which the GFP initiation codon (ATG) was mutated to ATT. H-JBMMSCs were transfected with 5'UTR-ORF-GFPmut for 24 hours and observed under a microscope.

Peptide synthesis

The amino acid sequence that could be translated was obtained from the gene sequence predicted by the ORF, and the peptide was synthesised (Jietai, Nanjing, China). During the osteogenic induction process, peptides were added simultaneously at a concentration of 10 μg/ml when the solution was changed. Osteogenic indexes were assessed after 5 days, 7 days and 2 weeks of induction.

Osteogenic differentiation

H-JBMMSCs are seeded in 6-well plates and cultured with osteogenic-induced conditioned medium (mesenchymal stem cell medium supplemented with 10 nM dexamethasone, 1.8 mM KH_2PO_4, 2 mM β-glycerophosphate and 100 μM/ml ascorbic acid). Cells were treated with 10 μg/ml control peptide or SNHG1 peptide once every 3 days during the culture process. After 5 days, an alkaline phosphatase (ALP) activity kit (Sigma-Aldrich, St Louis, MO, USA) was used to detect ALP activity. The protein concentration was used to standardise the OD value. After 7 days, western blot (WB) analysis was performed to measure the expression of target proteins. After 14 days, the cells were fixed with 70% alcohol, washed in PBS twice, and treated with Alizarin Red (Sigma-Aldrich). After drying the plate, 10% cetylpyridinium chloride was added for 30 minutes to detect the calcium ion content. The absorbance at 562 nm was measured and compared with the standard calcium curve to determine the concentration.

RNA isolation and qPCR

Total RNA was extracted from the cells using the TRIzol reagent (Invitrogen). One-microgram aliquots of RNA were reverse transcribed into cDNA (Invitrogen, Waltham, MA, USA). A QuantiTect SYBR Green PCR kit (Qiagen, Hilden, Germany) and an Archimed-X6 real-time PCR detection system (Rocgene, Beijing, China) were used for relative quantitative PCR. The relative expression levels of SNHG1 were normalised to those of GAPDH. The primers used in this study were as follows: human GAPDH, (forward) 5′- CGGACCAATACGACCAAATCCG -3′ and (reverse) 5′- AGCCACATCGCTCAGACACC -3′; and human SNHG1, (forward) 5′- ACAGCAGTTGAGGGTTTGCT -3′ and (reverse) 5′- GGGCCTGGATCATGTAAGAA -3′.

Western blot analysis

RIPA buffer containing protease and phosphatase inhibitors was used to extract proteins. Protein samples were blocked for 1 hour after gel electrophoresis and membrane transfer. The first antibody was incubated overnight in the refrigerator at 4°, and the second was incubated at room temperature for 1 hour. The samples were observed with western ECL substrates (Bio-Rad, Hercules, CA, USA). The primary antibodies used were anti-OCN (cat no. A20800, ABclonal), anti-BSP (cat no. bs-23258, Bioss), anti-GFP (cat no. 66002-1-lg, Proteintech), and anti-glyceraldehyde 3-phosphate dehydrogenase (GAPDH; cat no. G8795, Sigma-Aldrich).

Statistical analysis

Statistically significant differences ($P < 0.05$) were determined using a Student *t* test. GraphPad Prism 8 software (GraphPad, La Jolla, CA, USA) was utilised for all statistical analyses.

Results

Differential gene analysis

Ribo-seq was performed on h-JBMMSCs induced by osteogenic differentiation for 0 and 7 days, with 3 replicates in each group. The Pearson correlation coefficients (r) between the two replicate samples of each group were greater than 0.99, indicating high reproducibility of our experiments (Fig 1a and b). For any codon, frame 0/1/2 represents three nucleotides from 5' to 3', respectively. We found that the length of RPFs was approximately 29

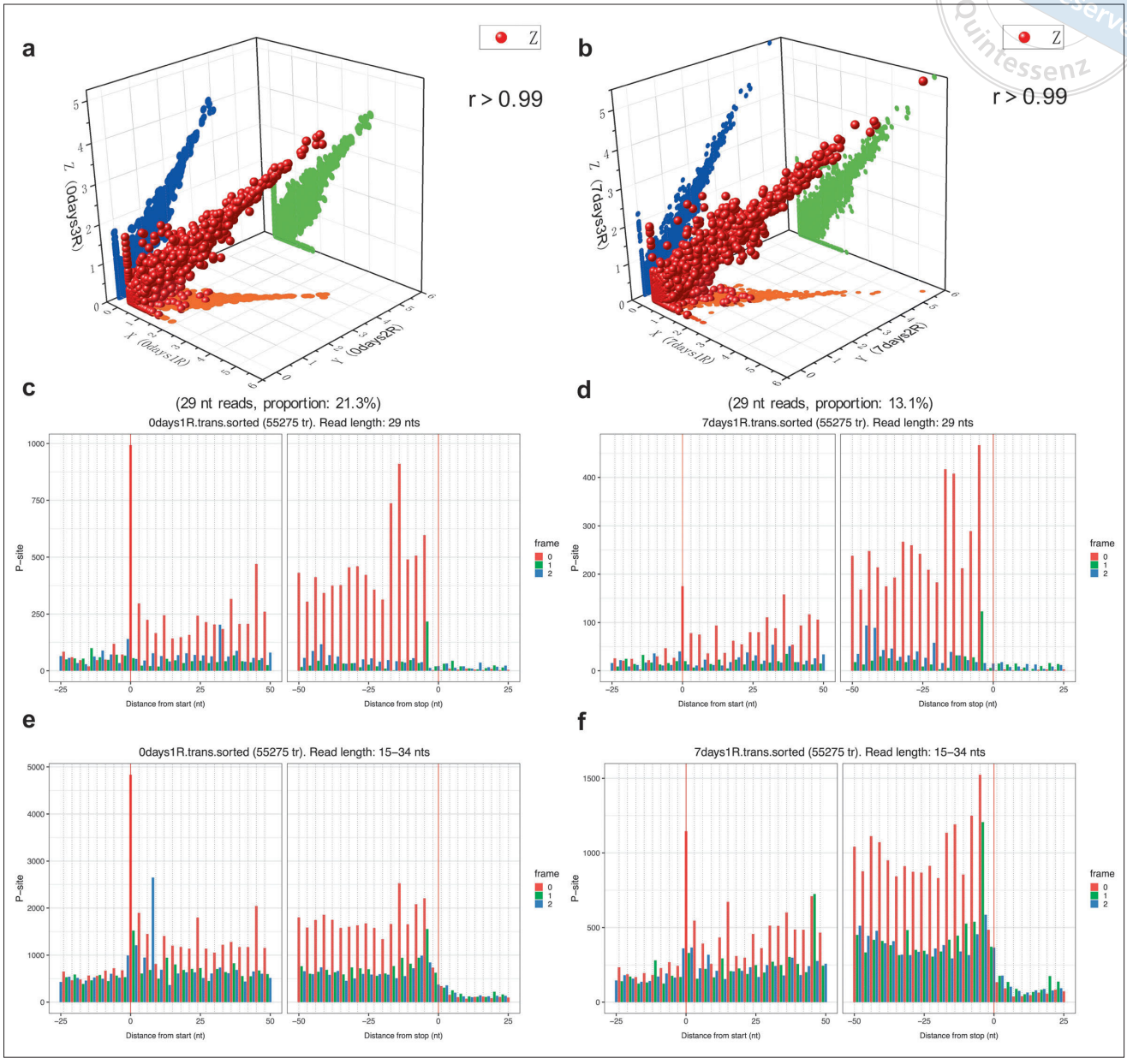

Fig 1a to f Ribo-seq data characteristics. 3D scatter plot of biological repeatability in the 0- and 7-day groups **(a and b)**. The Pearson correlation coefficients **(r)** between the two replicate samples of each group were greater than 0.99. The 29-nt **(c and d)** and 15-34-nt RPF distributions around the ribosomal P site **(e and f)**. Frame 0/1/2 represents three nucleotides of 5' to 3', respectively.

to 30 nt. When we used 29 nt readings to scan the start codon and stop codon, we observed a clear 3 nt periodicity from the distribution of the first base at the 5' end of the RPF (Fig 1c and d and Fig S1a [provided on request]). Trinucleotide periodicity was also observed when we scanned the start codon and stop codon with readings of 15-34 nt (Fig 1e and f and Fig S1e to h [provided on request]). These results demonstrate a characteristic feature of reliable translation-specific data.

Analysis of ribosome sequencing data revealed 1,548 differentially expressed translation genes compared with those at 0 days of osteogenic treatment, including 919 upregulated genes and 629 downregulated genes (Fig S2a, provided on request). KEGG analysis of the differential translation genes (DTGs) showed that they were enriched in p53, ECM-receptor interaction, cell cycle and other pathways (Fig 2a). TE can reflect the RNA utilisation rate, and gene TE was further analysed

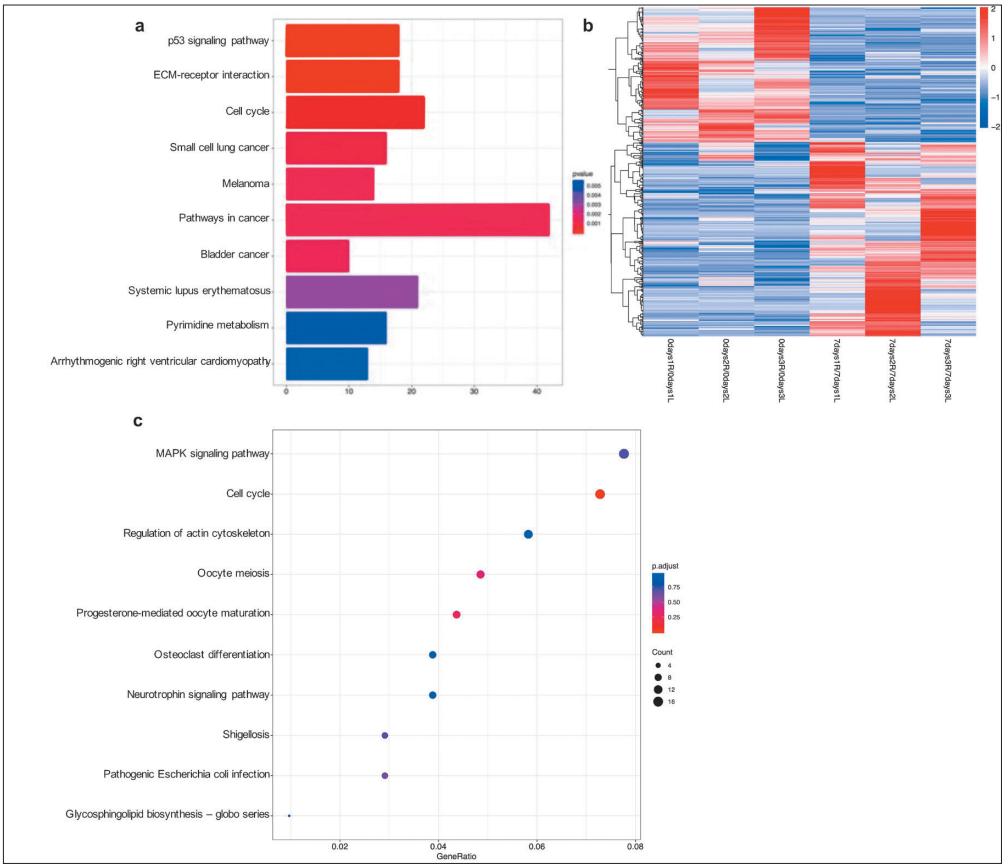

Fig 2a to c Differential translation gene analysis and differential TE gene analysis. KEGG analysis of differentially translated genes **(a)**. Cluster thermogram of genes with different translation efficiency **(b)**. KEGG analysis of differentially TE genes **(c)**.

by calculating the log2TE cumulative scores at 0 days and 7 days. The overall expression at 7 days was found to be greater than that at 0 days (Fig S2b, provided on request). Cluster analysis of the thermogram also revealed that the overall consistency of the upregulated genes in the group was significantly greater than that of the downregulated genes (Fig 2b). A total of 830 DTEGs were identified, with 488 genes being upregulated and 342 genes downregulated (Fig S2c, provided on request). KEGG analysis revealed enrichment of DTEGs in the MAPK pathway (Fig 2c).

In addition, most of the DTEGs (83.7%) were located on annotated protein-coding genes, but 16.4% of them were located in antisense RNA, long interspersed ncRNA (lincRNA), processing transcription and other noncoding genes (Fig 3a). Genes can be classified according to their biotype, an indicator of biological significance. In addition to protein-coding genes, they also include processed transcripts and pseudogenes. Processed transcripts encompass lncRNAs, ncRNAs and unclassified processed transcripts. Antisense RNAs and lincRNAs are types of lncRNAs. These results suggest that lncRNAs may have coding potential as ncRNAs.

Prediction and screening of ORFs

In addition to the 3-nt periodicity and RPF distribution, ribosome P sites are also used as discriminant conditions in the prediction and analysis of ORFs (Fig 3b). The frequency analysis of different codons at the ribosome P site showed that AGC, CUA, CUC, CUG and other codons tended to increase (Fig 3c). Moreover, a total of 53,432 ORFs were obtained, and 199 candidate translation ORFs were detected by removing the annotated protein-coding genes. Additionally, the cumulative analysis of the number of peptides of different lengths and the frequency of initial codon usage revealed 162 peptides of 0 to 10 aa, 27 peptides of 11 to 20 aa, 8 peptides of 21 to 30 aa and 2 peptides of 31 to 40 aa. The frequency of TTG and CTG usage was significantly greater than that of other codons (Fig 3d). The predicted lncRNA SNHG1 has three ORFs, two of which encode a 2-aa peptide and another initiation codon, CTG, and a 19-aa peptide (Fig S2d, provided on request). We consider that the lncRNA SNHG1 has potential translational value in h-JBMMSCs.

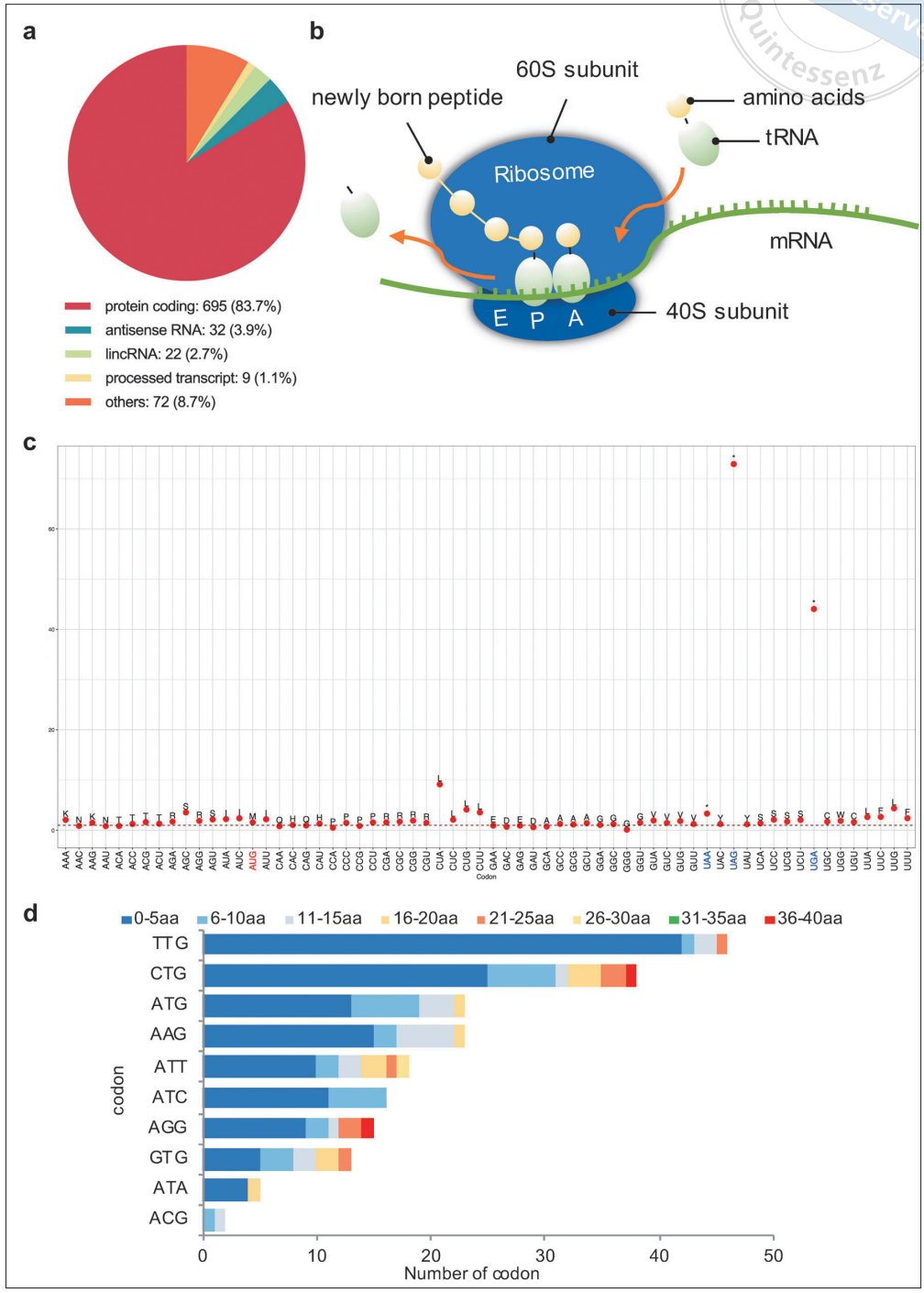

Fig 3a to d Analysis of the coding potential of noncoding RNAs. Proportion of genes with different TEs **(a)**. Schematic diagram of ribosome translation **(b)**. Frequency of differential codon usage at the ribosome P site. The abscissa represents 64 codons, the ordinate represents codon frequency, the red dots represent amino acids, and the uppercase letter corresponds to amino acid abbreviations. A frequency greater than 1 indicates upregulated amino acids, and a frequency less than 1 indicates downregulated amino acids. In the horizontal differential codon, red represents the classical start codon, blue represents the stop codon and black represents other codons **(c)**. The ORF predicts the initial codon usage frequency of noncoding RNA ORFs and the cumulative distribution of peptides of different lengths after removing the protein-coding gene **(d)**.

LncRNA SNHG1 inhibited the osteogenic differentiation of h-JBMMSCs

The mRNA expression level of SNHG1 was downregulated in h-JBMMSCs 7 days after osteogenic differentiation (Fig 4a). Then, we knocked down SNHG1 expression by infecting h-JBMMSCs with retrovirus (Fig 4b). After osteogenic induction for 5 days, compared with that in the sh-control group, ALP activity in the sh-SNHG1 group increased significantly (Fig 4c). In addition, after 7 days of induction, the expression levels of the OCN and BSP proteins in the sh-SNHG1 group were upregulated (Fig 4f and g). Two weeks later, the mediation of ARS in the sh-SNHG1 group was enhanced, and

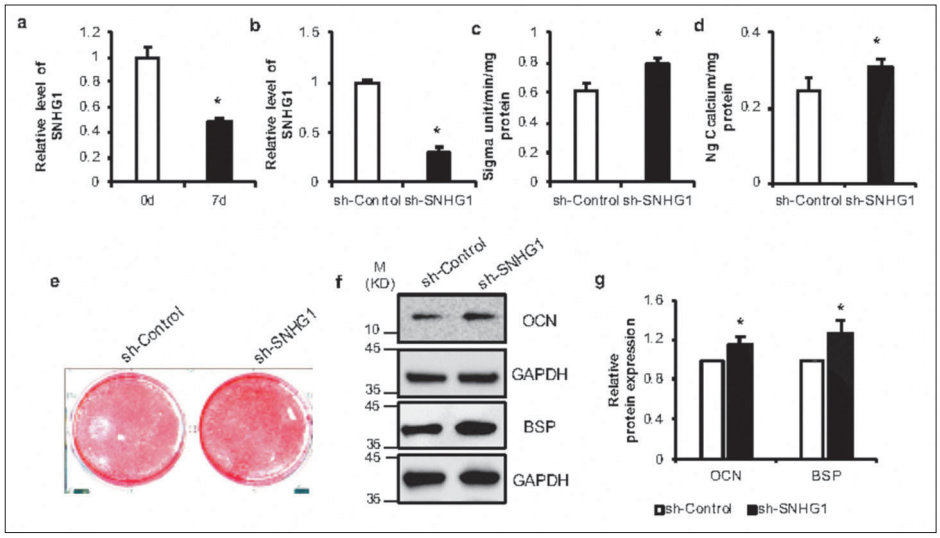

Fig 4a to g LncRNA SNHG1 knockdown enhanced osteogenic differentiation in h-JBMMSCs. The mRNA expression level of SNHG1 at 7 days after osteogenic differentiation, with GAPDH serving as a control **(a)**. SNHG1 was knocked down in h-JBMMSCs, and cells transfected with the empty vector served as controls **(b)**. ALP activity on day 5 **(c)**. Alizarin red staining **(d)** and calcium ion quantification on day 14 **(e)**. The protein levels of OCN, BSP and GAPDH were measured via Western blot assay **(f and g)**. Statistical analysis was performed using a Student *t* test. In the bar graphs, data are presented as mean ± SD. $^{*}P < 0.05$.

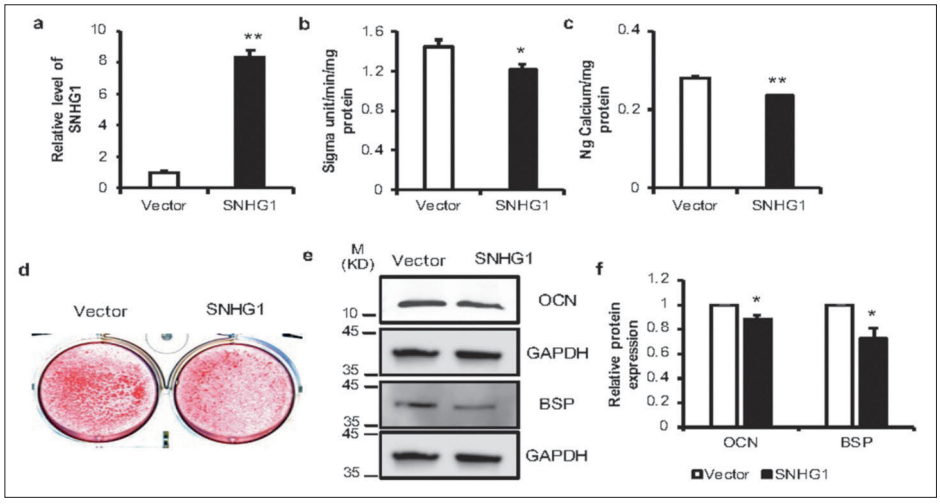

Fig 5a to f LncRNA SNHG1 overexpression inhibited osteogenic differentiation in h-JBMMSCs. SNHG1 was overexpressed in h-JBMMSCs, and cells transfected with the empty vector served as controls **(a)**. ALP activity on day 5 **(b)**. Calcium ion quantitative analysis **(c)** and Alizarin red staining on day 14 **(d)**. The protein levels of OCN, BSP and GAPDH were measured via Western blot assay **(e and f)**. Statistical analysis was performed using a Student *t* test. In the bar graphs, data are presented as mean ± SD. $^{*}P < 0.05$. $^{**}P < 0.01$.

the calcium ion concentration was increased (Fig 4d and e). These results indicate that knocking down SNHG1 in h-JBMMSCs promotes osteogenic differentiation.

Moreover, SNHG1 was overexpressed, and its expression of SNHG1 was increased (Fig 5a). After 5 days of osteogenic induction, ALP activity in the SNHG1 group decreased significantly compared to the Vector group (Fig 5b). After 7 days, the WB results showed that the expression of OCN and BSP was downregulated (Fig 5e and f). After 2 weeks, in the SNHG1 group, there was a decrease in the number of ARS and the calcium ion concentration (Fig 5c and d). These results indicate that the overexpression of SNHG1 in h-JBMMSCs inhibits osteogenic differentiation.

lncRNA SNHG1 encoded a small peptide and SNHG1-peptide inhibits the osteogenic differentiation of h-JBMMSCs

To investigate the activity of the start codon of the SNHG1 ORF, we created a 5'UTR-ORF-GFPmut construct (Fig 6a). Green fluorescence was observed under a microscope following the transfection of h-JBMMSCs (Fig 6b). WB results indicated the presence of the GFP fusion protein post-transfection of 5'UTR-ORF-GFPmut (Fig 6c). Moreover, h-JBMMSCs transfected with 5'UTR-ORF-GFPmut showed inhibited osteogenic differentiation (Fig 6d to h). Therefore, 57-nt sORF of the lncRNA SNHG1 might encode a 19-aa peptide.

To verify the function of the SNHG1 peptide, we synthesised a control peptide and an SNHG1-peptide.

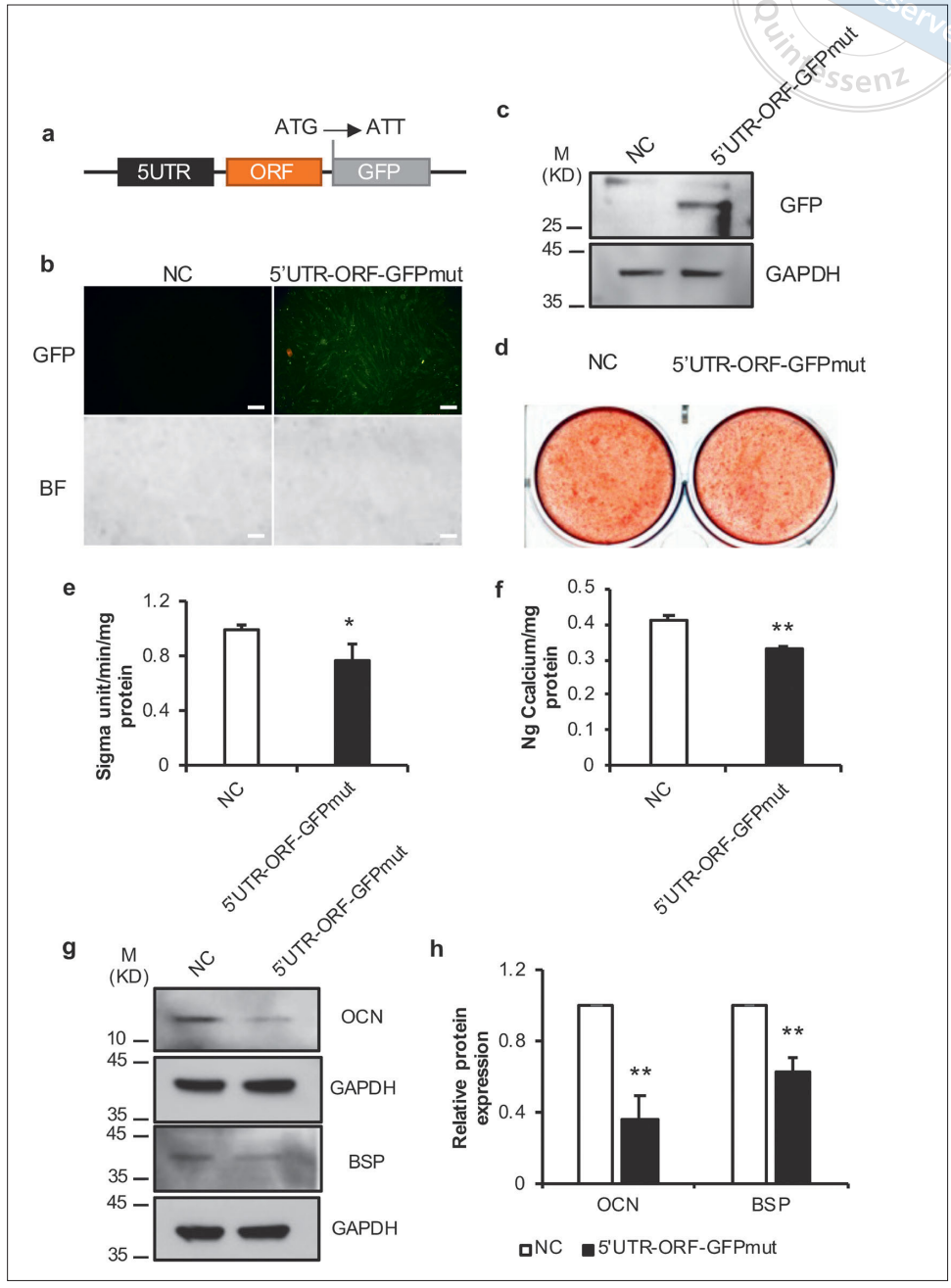

Fig 6a to h Transfection of the lncRNA SNHG1-encoded peptide and h-JBMMSCs with 5'UTR-ORF-GFPmut inhibited osteogenic differentiation. The 5'UTR-ORF-GFPmut virus was designed, and the sequence of the GFP-ORF start codon (ATG) was mutated to ATT **(a)**. GFP was expressed by h-JBMMSCs transfected with 5'UTR-ORF-GFPmut under a fluorescence microscope **(b)**. Western blot analysis showed that GFP was expressed in h-JBMMSCs transfected with 5'UTR-ORF-GFPmut **(c)**. ALP activity on day 5 **(d)**. Alizarin red staining **(e)** and calcium ion quantitative analysis on day 14 **(f)**. Protein levels of OCN, BSP and GAPDH were measured via Western blot assay **(g and h)**. Statistical analysis was performed using a Student *t* test. In the bar graphs, data are presented as mean ± SD. $^{*}P < 0.05$. $^{**}P < 0.01$.

Compared with the control peptide, SNHG1-peptide decreased ALP activity after 5 days of osteogenic induction (Fig 7a). At 7 days, SNHG1-peptide decreased the protein expression levels of OCN and BSP (Fig 7d and e). By 2 weeks, the ARS staining became lighter, and the level of calcium ions decreased (Fig 7b and c). These results indicate that the SNHG1-peptide inhibits osteogenic differentiation in h-JBMMSCs.

Discussion

Trinucleotide periodicity often indicates the coverage of ribosome fragments mapped to the subcodon position and tends to the first position.[40] It is commonly used to assess the quality of Ribo-seq data. Our results demonstrated good biological repeatability and a 3-nt periodicity in the group, which ensures the reliability of subse-

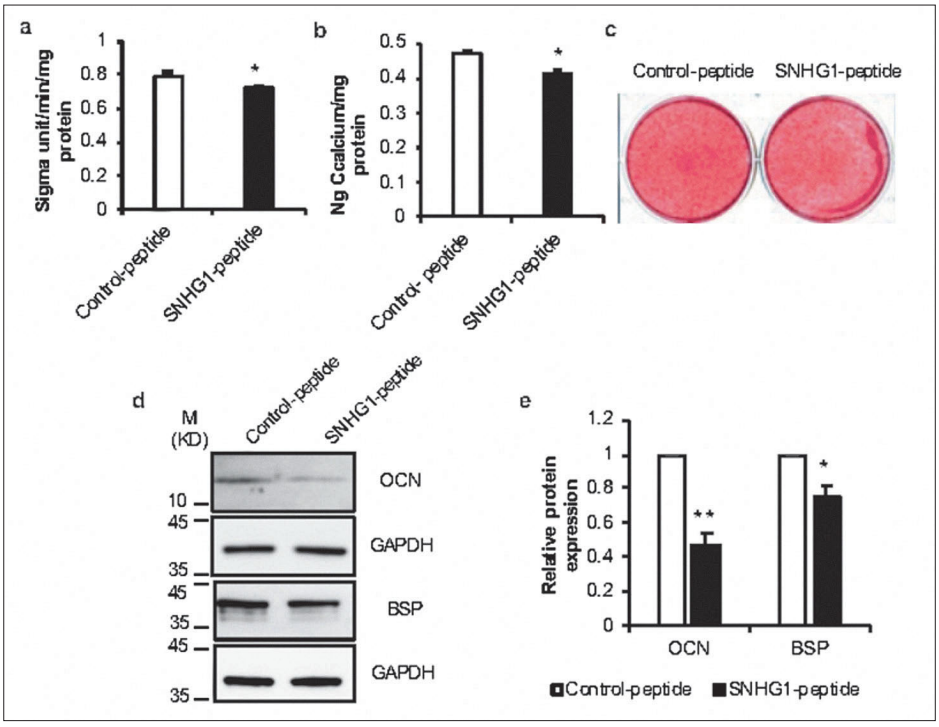

Fig 7a to e SNHG1-peptide inhibited the osteogenic differentiation of h-JBMMSCs. ALP activity on day 5 **(a)**. Calcium ion quantitative analysis **(b)** and Alizarin red staining on day 14 **(c)**. The protein levels of OCN, BSP and GAPDH were measured via Western blot assay **(d and e)**. Statistical analysis was performed using a Student *t* test. In the bar graphs, data are presented as mean ± SD. **P* < 0.05. ***P* < 0.01.

quent data analysis. The ribosome plays a crucial role in protein translation, thus impacting the growth, development and differentiation of cells. Knocking down RIOK3 significantly impairs ribosome function, influences the translation of intracellular proteins and diminishes the osteogenic differentiation of mouse BMMSCs (mBMMSCs).[41] In this study, compared to h-JBMMSCs at 0 days and 7 days post-osteogenic differentiation, there were more upregulated than downregulated genes in both the DTGs and DTEGs. The increase in the ribosome binding rate during osteogenic differentiation suggests that gene translation may have a regulatory function. Further bioinformatics analysis revealed that KEGG pathway analysis identified several pathways, such as the MAPK, p53 and ECM-receptor interaction pathways, were associated with osteogenic differentiation. The MAPK pathway is closely linked to osteogenic differentiation,[42,43] and lncRNA differentiation antagonising nonprotein coding RNA (DANCR) inhibits osteogenic differentiation of BMSCs.[44] The lncRNA SNHG1 negatively regulates the p38 MAPK signalling pathway, thus inhibiting the osteogenic differentiation of BMSCs.[34] The genes enriched in the MAPK signalling pathway include RAC1, MAPK8IP2, MAPK13, RPS6KA1, NFKB2 and FGF7, suggesting that these genes may act as regulatory factors in osteogenic differentiation. For instance, RAC1 can contribute to atherosclerosis,[45] but in MC3T3-E1 cells, OCN and runt-related transcription factor 2 (RUNX2) are upregulated by enhancing the expression of RAC1.[46]

We detected 53,432 ORFs, 199 of which were unannotated protein-coding genes according to ORF prediction. These 199 ORFs were predicted to encode micropeptides less than 40-aa in length. However, TE cannot distinguish between translating ribosomes and non-translating ribosomes based on the number of RPFs associated with transcripts.[29] To further highlight the active translation characteristics of RPFs, a predicted ribosome P site was proposed.[47] Through the prediction of ORFs and the analysis of ribosome P sites, we found that UUG and CUG were used more frequently as initial codons than was AUG. Among them, lncRNA SNHG1 was 57 nt long and its initial codon was CUG. Eukaryotic translation starts from the first AUG encountered by ribosomes on mRNA. However, the unexpected ribosome occupancy observed in the analysis of the initiation site indicates a significant number of non-AUG initiation events.[48] While the usage of start codons depends on genes and research, it has been demonstrated that CUG and UUG are utilised at a frequency of approximately 1% to 10% compared to AUG under optimal conditions, while AAG and AGG are largely unrecognised.[49,50] In mammals, when the POLG gene is encoded under optimal conditions, the initiation efficiency of the CUG codon is comparable to that of the AUG codon (~60% to 70%).[51] By integrating ORF

prediction, KEGG analysis and initial codon analysis, we selected SNHG1 for further investigation.

The expression of the lncRNA SNHG1 decreased after 7 days of osteogenic differentiation induced by h-JBMMSCs. Then, we knocked down and overexpressed SNHG1 in h-JBMMSCs for osteogenic induction. The activity of ALP in vitro is commonly used to detect the initial differentiation of BMSCs into osteoblasts, and is also a crucial factor in BMSC calcification.[52] The results of ALP activity, WB, ARS and calcium ion quantification all indicated that the lncRNA SNHG1 inhibited osteogenic differentiation. This finding is similar to previous research results showing that the lncRNA SNHG1 inhibits osteogenic differentiation via the miR-101/DKK1 axis.[53] To verify whether the lncRNA SNHG1 is translated, we designed lentivirus to add a GFP tag after the ORF of SNHG1 and mutated the start codon of GFP at the same time. However, our results showed that green fluorescence was observed under the microscope, and the WB results indicated that GFP was expressed in the cells. These results indicate that the lncRNA SNHG1 encodes a small peptide. Using the ORF sequence, we derived the corresponding amino acid sequence to synthesise small peptides in vitro and utilised them in the process of osteogenic differentiation induction. Compared to the control peptide, the SNHG1-peptide significantly reduced ALP activity and the expression of OCN and BSP. At the same time, the amount of ARS decreased, and the content of calcium ions decreased. These outcomes imply that the encoded products of lncRNAs may have similar function as lncRNAs.

Combining the results of the biological analysis and the SNHG1 experiment, we found that the lncRNA SNHG1 is a gene with upregulated TEs, but the SNHG1 mRNA level decreased after 7 days of osteogenic differentiation of h-JBMMSCs. Some studies have shown that genes are not completely consistent at the transcriptional and the translational levels, and the lower the transcription level, the greater the TE.[54,55] On the other hand, when h-JBMMSCs were transfected with 5'UTR-ORF-GFPmut or SNHG1-peptide acted on h-JBMMSCs, the osteogenic differentiation was inhibited. Combined with the upregulation of the TE of SNHG1, we speculated that SNHG1 expression would increase at the translational level but decrease at the protein level on the seventh day of osteogenic differentiation. For example, during the activation of Drosophila eggs, there is a poor correlation betwee changes in protein levels, and only 25% of the proteins encoded by translation upregulated genes are upregulated, and most of them are unchanged or downregulated.[56] It is speculated that the acceleration of translation is balanced by the degradation of proteins or that newly synthesised proteins account for only a small portion of the accumulated proteins, so the upregulation of translation expression of these proteins can hardly be detected.

These results also raise several questions. For example, 16.4% of genes with differential translation efficiency are noncoding genes, but only 199 noncoding genes contain sORFs. Thus, one question is: what is the role of these genes that may not be translated in binding to ribosomes? At the same time, there are still many limitations in this study. The existence of the endogenous SNHG1 peptide in h-JBMMSCs and its mechanism of inhibiting osteogenic differentiation need further study.

Conclusion

By analysing Ribo-seq data, it was found that the osteogenic differentiation of h-JBMMSCs may be regulated by translation. One hundred and ninety-nine candidate sORFs of ncRNAs were identified, and UUG and CUG were the main initiation codons, which provided evidence for non-AUG initiation. The lncRNA SNHG1, which encodes a small peptide of 19-aa, was shown to inhibit the osteogenic differentiation of h-JBMMSCs. This peptide inhibits the osteogenic differentiation of h-JBMMSCs and may have a potential role in the treatment of osteopetrosis.

Conflicts of interest

The authors declare no conflicts of interest related to this study.

Author contribution

Dr Hua LIU performed the experiments and was a major contributor to the writing of manuscript; Drs Zhi Peng FAN, Hui Na LIU and Qiu Bo YANG conceived and designed the study. All the authors have read and approved the final manuscript.

(Received Apr 09, 2024; accepted Aug 13, 2024)

References

1. Ullah I, Subbarao RB, Rho GJ. Human mesenchymal stem cells - Current trends and future prospective. Biosci Rep 2015;35:e00191.
2. Lloyd B, Tee BC, Headley C, Emam H, Mallery S, Sun Z. Similarities and differences between porcine mandibular and limb bone marrow mesenchymal stem cells. Arch Oral Biol 2017;77:1–11.
3. Zhang W, Dong ZW, Li DK, et al. Cathepsin K deficiency promotes alveolar bone regeneration by promoting jaw bone marrow mesenchymal stem cells proliferation and differentiation via glycolysis pathway. Cell Prolif 2021;54:e13058.
4. Fu X, Liu G, Halim A, Ju Y, Luo Q, Song AG. Mesenchymal stem cell migration and tissue repair. Cells 2019;8:784.
5. Zong C, Zhao L, Huang C, Chen Y, Tian L. Isolation and culture of bone marrow mesenchymal stem cells from the human mandible. J Vis Exp 2022;13:(182).
6. Li C, Wang FF, Zhang R, Qiao P, Liu H. Comparison of proliferation and osteogenic differentiation potential of rat mandibular and femoral bone marrow mesenchymal stem cells in vitro. Stem Cells Dev 2020;29:728–736.
7. Luo S, Pei F, Zhang W, et al. Bone marrow mesenchymal stem cells combine with treated dentin matrix to build biological root. Sci Rep 2017;12:44635.
8. Song W, Xie JH, Li JY, Bao C, Xiao Y. The emerging roles of long noncoding RNAs in bone homeostasis and their potential application in bone-related diseases. DNA Cell Biol 2020;39: 926–937.
9. Patil S, Dang K, Zhao X, Gao Y, Qian A. Role of LncRNAs and CircRNAs in bone metabolism and osteoporosis. Front Genet 2020;13:584118.
10. Tang S, Xie ZY, Wang P, et al. LncRNA-OG promotes the osteogenic differentiation of bone marrow-derived mesenchymal stem cells under the regulation of hnRNPK. Stem Cells 2019;37:270–283.
11. Zhou P, Li Y, Di RL, et al. H19 and Foxc2 synergistically promotes osteogenic differentiation of BMSCs via Wnt-β-catenin pathway. J Cell Physiol 2019;234:13799–13806.
12. Wang W, Li T, Feng S. Knockdown of long non-coding RNA HOTAIR promotes bone marrow mesenchymal stem cell differentiation by sponging microRNA miR-378g that inhibits nicotinamide N-methyltransferase. Bioengineered 2021;12:12482–12497.
13. Tong X, Gu PC, Xu SZ, Lin XJ. Long non-coding RNA-DANCR in human circulating monocytes: A potential biomarker associated with postmenopausal osteoporosis. Biosci Biotechnol Biochem 2015;79:732–737.
14. Gregson CL, Armstrong DJ, Bowden J, et al. UK clinical guideline for the prevention and treatment of osteoporosis. Arch Osteoporos 2022;17:58 [erratum 2022;17:80].
15. Song J, Kim D, Han J, Kim Y, Lee M, Jin EJ. PBMC and exosome-derived Hotair is a critical regulator and potent marker for rheumatoid arthritis. Clin Exp Med 2015;15:121–126.
16. Winkle M, EI-Daly SM, Fabbri M, Calin GA. Noncoding RNA therapeutics - Challenges and potential solutions. Nat Rev Drug Discov 2021;20:629–651.
17. Huang JZ, Chen M, Chen D, et al. A peptide encoded by a putative lncRNA HOXB-AS3 suppresses colon cancer growth. Mol Cell 2017;68:171–184.e6.
18. Zhu S, Wang JZ, Chen D, et al. An oncopeptide regulates m6A recognition by the m6A reader IGF2BP1 and tumorigenesis. Nat Commun 2020;11:1685.
19. Makarewich CA, Olson EN. Mining for micropeptides. Trends Cell Biol 2017;27:685–696.
20. Ingolia NT, Hussmann JA, Weissman JS. Ribosome profiling: Global views of translation. Cold Spring Harb Perspect Biol 2019;11:a032698.
21. Sieber P, Platzer M, Schuster S. The definition of open reading frame revisited. Trends Genet 2018;34:167–170.
22. Malekos E, Carpenter S. Short open reading frame genes in innate immunity: From discovery to characterization. Trends Immunol 2022;43:741–756.
23. Chen Y, Long WL, Yang LQ, et al. Functional peptides encoded by long non-coding RNAs in gastrointestinal cancer. Front Oncol 2021;23:777374.
24. Plaza S, Menschaert G, Payre F. In search of lost small peptides. Annu Rev Cell Dev Biol 2017;33:391–416.
25. Xing J, Liu H, Jiang W, Wang L. LncRNA-encoded peptide: Functions and predicting methods. Front Oncol 2020;10:622294.
26. Orr MW, Mao YH, Storz G, Qian SB. Alternative ORFs and small ORFs: Shedding light on the dark proteome. Nucleic Acids Res 2020;48:1029–1042.
27. Sandmann CL, Schulz J, Ruiz-Orera J, et al. Evolutionary origins and interactomes of human, young microproteins and small peptides translated from short open reading frames. Mol Cell 2023;83:994-1011.e18.
28. Calviello L, Mukherjee N, Wyler E, et al. Detecting actively translated open reading frames in ribosome profiling data. Nat Methods 2016;13:165–170.
29. Choi SW, Kim HW, Nam JW. The small peptide world in long noncoding RNAs. Brief Bioinform 2019;20:1853–1864.
30. Batista PJ, Chang HY. Long noncoding RNAs: Cellular address codes in development and disease. Cell 2013;152:1298–1307.
31. Matsumoto A, Pasut A, Mastumoto M, et al. mTORC1 and muscle regeneration are regulated by the LINC00961-encoded SPAR polypeptide. Nature 2017;541:228–232.
32. Li B, Li A, You Z, Xu J, Zhu S. Epigenetic silencing of CDKN1A and CDKN2B by SNHG1 promotes the cell cycle, migration and epithelial-mesenchymal transition progression of hepatocellular carcinoma. Cell Death Dis 2020;11:823.
33. Tan X, Chen WB, Lv DJ, et al. LncRNA SNHG1 and RNA binding protein hnRNPL form a complex and coregulate CDH1 to boost the growth and metastasis of prostate cancer. Cell Death Dis 2021;12:138 [erratum 2024;15:213].
34. Jiang YP, Wu W, Jiao G, Chen Y, Liu H. LncRNA SNHG1 modulates p38 MAPK pathway through Nedd4 and thus inhibits osteogenic differentiation of bone marrow mesenchymal stem cells. Life Sci 2019;228:208–214.
35. Ba P, Duan X, Fu G, Lv S, Yang P, Sun Q. Differential effects of p38 and Erk1/2 on the chondrogenic and osteogenic differentiation of dental pulp stem cells. Mol Med Rep 2017;16:63–68.
36. Li Z, Guo X, Wu S. Epigenetic silencing of KLF2 by long noncoding RNA SNHG1 inhibits periodontal ligament stem cell osteogenesis differentiation. Stem Cell Res Ther 2020;11:435.
37. Yu X, Rong PZ, Song MS, et al. lncRNA SNHG1 induced by SP1 regulates bone remodeling and angiogenesis via sponging miR-181c-5p and modulating SFRP1/Wnt signaling pathway. Mol Med 2021;27:141.
38. Mi S, Du JY, Liu J, et al. FtMt promotes glioma tumorigenesis and angiogenesis via lncRNA SNHG1/miR-9-5p axis. Cell Signal 2020;75:109749.
39. Wang Z, Wang RH, Wang K, Liu X. Upregulated long noncoding RNA Snhg1 promotes the angiogenesis of brain microvascular endothelial cells after oxygen-glucose deprivation treatment by targeting miR-199a. Can J Physiol Pharmacol 2018;96:909–915.
40. Guo H, Ingolia NT, Weissman JS, Bartel DP. Mammalian microRNAs predominantly act to decrease target mRNA levels. Nature 2010;466:835–840.

41. Zong HX, Liu YQ, Wang XL, et al. RIOK3 potentially regulates osteogenesis-related pathways in ankylosing spondylitis and the differentiation of bone marrow mesenchymal stem cells. Genomics 2023;115:110730.
42. Zhang Y, Gu XF, Li D, Cai L, Xu Q. METTL3 regulates osteoblast differentiation and inflammatory response via Smad signaling and MAPK signaling. Int J Mol Sci 2019;21:199.
43. Li J, Du H, Ji X, et al. ETV2 promotes osteogenic differentiation of human dental pulp stem cells through the ERK/MAPK and PI3K-Akt signaling pathways. Stem Cell Res Ther 2022;13:495.
44. Zhang J, Tao Z, Wang Y. Long non-coding RNA DANCR regulates the proliferation and osteogenic differentiation of human bone-derived marrow mesenchymal stem cells via the p38 MAPK pathway. Int J Mol Med 2018;41:213–219.
45. Healy A, Berus JM, Christensen JL, et al. Statins disrupt macrophage Rac1 regulation leading to increased atherosclerotic plaque calcification. Arterioscler Thromb Vasc Biol 2020;40:714–732.
46. Li X, Ji JB, Wei W, Liu L. MiR-25 promotes proliferation, differentiation and migration of osteoblasts by up-regulating Rac1 expression. Biomed Pharmacother 2018;99:622–628.
47. Ingolia NT. Ribosome footprint profiling of translation throughout the genome. Cell 2016;165:22–33.
48. Fedorova AD, Kiniry SJ, Andreev DE, Mudge JM, Baranov PV. Thousands of human non-AUG extended proteoforms lack evidence of evolutionary selection among mammals. Nat Commun 2022;13:7910.
49. Peabody DS. Translation initiation at non-AUG triplets in mammalian cells. J Biol Chem 1989;264:5031–5035.
50. Kearse MG, Wilusz JE. Non-AUG translation: A new start for protein synthesis in eukaryotes. Genes Dev 2017;31:1717–1731.
51. Loughran G, Zhdanov AV, Mikhaylova MS, et al. Unusually efficient CUG initiation of an overlapping reading frame in POLG mRNA yields novel protein POLGARF. Proc Natl Acad Sci U S A 2020;117:24936–24946.
52. Chen X, Yang L, Ge D, et al. Long non-coding RNA XIST promotes osteoporosis through inhibiting bone marrow mesenchymal stem cell differentiation. Exp Ther Med 2019;17:803–811.
53. Xiang J, Fu HQ, Xu Z, Fan WJ, Liu F, Chen B. lncRNA SNHG1 attenuates osteogenic differentiation via the miR-101/DKK1 axis in bone marrow mesenchymal stem cells. Mol Med Rep 2020;22:3715–3722.
54. Sendoel A, Dunn JG, Rodriguez EH, et al. Translation from unconventional 5' start sites drives tumour initiation. Nature 2017;541:494–499.
55. Lukoszek R, Feist P, Ignatova Z. Insights into the adaptive response of Arabidopsis thaliana to prolonged thermal stress by ribosomal profiling and RNA-Seq. BMC Plant Biol 2016;16:221.
56. Kronja I, Yuan B, Eichhorn SW, et al. Widespread changes in the posttranscriptional landscape at the Drosophila oocyte-to-embryo transition. Cell Rep 2014;7:1495–1508.

fdi World Dental Congress

SHANGHAI 2025

4 DAY exhibition

4 DAY scientific programme

60,000m² exhibition area

35,000+ visitors

8,000 delegates

700+ exhibiting companies

100+ Worldwide speakers

200+ national speakers

Early bird registration deadline: **2 June 2025**

Register Here

See you in SHANGHAI

9 - 12 September 2025

Monitoring Role of Non-invasive Examinations on the Clinical Efficacy of Photodynamic Therapy for Oral Potentially Malignant Disorders

Xing Yun LIU[1], Qian Yun GUO[1], Qian WANG[1], Si XU[1], Zhe CHENG[1], Lei ZHANG[1], Yu Tian WANG[1], Xiang GUO[1], Xiao Dan LIU[1], Wen Wen LI[1], Xing WANG[1], Shu Fang LI[1], Zi Jian LIU[1], Hong Mei CUI[1], Ming Xing LU[1], Jian Qiu JIN[1], Ying HAN[1], Hong Wei LIU[1]

Objective: *To assess the clinical efficacy of 5-aminolaevulinic acid photodynamic therapy (5-ALA-PDT) in treating oral potentially malignant disorders (OPMDs) and investigate the utility of toluidine blue staining and autofluorescence examination for monitoring the efficacy of 5-ALA-PDT.*

Methods: *A prospective cohort study was conducted, including 75 OPMDs patients who underwent 5-ALA-PDT and follow-up observation. The patients' lesion size and clinical presentation were recorded to evaluate the clinical efficacy of 5-ALA-PDT. Toluidine blue staining and autofluorescence examination were performed as auxiliary monitoring methods, aiming to assess their diagnostic capabilities as non-invasive examinations for detecting pathological oral epithelial dysplasia (OED) and explore their monitoring value for the clinical efficacy of 5-ALA-PDT.*

Results: *Toluidine blue staining showed a sensitivity of 62.2% and a specificity of 42.9% for diagnosing OED, whereas autofluorescence examination showed a sensitivity of 67.2% and a specificity of 64.3%. The parallel combination of both examinations increased the sensitivity to 77.0%, whereas the series combination increased the specificity to 71.4%. After 5-ALA-PDT, 38.7% of patients with OPMDs achieved complete remission, with an overall response rate of 92%. Persistent positive toluidine blue staining after 5-ALA-PDT treatment was significantly associated with treatment failure. The clinical efficacy of 5-ALA-PDT gradually decreased in patients with aggravation, stable or improved lesions from non-invasive examinations both before and after treatment.*

Conclusion: *5-ALA-PDT demonstrates significant efficacy in treating OPMDs by effectively eliminating lesions. Toluidine blue staining and autofluorescence examination have certain diagnostic capabilities for OED and can be used for monitoring efficacy during 5-ALA-PDT treatment.*

Keywords: *autofluorescence imaging, oral potentially malignant disorders, photodynamic therapy, toluidine blue*

Chin J Dent Res 2025;28(1):45–54; doi: 10.3290/j.cjdr.b6097614

Oral potentially malignant disorders (OPMDs) are a group of diseases occurring in the oral mucosa with the potential for malignant transformation, including oral leucoplakia (OLK), oral erythroplakia (OEK), oral submucous fibrosis, oral lichen planus (OLP) and oral

1 Department of Oral Medicine, Peking University School and Hospital of Stomatology & National Center of Stomatology & National Clinical Research Center for Oral Diseases & National Engineering Research Center of Oral Biomaterials and Digital Medical Devices & Beijing Key Laboratory of Digital Stomatology & NHC Research Center of Engineering and Technology for Computerized Dentistry & NMPA Key Laboratory for Dental Materials, Beijing, P.R. China.

Corresponding authors: Dr Ying HAN and Dr Hong Wei LIU, Department of Oral Medicine, Peking University School and Hospital of Stomatology, #22 Zhongguancun South Street, Haidian District, Beijing 100081, P.R. China. Tel: 86-10-82195362. Emails: 13683375487@163.com; hongweil2569@163.com

This study was supported by the National Natural Science Foundation of China (U19A2005; 81771071), the Natural Science Foundation of Beijing Municipality (7181002), the Special Fund for the Development of Capital Health Care (2018-1-1021) and Clinical Research Foundation of Peking University School and Hospital of Stomatology (PKUSS-2023CRF304).

lichenoid lesions.[1] The overall prevalence of OPMDs is approximately 4.47%,[2] with an overall malignant transformation rate of 7.9%.[3] It is estimated that 70% to 90% of oral squamous cell carcinomas arise from OPMDs.[4] Therefore, the diagnosis, treatment, monitoring of malignant transformation and follow-up management of OPMDs are crucial for preventing the occurrence and development of oral cancer and improving patient survival rates.

Photodynamic therapy (PDT) is a treatment method that involves the application of photosensitisers locally or systemically, which accumulate in abnormal proliferating tumour tissue. Subsequent irradiation of the tissue with a specific wavelength light source induces photobiological reactions, generating a large amount of reactive oxygen species and destroying tumour cells.[5-7] PDT has gradually become an important therapeutic approach for the treatment of tumours and precancerous lesions due to its high selectivity, minimal damage and rapid recovery time.[8,9] 5-aminolevulinic acid (5-ALA) is the most commonly used photosensitiser in treating OPMDs.[10,11] Currently, there are more than 10 studies worldwide exploring the efficacy of 5-ALA-PDT in treating OPMDs, but none have investigated the monitoring ability of non-invasive examinations for the efficacy of 5-ALA-PDT.

Methods for the diagnosis and monitoring of malignant transformation in OPMDs include clinical, histopathological and auxiliary examinations. The accuracy of clinical examination relies on the experience of the dental practitioner and can lead to missed or misdiagnosed cases. Histopathological examination is limited by factors such as trauma, time consumption and patient discomfort, making it difficult to use as a long-term monitoring method in clinical follow-up management. In recent years, many researchers have been dedicated to finding non-invasive or minimally invasive auxiliary examination methods to alleviate patient suffering and assist in clinical diagnosis and prognosis assessment.[12,13]

Toluidine blue, as an acidic metachromatic dye, has a strong affinity for nucleic acids, making it easier to stain tissues with epithelial dysplasia or tumour tissue.[14,15] VELscope (LED Dental, Vancouver, Canada) is the most widely used autofluorescence examination device, which emits blue light to excite endogenous fluorophores and is used to differentiate normal, abnormal proliferative and tumour tissue.[16,17] Studies have shown that these two non-invasive examinations have significant auxiliary value in the early diagnosis of OPMDs.[18-20] However, there is currently no research exploring their application in monitoring during 5-ALA-PDT.

This study prospectively collected data and conducted follow-up management of patients with OPMDs receiving 5-ALA-PDT to explore its clinical efficacy in treating OPMDs. Additionally, the study incorporated toluidine blue staining and autofluorescence examination into the assessment of 5-ALA-PDT efficacy and follow-up observation, aiming to provide more objective and convenient methods for monitoring during treatment.

Materials and methods

Patient inclusion and exclusion

This study was a prospective follow-up cohort study conducted from January 2016 to August 2023 at the Department of Oral Diseases, Peking University School of Stomatology. Patients diagnosed with OPMDs based on clinical and histopathological assessments, who underwent 5-ALA-PDT treatment and received non-invasive examinations (toluidine blue staining, autofluorescence examination) during follow-up, were included. The clinical diagnostic criteria for OPMDs followed the WHO consensus,[1,21] with histopathological results serving as the diagnostic gold standard. Patients with severe systemic infections, uncontrolled systemic diseases, severe mental illness or intolerance to or the inability to complete PDT treatment were excluded.

Baseline data collection

At the initial visit, patients' clinical basic information was collected, including sex, date of birth, medical history, smoking history, alcohol consumption history, betel nut chewing history, symptoms and course of disease. Patients underwent a comprehensive examination of the oral mucosa and routine oral examination, and the nature, location, number, size (cm^2), clinical type, oral hygiene status, local irritants and initial clinical diagnosis of the lesions were recorded. Lesions were photographed using a digital single-lens reflex camera. Clinical types of OLK included homogeneous and non-homogeneous (verrucous type, granular type, ulcerative type). Other OPMDs were not classified into subtypes.

Toluidine blue staining examination

Patients were instructed to rinse their mouths with water for 30 seconds. Using a dry cotton swab, the liquid on the surface of the lesion was wiped away. A new cotton swab was dipped in 1% acetic acid solution and applied

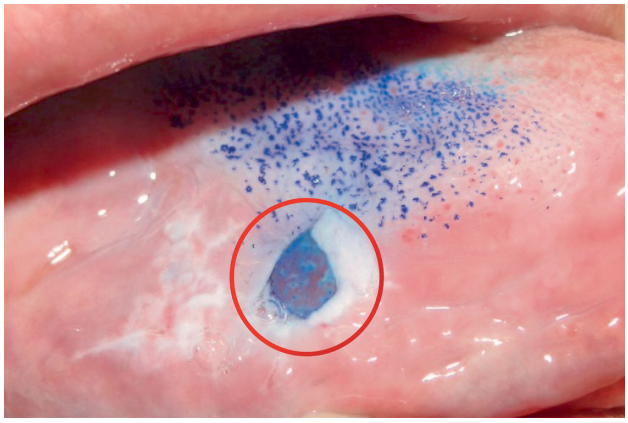

Fig 1 Positive toluidine blue staining on the right ventral tongue, ulcerative type oral leucoplakia with moderate epithelial dysplasia.

to the lesion surface for 30 seconds to remove the saliva film. Subsequently, another cotton swab was dipped in 1% toluidine blue solution and applied to the lesion surface for 30 seconds. During this period, patients were instructed not to close their mouths, and then to rinse their mouths with water three times. A cotton swab dipped in 1% acetic acid solution was used to wipe the lesion surface to remove mechanical staining, and finally, patients were asked to rinse their mouths with water for 30 seconds. Lesions that still showed patchy staining after bleaching were judged and recorded as positive. Lesions without staining were recorded as negative, whereas those with light staining that was difficult to determine were considered suspicious (Fig 1).

Autofluorescence examination

The examination was conducted in a dark environment. The examiner held a VELscope autofluorescence instrument, allowing fluorescence to be projected vertically onto the lesion site. The lesion was observed through the eyepiece, and the fluorescence photograph results were stored using an iPod touch 4. Examination results were recorded as negative, suspicious or positive. The judgment criteria for autofluorescence detection results were that normal tissue exhibited a faint green fluorescence after fluorescence irradiation, indicating a negative result. Positive results were characterised by the absence of abnormal black fluorescence in irregular, asymmetrical shapes after fluorescence irradiation, with normal green fluorescence observed in the contralateral lesion-free area. Suspicious results were recorded for cases with fluorescence attenuation that was difficult to determine as physiological or abnormal (Fig 2).

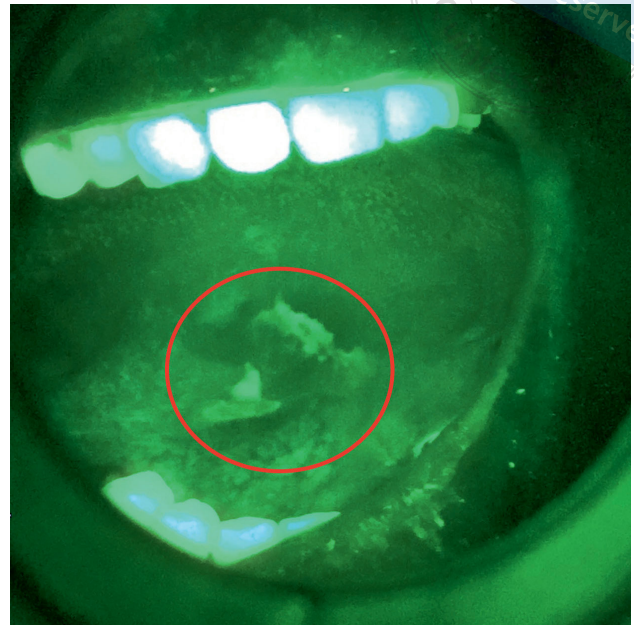

Fig 2 VELscope image of the left ventral tongue (granular type oral leucoplakia with moderate oral epithelial dysplasia) showed fluorescence visualisation loss.

Histopathological examination

For lesions that did not regress after local irritation was removed for 2 weeks, the most typical area of the lesion was selected for a local biopsy or excision biopsy specimen to be taken. Tissue samples were fixed in formalin solution and embedded in paraffin after immersion. After slicing, haematoxylin-eosin staining was performed, followed by microscopic examination. Oral pathologists made histopathological diagnoses based on disease diagnostic criteria. For cases of oral epithelial dysplasia (OED), the degree was classified into three categories according to WHO standards: mild, moderate and severe. If there were two or more degrees of OED, the result was based on the more severe degree. Lesions showing suspicious early carcinoma or early infiltration were classified as oral cancer.

Clinical typing, toluidine blue staining results, autofluorescence examination results and histopathological examination results were primarily determined by one physician, with two additional physicians providing secondary review and confirmation.

Follow-up visits and data collection

During each visit, changes in the patient's general condition were first recorded, including symptoms, habits and systemic diseases. Before each 5-ALA-PDT treat-

ment, clinical examination, toluidine blue staining examination and autofluorescence examination were conducted, and the results were recorded and retained with photographs. Changes in non-invasive examination results compared to baseline status were recorded as reduction (positive to suspicious/positive to negative/suspicious to negative), no change or aggravation (negative to suspicious/negative to positive/suspicious to positive).

According to the expert consensus on 5-ALA-PDT for oral potentially malignant disorders by the Chinese Stomatological Association,[22] standardised 5-ALA-PDT treatment was performed. A 20% concentration of 5-ALA gel was topically incubated for at least 2 hours. After thorough fluorescence distribution was confirmed by Wood's lamp, local anaesthesia was administered. A 635-nm, 600-mw laser light source was used with the fibre optic head positioned 2 cm from the lesion surface and perpendicular to the lesion area. The diameter of the irradiation spot was adjusted to 1 cm, and each spot was irradiated for 3 to 4 minutes to ensure a light flux within the range of 50 to 150 J/cm^2.

Treatment intervals were adjusted based on the severity of the patient's condition and treatment response, and treatment was administered every 1 to 3 weeks until the lesion disappeared or until an oral mucosal disease specialist deemed it appropriate to stop. The number of treatments, treatment parameters and treatment response were recorded.

A follow-up visit was scheduled 2 to 4 weeks after the end of the PDT course. Patient symptoms, clinical manifestations, lesion size, toluidine blue staining examination and autofluorescence examination results were recorded, and photographs were taken and retained. The clinical efficacy of PDT was assessed based on the size of the lesion and clinical presentation.

Evaluation criteria

Diagnostic ability of non-invasive examinations for detecting OED

Using the presence of OED in histopathological diagnosis as the gold standard, the sensitivity, specificity, accuracy, positive predictive value, negative predictive value and Youden index of toluidine blue staining and autofluorescence examination were calculated. Receiver operating characteristic curves were plotted, and the area under the curve (AUC) was calculated.

In a parallel test, if either of the two non-invasive examination results is positive, it is considered positive; both results must be negative to be considered negative.

In a series test, if one of the two non-invasive examination results is negative, it is considered negative; both results must be positive to be considered positive.

$$Sensitivity = \left(\frac{True\ Positives}{True\ Positives\ +\ False\ Negatives}\right) \times 100\%$$

Representing the ability of a diagnostic method to correctly detect actual patients.

$$Specificity = \left(\frac{True\ Negatives}{True\ Negatives\ +\ False\ Positives}\right) \times 100\%$$

Representing the ability of a diagnostic method to correctly detect actual non-patients.

$$Positive\ Predictive\ Value = \left(\frac{True\ Positives}{True\ Positives\ +\ False\ Positives}\right) \times 100\%$$

Indicating the proportion of truly diseased patients among those indicated as diseased by a diagnostic method.

$$Negative\ Predictive\ Value = \left(\frac{True\ Negatives}{True\ Negatives\ +\ Negatives}\right) \times 100\%$$

Indicating the proportion of truly non-diseased individuals among those indicated as non-diseased by a diagnostic method.

$$Accuracy = \left(\frac{True\ Positives\ +\ True\ Negatives}{Total\ cases}\right) \times 100\%$$

Indicating the proportion of correctly diagnosed patients and non-patients among all individuals undergoing diagnosis.

Clinical efficacy evaluation of 5-ALA-PDT

Clinical efficacy evaluation was conducted 2-4 weeks after the completion of 5-ALA-PDT treatment, according to the following criteria:

- Complete response (CR): The target lesion was found to have disappeared upon clinical examination.
- Partial response (PR): Compared to baseline, the size of the lesion has decreased by ≥ 20% or there is a transition from a severe clinical type to a milder clinical type, or toluidine blue staining or autofluorescence examination result has turned negative.
- No response (NR): The lesion area has decreased by < 20% or has increased in size, or the clinical type has aggravated, or toluidine blue staining or autofluorescence examination result has turned positive.

The overall response (OR) rate was ((CR + PR) / (CR + PR + NR)) × 100%.

Table 1 Demographics of patients who received 5-ALA-PDT.

Variable		Male	Female	Total
Total		35 (46.7%)	40 (53.3%)	75 (100.0%)
Age (year)	Mean ± SD	51.99 ± 13.96	56.25 ± 12.25	54.26 ± 13.16
Systemic diseases	Yes	21 (60.0%)	25 (62.5%)	46 (61.3%)
	No	14 (40.0%)	15 (37.5%)	29 (38.7%)
Smoking	Yes	25 (71.4%)	0 (0.0%)	25 (33.3%)
	No	10 (28.6%)	40 (100.0%)	50 (66.7%)
Drinking	Yes	21 (60.0%)	3 (7.5%)	24 (32.0%)
	No	14 (40.0%)	37 (92.5%)	51 (68.0%)
Disease classification	OLK	33 (94.3%)	31 (77.5%)	64 (85.3%)
	OEK	2 (5.7%)	6 (15.0%)	8 (10.7%)
	Other OPMDs	0 (0.0%)	3 (7.5%)	3 (4.0%)
Clinical types of OLK	Homogenous	17 (51.5%)	7 (22.6%)	24 (37.5%)
	Non-homogenous	16 (48.5%)	24 (77.4%)	40 (62.5%)
Lesion location	High-risk areas[a]	20 (57.1%)	21 (52.5%)	41 (54.7%)
	Others	15 (42.9%)	19 (47.5%)	34 (45.3%)
OED	No	7 (20.0%)	7 (17.5%)	14 (18.7%)
	Mild	10 (28.6%)	10 (25.0%)	20 (26.7%)
	Moderate	10 (28.6%)	15 (37.5%)	25 (33.3%)
	Severe	8 (22.9%)	8 (20.0%)	16 (21.3%)
Clinical efficacy of 5-ALA-PDT	CR	12 (34.3%)	17 (42.5%)	29 (38.7%)
	PR	22 (62.9%)	18 (45.0%)	40 (53.3%)
	NR	1 (2.9%)	5 (12.5%)	6 (8.0%)

[a]High-risk areas refer to the margin and ventral surface of the tongue and floor of the mouth

SD, standard deviation.

Statistical analysis

The statistical analysis was performed using SPSS version 26.0 software (IBM, Chicago, IL, USA). Normally distributed continuous variables were expressed as mean ± standard deviation (SD), while non-normally distributed continuous variables were presented as median (Md) and interquartile range (P25, P75). Categorical variables were presented as frequency and percentage.

For continuous variables, normality and homogeneity of variance were assessed. If the assumptions were met, a Student *t* test or analysis of variance (ANOVA) was used for between-group comparisons. If the assumptions were violated, a Mann-Whitney U test or Kruskal-Wallis test was applied. The between-group comparison of categorical variables and correlation analysis were conducted using a chi-square test. All reported *P* values were based on two-tailed tests, with the level of statistical significance set at $P < 0.05$.

Results

Demographic information

A total of 75 patients were included, with 35 men and 40 women, yielding a male-to-female ratio of approximately 1:1.14. The mean age was 54.26 ± 13.16 years. Among them, 64 cases were diagnosed as OLK and eight as OEK, and the remaining three cases included oral lichen planus, oral lichenoid lesions and chronic discoid lupus erythematosus, respectively. Among OLK patients, 24 cases were of the homogeneous type and 40 cases were non-homogeneous. Baseline histopathological examination revealed 14 cases with no OED, with 20 cases of mild, 25 cases of moderate and 16 cases of severe OED. Patients' basic information is summarised in Table 1.

The 75 OPMD patients received between one and 23 sessions of 5-ALA-PDT, with a median of 4 (2, 6) sessions. The overall response rate of 5-ALA-PDT in

Table 2 Relationship between baseline results of two non-invasive examinations.

Non-invasive examination results		Autofluorescence examination		Total
		Positive	Negative	
Toluidine blue staining	Positive	37	9	46
	Negative	9	20	29
Total		46	29	75

Table 3 Correlation between baseline non-invasive examination results and clinical information.

Clinical information		Toluidine blue staining	*P* value	Autofluorescence examination	*P* value
		Positive/negative		Positive/negative	
Total		46/29	NA	46/29	NA
Disease classification	OLK	36/28	0.117	38/26	0.202
	OEK	7/1		7/1	
	Other OPMDs	3/0		1/2	
Lesion location	High-risk areas[a]	23/18	0.307	24/17	0.585
	Others	23/11		22/12	
Clinical types of OLK	Homogenous	8/16	0.004*	10/14	0.025*
	Non-homogenous	28/12		28/12	
OED	No	8/6	0.721	5/9	0.029*
	Yes	38/23		41/20	
5-ALA-PDT clinical efficacy	OR	41/28	0.396	42/27	0.780
	NR	5/1		4/2	

[a]High-risk areas refer to the margin and ventral surface of the tongue and floor of the mouth

*$P < 0.05$, statistically significant.

NA, not applicable; OR, overall response.

treating OPMDs was 92%, with 29 cases achieving CR and 40 achieving PR. Among OLK patients, the CR rate was 40.6% (26/64) and the overall response rate was 93.7% (60/64). The CR rates for ulcerative OLK (60.0%, 9/15), granular OLK (50.0%, 10/20), homogeneous OLK (25.0%, 6/24) and verrucous OLK (20.0%, 1/5) decreased in this order, though the differences were not statistically significant. In OEK patients, the CR rate with 5-ALA-PDT was 37.5% (3/8) and the overall response rate was 87.5% (7/8). There was no significant difference in the efficacy rates of 5-ALA-PDT among different disease types.

Correlation between baseline non-invasive examination results and clinical information

At baseline, 61.3% of patients tested positive for toluidine blue staining, and 61.3% tested positive for autofluorescence examination, with 49.3% showing positive results for both non-invasive examinations. The concordance rate of the two non-invasive examination results at baseline was 76%, as shown in Table 2. Comparing the baseline non-invasive examination results with clinical information revealed significant associations. Positive toluidine blue staining was notably associated with the non-homogeneous type of OLK ($P = 0.004$). Positive autofluorescence examination was significantly associated with non-homogeneous type OLK ($P = 0.025$) and the presence of OED ($P = 0.029$); however, there was no significant correlation between baseline non-invasive examination results and disease type, lesion site or efficacy of 5-ALA-PDT. The proportional relationship between the two non-invasive examination results and OLK clinical subtypes and the degree of OED is presented in Table 3 and Fig 3.

Non-invasive examination for diagnosing OED

The diagnostic performance of two non-invasive examination methods was evaluated based on the presence of OED as a positive result in histopathology (Table 4). When each non-invasive method was applied individually, autofluorescence examination demonstrated higher sensitivity (67.2%), specificity (64.3%), positive predictive value (89.1%) and accuracy (66.7%) compared to toluidine blue staining (sensitivity 62.2%, specificity 42.9%, positive predictive value 82.6%, accuracy 58.7%). However, toluidine blue staining exhibited a higher

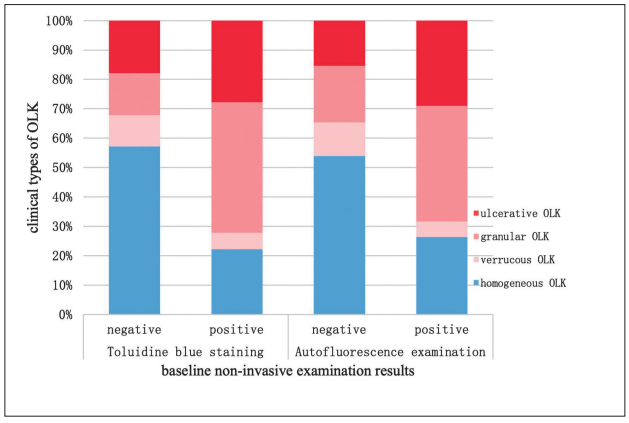

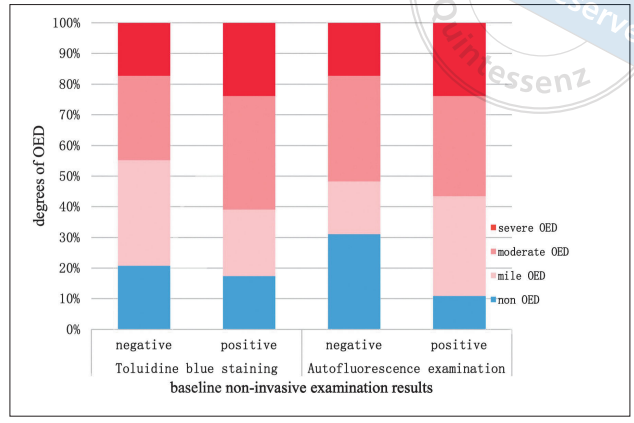

Fig 3 Relationship between baseline non-invasive examination results and clinical types of OLK and OED. At baseline, there was a significant correlation between toluidine blue staining positivity and clinical type of OLK being heterogeneous ($P = 0.004$), while positivity in autofluorescence examination was significantly associated with heterogeneous OLK ($P = 0.029$) and presence of OED ($P = 0.025$).

Table 4 Diagnostic performance of the two non-invasive examination methods for detecting OED.

Examination method	Sensitivity	Specificity	Positive predictive value	Negative predictive value	Accuracy	AUC
Toluidine blue staining	62.2%	42.9%	82.6%	79.3%	58.7%	0.526
Autofluorescence examination	67.2%	64.3%	89.1%	69.0%	66.7%	0.657
Serial test	54.1%	71.4%	89.2%	73.7%	57.3%	0.628
Parallel test	77.0%	21.4%	81.0%	82.4%	66.7%	0.492

AUC, area under the receiver operating characteristic curve.

negative predictive value (79.3%) than autofluorescence examination (69.0%). When the two methods were used in combination, there was an improvement in specificity (71.4%) and positive predictive value (89.2%) for the serial test, and an increase in sensitivity (77.0%) and negative predictive value (82.4%) for the parallel test.

Correlation between changes in non-invasive examination results during follow-up and clinical efficacy of 5-ALA-PDT

All 75 patients underwent toluidine blue staining and autofluorescence examination during treatment follow-up, and the results are presented in Table 5. It was found that the NR rate in patients with positive toluidine blue staining after treatment completion was 35.7%, significantly higher than the rate in patients with negative staining (1.6%; $P < 0.001$). Additionally, patients with a reduction in toluidine blue staining results had the highest rate of CR, while those with no change had the highest rate of PR, and those with aggravation had the highest rate of NR, with statistically significant differences ($P = 0.040$). There was no significant difference in the distribution of 5-ALA-PDT efficacy between patients with positive and negative autofluorescence examination results after treatment completion ($P = 0.067$). However, the CR rates gradually decreased and NR rates gradually increased with decreasing reduction, no change and aggravation in autofluorescence examination results before and after treatment ($P = 0.009$).

During the treatment and follow-up process, 35 patients underwent toluidine blue staining and autofluorescence examination at each visit, along with an evaluation of clinical classification. The duration of clinical classification positivity (considering OLK converting from a non-homogeneous to homogeneous type or the disappearance of red lesions in OEK as negative), toluidine blue positivity and VELscope positivity were recorded and calculated statistically. The median duration of clinical classification positivity was 4.0 (2.0, 9.5) weeks, toluidine blue positivity was 4.0 (4.0, 8.0) weeks, and VELscope positivity was 4.0 (2.0, 8.0) weeks. A Mann-Whitney U test indicated no significant differences in the duration of clinical classification positivity, toluidine blue positivity and VELscope positivity ($P > 0.05$).

A Spearman rank correlation test revealed a significant positive correlation among the durations of clin-

Table 5 Correlation between changes in non-invasive examination results and clinical efficacy.

Non-invasive examination results and changes		CR	PR	NR	*P* value
Toluidine blue staining after treatment	Negative	28 (45.9%)	32 (52.5%)	1 (1.6%)	< 0.001*
	Positive	1 (7.1%)	8 (57.1%)	5 (35.7%)	
Change in toluidine blue staining	Reduced	23 (50.0%)	21 (45.7%)	2 (4.3%)	0.040*
	No change	5 (20.0%)	17 (68.0%)	3 (12.0%)	
	Aggravated	1 (25.0%)	2 (50.0%)	1 (25.0%)	
Autofluorescence after treatment	Negative	23 (41.8%)	30 (54.5%)	2 (3.6%)	0.067
	Positive	6 (30.0%)	10 (50.0%)	4 (20.0%)	
Change in autofluorescence examination	Reduced	21 (56.8%)	16 (43.2%)	0 (0.0%)	0.009*
	No change	7 (21.9%)	20 (62.5%)	5 (15.6%)	
	Aggravated	1 (16.7%)	4 (66.7%)	1 (16.7%)	

*$P < 0.05$, statistically significant.

ical classification positivity, toluidine blue positivity and VELscope positivity. The correlation coefficient between the duration of clinical classification positivity and toluidine blue positivity was 0.574 ($P = 0.010$), between clinical classification positivity and VELscope positivity was 0.640 ($P = 0.008$), and between toluidine blue positivity and VELscope positivity was 0.468 ($P = 0.032$).

Discussion

This study included a total of 75 patients with OPMDs who underwent 5-ALA-PDT treatment and follow-up. Among them, 64 cases were OLK, eight were OEK and the remaining three were distributed as oral lichen planus, oral lichenoid lesions and chronic discoid lupus erythematosus. The overall response rate for 5-ALA-PDT treatment was 92%, with 38.7% achieving CR and 53.3% achieving PR. A meta-analysis conducted in 2022 showed an overall response rate of 93.7% for PDT treatment of OPMDs, with 35.3% CR among 235 cases of OLK and 91.8% among 61 cases of OEK, which is consistent with the results of this study.[23] This suggests that 5-ALA-PDT is effective in removing OPMD lesions.

The baseline results of toluidine blue staining were significantly correlated with clinical types of OLK, whereas positive results of autofluorescence examination were significantly correlated with non-homogeneous OLK and the presence of OED. This indicates that these two non-invasive examinations can be used to assess the malignancy of OPMD lesions, highlighting the importance of increased attention to patients with positive results from non-invasive examinations.

The diagnostic performance results suggested that autofluorescence examination had a slightly better diagnostic ability for detecting OED compared to toluidine blue staining. Parallel use of both methods increased the sensitivity to 77.0%, whereas series use increased the specificity to 71.4%, suggesting that combining these methods may enhance diagnostic accuracy in clinical practice. The meta-analysis results reported by Walsh et al[24] showed that the sensitivity of vital staining methods for diagnosing OPMDs or OSCC was 0.86, with a specificity of 0.68, while optical methods had a sensitivity of 0.87 and a specificity of 0.50, and the combined use of staining and optical examination methods can improve diagnostic specificity.[24] The application of non-invasive examination methods to assist in the diagnosis and detection of OPMDs is a future trend. Toluidine blue staining and autofluorescence examination have the advantages of being completely non-invasive, easy to operate and efficient, and they have certain discriminatory abilities for OED. Future research should further explore their combined application and diagnostic accuracy.

In this study, non-invasive examination methods were used to assist in the examination during 5-ALA-PDT treatment. It was found that patients with positive results for toluidine blue staining at the end of treatment had poorer efficacy of 5-ALA-PDT. The efficacy of 5-ALA-PDT decreased progressively with the reduction, stability or aggravation of non-invasive examination results both before and after treatment, indicating that non-invasive examination methods can be used to monitor the efficacy of 5-ALA-PDT treatment and assist in judging the treatment effect during follow-up.

Furthermore, we believe that non-invasive examination results can be used as one of the criteria for determining whether to discontinue 5-ALA-PDT treatment.[25] If patients' clinical lesions disappear but the non-invasive examination results remain positive, 5-ALA-PDT treatment should continue until the non-invasive examination results become negative. Conversely, if patients' clinical lesions are relatively refractory and difficult to resolve, non-invasive examination results should also be considered. If they all turn negative, this

indicates a reduced risk of lesion malignancy, and laser ablation treatment or follow-up observation alone may be considered.

A total of 35 patients underwent non-invasive examination monitoring during each visit of the treatment follow-up. We found no significant difference in the duration of positivity between toluidine blue staining and VELscope concerning non-homogeneous clinical classifications or erythematous red lesions. This indicates that toluidine blue staining and VELscope examinations can promptly and effectively reflect changes in lesions. The results of toluidine blue staining and VELscope are distinct and easy to differentiate. Compared to distinguishing clinical manifestations of lesions, the positive or negative results of non-invasive examinations are more indicative, facilitating other non-specialised clinicians in assessing OPMDs when the clinical risk is difficult to determine.

Conclusion

This study demonstrates that 5-ALA-PDT treatment is significantly effective for OPMDs. Toluidine blue staining and autofluorescence examination have certain diagnostic capabilities for OED and can be used for monitoring during 5-ALA-PDT treatment. It is still necessary to increase the sample size and extend the follow-up period in the future in order to explore the long-term efficacy of 5-ALA-PDT treatment as well as its correlation with non-invasive examination results.

Conflicts of interest

The authors declare no conflicts of interest related to this study.

Author contribution

Dr Xing Yun LIU contributed to the data analyses and manuscript draft; Drs Ying HAN and Hong Wei LIU devised the study design and revised the manuscript; Drs Qian Yun GUO, Qian WANG and Si XU contributed to the data analysis and manuscript preparation; Drs Zhe CHENG, Lei ZHANG, Yu Tian WANG, Xiang GUO, Xiao Dan LIU and Wen Wen LI contributed to the data collection and analysis; Drs Xing WANG, Shu Fang LI, Zi Jian LIU, Hong Mei CUI, Ming Xing LU and Jian Qiu JIN contributed to the data collection and patients treatment.

(Received May 19, 2024; accepted Oct 28, 2024)

References

1. Warnakulasuriya S, Kujan O, Aguirre-Urizar JM, et al. Oral potentially malignant disorders: A consensus report from an international seminar on nomenclature and classification, convened by the WHO collaborating centre for oral cancer. Oral Dis 2021;27:1862–1880.
2. Zhang C, Li BJ, Zeng X, Hu XS, Hua H. The global prevalence of oral leukoplakia: a systematic review and meta-analysis from 1996 to 2022. BMC Oral Health 2023;23:645.
3. Iocca O, Sollecito TP, Alawi F, et al. Potentially malignant disorders of the oral cavity and oral dysplasia: A systematic review and meta-analysis of malignant transformation rate by subtype. Head Neck 2020;42:539–555.
4. Mello FW, Miguel AFP, Dutra KL, et al. Prevalence of oral potentially malignant disorders: A systematic review and meta-analysis. J Oral Pathol Med 2018;47:633–640.
5. Dabrowski JM, Arnaut LG. Photodynamic therapy (PDT) of cancer: From local to systemic treatment. Photochem Photobiol Sci 2015;14:1765–1780.
6. Kolarikova M, Hosikova B, Dilenko H, et al. Photodynamic therapy: Innovative approaches for antibacterial and anticancer treatments. Med Res Rev 2023;43:717–774.
7. Agostinis P, Berg K, Cengel KA, et al. Photodynamic therapy of cancer: An update. CA Cancer J Clin 2011;61:250–281.
8. Alvarez N, Sevilla A. Current advances in photodynamic therapy (PDT) and the future potential of PDT-combinatorial cancer therapies. Int J Mol Sci 2024;25:1023.
9. Correia JH, Rodrigues JA, Pimenta S, Dong T, Yang Z. Photodynamic therapy review: Principles, photosensitizers, applications, and future directions. Pharmaceutics 2021;13:1332.
10. Howley R, Chandratre S, Chen B. 5-aminolevulinic acid as a theranostic agent for tumor fluorescence imaging and photodynamic therapy. Bioengineering (Basel) 2023;10:496.
11. Shinoda Y, Kato D, Ando R, et al. Systematic review and meta-analysis of in vitro anti-human cancer experiments investigating the use of 5-aminolevulinic acid (5-ALA) for photodynamic therapy. Pharmaceuticals (Basel) 2021;14:229.
12. Patton LL, Epstein JB, Kerr AR. Adjunctive techniques for oral cancer examination and lesion diagnosis: a systematic review of the literature. J Am Dent Assoc 2008;139:896–905.
13. Macey R, Walsh T, Brocklehurst P, et al. Diagnostic tests for oral cancer and potentially malignant disorders in patients presenting with clinically evident lesions. Cochrane Database Syst Rev 2015;2015:CD010276.
14. Sridharan G, Shankar AA. Toluidine blue: A review of its chemistry and clinical utility. J Oral Maxillofac Pathol 2012;16:251–255.
15. Mills S. How effective is toluidine blue for screening and diagnosis of oral cancer and premalignant lesions? Evid Based Dent 2022;23:34-35.
16. Monici M. Cell and tissue autofluorescence research and diagnostic applications. Biotechnol Annu Rev 2005;11:227–256.
17. Fernandes JR, Dos Santos LCF, Lamers ML. Applicability of autofluorescence and fluorescent probes in the trans-surgical of oral carcinomas: a systematic review. Photodiagnosis Photodyn Ther 2023;41:103238.
18. Kim DH, Song EA, Kim SW, Hwang SH. Efficacy of toluidine blue in the diagnosis and screening of oral cancer and precancer: A systematic review and meta-analysis. Clin Otolaryngol 2021;46:23–30.

19. Flores Dos Santos LC, Fernandes JR, Lima IFP, Bittencourt LDS, Martins MD, Lamers ML. Applicability of autofluorescence and fluorescent probes in early detection of oral potentially malignant disorders: A systematic review and meta-data analysis. Photodiagnosis Photodyn Ther 2022;38:102764.
20. Wang Q, Xu S, Han Y, et al. Clinical application value of toluidine blue staining in the early diagnosis of oral potential malignant disorders and oral squamous cell carcinoma [in Chinese]. Zhongguo Shi Yong Kou Qiang Ke Za Zhi 2020;13:738–744.
21. Muller S, Tilakaratne WM. Update from the 5th edition of the World Health Organization classification of head and neck tumors: Tumours of the oral cavity and mobile tongue. Head Neck Pathol 2022;16:54–62.
22. Liu ZJ, Wang X, Han Y, Liu HW. Clinical problems and outcome indicators in the expert consensus determined by the Delphi method of 5-aminolevulinic acid photodynamic therapy for the treatment of oral potential malignant diseases [in Chinese]. Kou Qiang Ji Bing Fang Zhi 2022;30:330–337.
23. Binnal A, Tadakamadla J, Rajesh G, Tadakamadla SK. Photodynamic therapy for oral potentially malignant disorders: A systematic review and meta-analysis. Photodiagnosis Photodyn Ther 2022;37:102713.
24. Walsh T, Macey R, Kerr AR, Lingen MW, Ogden GR, Warnakulasuriya S. Diagnostic tests for oral cancer and potentially malignant disorders in patients presenting with clinically evident lesions. Cochrane Database Syst Rev 2021;7:CD010276.
25. Jin JQ, Han Y, Yang G, et al. Photodynamic therapy for oral erythroplakia transformed from oral lichen planus: A case report [in Chinese]. Zhongguo Kou Qiang Yi Xue Ji Xu Jiao Yu Za Zhi 2022;25:229–235.

Role of Biosynthetic Gene Cluster BGC3 in the Cariogenic Virulence of *Streptococcus mutans*

Jing Yi YANG[1,#], Yi Xin ZHANG[2,#], Yu Wei ZHANG[3,#], Ying CHEN[1,4], Min Di XU[1], Dan Dan WANG[1], Yi Hua CHEN[3], Yi Xiang WANG[1,2], Bin XIA[1]

Objective: *To investigate the role of the biosynthetic gene cluster BGC3 of Streptococcus mutans (S. mutans) in the process of dental caries.*

Methods: *BGC3 and ΔBGC3 S. mutans strains were constructed and their growth curves were evaluated. Acid production capacity was assessed by evaluating pH reduction levels over identical culture periods. The survival of bacteria in phosphate citrate buffer solution (pH 3.0) was quantified. The expression levels of virulence genes (atpF, gtfC, gtfD, spaP, vicR and ftf) were analysed using the qPCR. Co-culture experiments were conducted to evaluate bacterial adaptability. Bacterial viability was determined by microscopical examination of live/dead staining.*

Results: *Deletion of BGC3 did not significantly impact S. mutans growth or acid production in biofilms. The ΔBGC3 strain exhibited enhanced acid resistance and higher expression levels of virulence genes compared to the wild type. In addition, ΔBGC3 exhibited superior bacterial viability in the co-culture system.*

Conclusion: *BGC3 affected the acid resistance and expression of caries-related genes in S. mutans. The BGC3 knockout strain exhibited a more robust survival capability than the wild-type strain.*

Keywords: *biofilm, biosynthetic gene clusters, dental caries, Streptococcus mutans, virulence genes*

Chin J Dent Res 2025;28(1):55–62; doi: 10.3290/j.cjdr.b6097621

1 Department of Pediatric Dentistry, Peking University School and Hospital of Stomatology & National Center for Stomatology, Beijing, P.R. China.
2 Central laboratory, Peking University School and Hospital of Stomatology, Beijing, P.R. China.
3 State Key Laboratory of Microbial Resources, Institute of Microbiology, Chinese Academy of Sciences, Beijing, P.R. China.
4 Department of Stomatology Shenzhen Children's Hospital, Shenzhen, P.R. China.
# These authors contributed equally to this work.

Corresponding authors: Dr Yi Xiang WANG, Central laboratory, Peking University School and Hospital of Stomatology, No. 22 Zhongguancun Avenue South, Haidian District, Beijing 100081, P.R. China. Email: kqwangyx@sina.com.

Dr Bin XIA, Department of Pediatric Dentistry, Peking University School and Hospital of Stomatology & National Center for Stomatology, No. 22 Zhongguancun Avenue South, Haidian District, Beijing 100081, P.R. China. Email: xiabin@pkuss.bjmu.edu.cn.

This study was supported by several grants: the National Key Research and Development Program of China (grant no. 2021YFC2301000), the Nature Science Foundation of Beijing Municipality (grant no. 7232218) and the National Nature Science Foundation of China (grant no. 81970920).

Dental caries is one of the most common chronic diseases globally and a major public health challenge. It is a multifactorial disease and one in which bacterial biofilm, commonly called dental plaque, is thought to play a role in the occurrence and progression.[1] *Streptococcus mutans* (*S. mutans*), a prominent member of the Streptococcus genera in the natural oral microbiota, is prevalent in various oral habitats, including saliva, dental plaque, gingival crevicular fluid and carious teeth.[2] By the 1960s, clinical and animal research had established *S. mutans* as a significant pathogen in dental caries.[3] Subsequent studies have reinforced its crucial role in caries development with its acid production, acid tolerance, adhesion and biofilm formation abilities.[4,5]

Biosynthetic gene clusters (BGCs) are sequences of nucleotides containing specific genetic information. The small-molecule products encoded by these clusters have been recognised for their unique biochemical potential.[6] These molecules are critical mediators in microbial communities, facilitating microbe-microbe

Table 1 Strains and plasmids used in this study.

Strain/Plasmid		Characteristics	Sources
Strain	*S. mutans* CIM3001	Wild type	This study
	S. mutans CIM3001ΔBGC3	BGC3 in-frame deletion mutant	This study
Plasmid	pIFDC2	Amp^r, IFDC2 cassette	Baker et al[5]

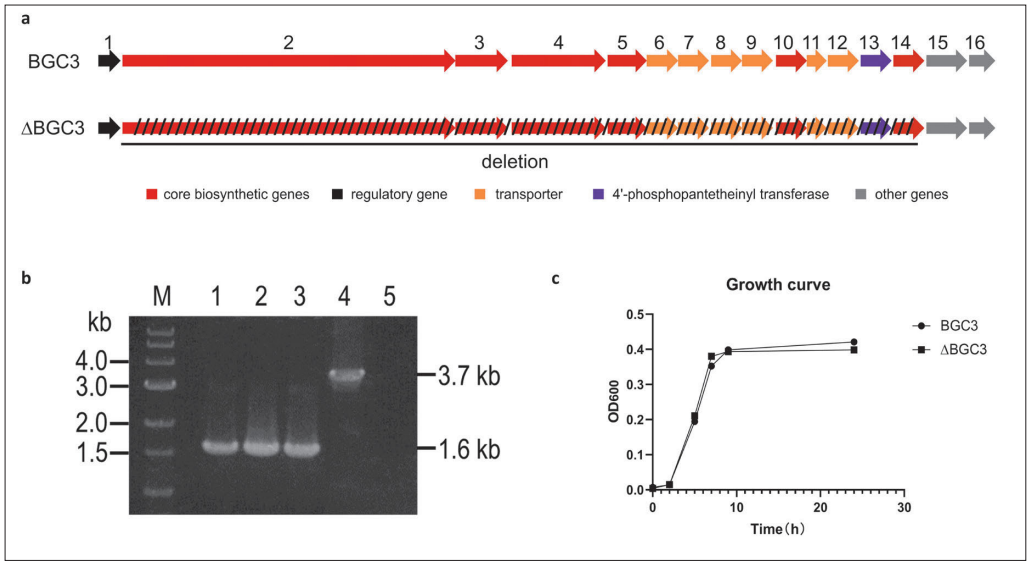

Fig 1a to c Construction, PCR verification and growth curves of *S. mutans* CIM3001ΔBGC3 and CIM3001BGC3 strains. The genes are sequentially encoded as 1 to 16 from left to right, and their functional predictions and proteins are shown in Table 3. The slash represents the in-frame deletion part. The genes are indicated by arrows with different colours **(a)**. Lane M shows the DNA marker; lanes 1 to 3 present the PCR verifications of *S. mutans* CIM3001ΔBGC3 strains; lane 4 illustrates the PCR verification of a BGC3 gene cluster disrupted mutant with an IFDC2 cassette; and lane 5 is the negative control using the genomic DNA of *S. mutans* CIM3001 **(b)**. Growth curves of BGC3 and ΔBGC3 strains in brain heart infusion (BHI) media over 24 hours under anaerobic conditions **(c)**.

and host-microbe interactions. Their functions span antimicrobial activity, signalling activation, immune regulation and biofilm formation.[7]

Recent investigations have revealed that the genome of *S. mutans* encompassed numerous BGCs associated with microbial secondary metabolism. These include non-ribosomal peptide synthetase (NRPS), polyketide synthase (PKS) and hybrid PKS/NRPS gene clusters.[6] Notably, previous studies have identified specific hybrid PKS/NRPS gene clusters in *S. mutans*, namely *mub*, muc and *muf*, that contribute to various physiological activities. These activities encompass interspecies competition, oxidative stress response and biofilm formation, offering new avenues for understanding the cariogenic mechanisms of *S. mutans* and strategies for caries prevention.[8-10]

In a prior investigation, 169 *S. mutans* genomes were analysed, leading to the identification 136 of hybrid PKS/NRPS gene clusters ranging from 12.6 to 36.2 kb in length. These gene clusters were divided into six groups based on their gene composition and organisation.[6] Group III, referred to as BGC3 in this study, consists of 29 hybrid PKS/NRPS gene clusters. BGC3 encodes two PKS modules, three NRPS modules, six transporter proteins, etc. It can release thioester-tethered product reductively, and may also hydrolyse incorrectly loaded elongation units in thiolation domains.[6] However, its biological functional attributes remain unexplored.

Expanding on this research, the current study analysed 413 *S. mutans* genomes from the NCBI database (as of 20 March 2023). Of these, 97 were found to contain BGC3 (NCBI accession number NZ_JAPMUF000000000.1). This finding ranks BGC3 as the second most prevalent gene cluster responsible for mutanobactin production, following Group I which was found to be associated with survival of *S. mutans* in a biofilm environment.[6]

To investigate the impact of BGC3 on the cariogenic properties of *S. mutans*, we isolated the *S. mutans* CIM3001 strain, containing BGC3, from the oral cavity and created a mutant strain, *S. mutans* CIM3001ΔBGC3 (hereafter called ΔBGC3, with the characteristic of being susceptible to gene editing), for experimental purposes.

Table 2 Primers used in this study.

Primers	Sequence (5' to 3')	Description
ldhF-BsaI	CAGGTCTCTGAGCAACAATAACACTCATAGC	IFDC2 cassette PCR
ermR-BsaI	GTGGTCTCAGAAGCTGTCAGTAGTATACCTAA	
BGC3ko-upF	ATCGTTTGCCCCATATAATC	BGC3 in-frame deletion
BGC3ko-upR	GTGGTCTCAGCTCTGTTCTTTTGCTGAGGCTGT	
BGC3ko-upR2	GTGGTCTCATGTTCTTTTGCTGAGGCTGT	
BGC3ko-dnF	CAGGTCTCTCTTCCACTTTATCCACCAACT	
BGC3ko-dnF2	CAGGTCTCTAACACACTTTATCCACCAACT	
BGC3ko-dnR	TAGTTCCGTTATTGTTTCCA	
BGC3-vF	TAAGCTCAAAAGTAAAATGGC	mutant verification
BGC3-vR	TTCATGTCATAGTTATCCGTT	
atpF-F	TTGATAACGCTAAGGAAACTGGTA	H^+-translocating F-ATPase
atpF-R	AACGCTTGATAGGGCTTCTG	
gtfC-F	TCAGACAACACCTTCCTTCCTA	Glucosyltransferase SI (GTFC)
gtfC-R	GAGCACCAGTGACCATATAACC	
gtfD-F	GCCTTTTTACGCTTGTTTGT	Glucosyltransferase I (GTFD)
gtfD-R	CCATATTCATATTCTCCGCC	
spaP-F	TCCGTGCCGATAATCCAAGA	Surface-associated protein P1
spaP-R	CGCCTGTTTGTCCCATTTGT	
vicR-F	GCATCACTTAGCGACACACA	Two-component regulatory system regulator
vicR-R	CAGACGACGAACAGTAACATCAA	
ftf-F	CGAACGGCGACTTACTCTTAT	Fructosyltransferase (FTF)
ftf-R	TTACCTGCGACTTCATTACGATT	
BGC3-F	GTCTTGATAGCAAAGGTGAA	Specific DNA primers
BGC3-R	TATCAAAATAAAACGGCAACC	
BGC3ko-F	TAAAGTCAACAGAGTTTCTC	Specific DNA primers
BGC3ko-R	TAATTCTTGTTTGGTGAAAG	

Materials and methods

Bacterial strains, plasmids and culture conditions

The bacterial strains and plasmids utilised in this study are enumerated in Table 1. *S. mutans* strains were cultured anaerobically on brain-heart infusion (BHI) agar plates or in BHI broth (Oxoid, Basingstoke, England) at 37°C. Antibiotic-resistant colonies were selected on BHI plates supplemented with erythromycin (12.5 μg/ml), whereas p-Cl-Phe-sensitive colonies were selected on BHI plates containing 4 mg/ml p-Cl-Phe.

General DNA manipulations

DNA extraction and genome sequencing of *S. mutans* CIM3001 were conducted by Novogene (Beijing, China). All polymerase chain reaction (PCR) primers used were synthesised by Azenta Life Sciences (Beijing, China) and are detailed in Table 2. The PCRs were performed using Taq DNA polymerase or Phanta DNA polymerase (Vazyme, Nanjing, China), following the protocols provided by the manufacturer. Golden Gate cloning was executed as previously described.[11] Genomic DNAs from various *S. mutans* strains were prepared as outlined in the literature.[12] For natural transformation experiments, cells were incubated in Todd-Hewitt medium (Becton-Dickinson, Sparks, MD, USA) enriched with 0.3% yeast extract, with the comprehensive natural transformation procedure described in an earlier report.[13]

Construction of the gene cluster in-frame deletion mutant

The BGC3 and ΔBGC3 genes are shown in Fig 1a. The in-frame deletion mutant of the BGC3 gene cluster, *S. mutans* CIM3001ΔBGC3, was constructed through a two-stage homologous recombination process. Initially, two DNA fragments flanking the BGC3 gene cluster, measuring 0.5 and 0.8 kb, were PCR-amplified using the primers BGC3ko-upF/R and BGC3ko-dnF/R, with genomic DNA from *S. mutans* CIM3001 as the template. Concur-

Table 3 Genes of BGC3 and their function predictions and proteins.

Gene	Function prediction	Protein (NCBI Reference Sequence)
1	Helix-turn-helix domain-containing protein	WP_002277533.1
2	T-KS-AT(Malonyl-CoA)-T-C-A(Phe)-T-C-A(Glu)-T	WP_195426493.1
3	KS-T	WP_002285336.1
4	C-A(Ser)-T-R	WP_195426492.1
5	Class I SAM-dependent methyltransferase	WP_002277529.1
6	Macrolide transporter	WP_002269643.1
7	ABC transporter ATP-binding protein	WP_002283253.1
8	ABC transporter permease	WP_002278315.1
9	ABC transporter permease	WP_002264134.1
10	acyl-CoA ligase	WP_002285333.1
11	ABC transporter ATP-binding protein	WP_002264137.1
12	ABC transporter permease	WP_002277525.1
13	4'-phosphopantetheinyl transferase superfamily protein	WP_195426491.1
14	Thioesterase	WP_002264142.1
15	Methionine adenosyltransferase	WP_002283366.1
16	SDR family oxidoreductase	WP_002278149.1

rently, a 2.1 kb IFDC2 cassette was PCR-amplified using the primer pair ldhF-BsaI/ermR-BsaI with pIFDC2 as the template. These flanking fragments and the IFDC2 cassette were then joined through Golden Gate cloning and introduced into *S. mutans* CIM3001. Erythromycin-resistant colonies on BHI plates were selected and PCR-validated as BGC3 cluster-disrupted mutants using the primer pair BGC3-vF/R. Subsequently, the IFDC2 cassette was removed via a second homologous recombination round. Here, fragments flanking the IFDC2 cassette (0.5 and 0.8 kb) were PCR-amplified using primers BGC3ko-upF/R2 and BGC3ko-dnF2/R, ligated and transformed into the BGC3-disrupted mutant. Colonies capable of growing on BHI plates supplemented with p-Cl-Phe were selected and PCR-confirmed as *S. mutans* CIM3001ΔBGC3 using the primer pair BGC3-vF/R, with final validation by sequencing.

Growth conditions and growth curves

BGC3 and ΔBGC3 strains were cultured anaerobically in BHI broth (Difco) or on BHI agar plates (pH 7.0) at 37°C (85% N_2, 10% CO_2, 5% H_2). Overnight cultures of *S. mutans* were diluted in fresh BHI to an optical density at 600 nm (OD_{600}) of 0.5, representing log-phase bacteria, and further diluted 100-fold in BHI medium containing 2% (w/v) sucrose for biofilm formation. The bacterial concentration was adjusted to OD_{600} = 1.00, and 5% of the inoculum was added to the new BHI broth medium for cultivation. Growth curve was determined by measuring the OD_{600} values was measured at 2, 5, 8, 10 and 24 hours, respectively.

Differences in acid production, acid tolerance and expression of adhesion-related genes

BGC3 and ΔBGC3 strains were cultivated in BHI broth (pH 7.0) and BHI broth with 2% (w/v) sucrose (pH 7.0), respectively. After overnight cultivation, the supernatants were collected for measuring pH value by using a PHS-3C precision pH meter (INESA Scientific Instrument Co, Shanghai, China). The acid production capacity of the indicated strains was determined by the changes in pH.

The harvested bacteria at the mid-logarithmic growth phase were resuspended to an optical density at 600 nm (OD_{600}) of 0.2 in phosphate-citrate buffer solution (pH 3.0) and incubated at 37°C for 90 minutes. Viable cell counts were performed on the samples after 24 hours of incubation.

To assess the differences in acid resistance and adhesion gene expression levels between the BGC3 and ΔBGC3 strains, SYBR reverse transcription-quantitative PCR was employed, targeting the acid resistance-related gene *atpF* and the adhesion-related genes *gtfC*, *gtfD*, *spaP*, *vicR* and *ftf*. Bacterial RNA extraction was conducted using an RNAprep Pure Cell/Bacteria Kit. The extracted total RNA was then reverse-transcribed with the targeted primers listed in Table 2. qPCR reactions were carried out on an ABI 7500 Real Time PCR system using the GoTaq qPCR Master Mix kit (SYBR Green Reagent), in a total reaction volume of 20 µl. The qPCR protocol included an initial 10 minutes at 95°C, followed by 40 cycles of 95°C for 15 seconds and 60°C for 1 minute. The expression levels of the candidate genes were quantified using the $2^{-\Delta\Delta Ct}$ method.

Microscopic examination of live/dead staining

The bacterial viability was assessed using a SYTO9-PI Live and Dead Bacterial Stain Kit. This kit comprises SYTO9, a green fluorescent dye that permeates both live and dead cells, and propidium iodide, a red fluorescent dye that only enters dead or dying cells with compromised cell membranes. As previously mentioned, biofilms cultured for 2 hours and 16 hours on cover glasses were stained with a 1:1 (volume ratio) mixture of SYTO9 and propidium iodide solution for 15 minutes, adhering to the guidelines provided by the manufacturer.[14] The biofilms were washed with deionised water to remove residual dye.

Images were obtained using a con-focal laser scanning microscope (CLSM) (OLYMPUS, Tokyo, Japan) with 63× oil immersion objectives. Image-Pro Plus 6.0 software (Media Cybernetics, Bethesda, MD, USA) was employed to analyse the images, based on three duplicate samples from each group.

Co-culture assay

The same concentration of BGC3 and ΔBGC3 bacterial fluids (OD_{600} = 1.00) were inoculated into BHI medium in 6-well plates at a ratio of 100 μl: 100 μl for cultivation at indicated time points. At 3, 24 and 47 hours after co-culture, bacteria were harvested and subjected to extract DNA using the TIANamp Bacterial DNA Kit. The qPCR was performed on an ABI 7500 Real Time PCR machine. qPCR reactions were set as described above, except using BGC3 and ΔBGC3 specific primers (Table 2).

Statistical analysis

All experiments were conducted with a minimum of three technical and three biological replicates. Statistical analyses for growth curve and expression levels of targeted genes were performed using a Student t test. Statistical analysis for co-culture was carried out using a two-way analysis of variance. The data were analysed using GraphPad Prism (version 8.0.2) software (GraphPad Software, San Diego, CA, USA), with the level of statistical significance set at $P < 0.05$.

Results

Construction of ΔBGC3 strain and investigating the growth curves of BGC3 and ΔBGC3 strains

We mapped the structure of the BGC3 gene cluster based on the published reference (Fig 1a).[6] To determine the impact of BGC3 deletion on the growth of *S. mutans*, the *S. mutans* CIM3001 ΔBGC3 strain was successfully generated after screening by PCR (Fig 1b). The ΔBGC3 mutant strain exhibited a growth profile similar to the wild-type strain (Fig 1c), suggesting that the absence of BGC3 did not significantly affect the growth of *S. mutans*.

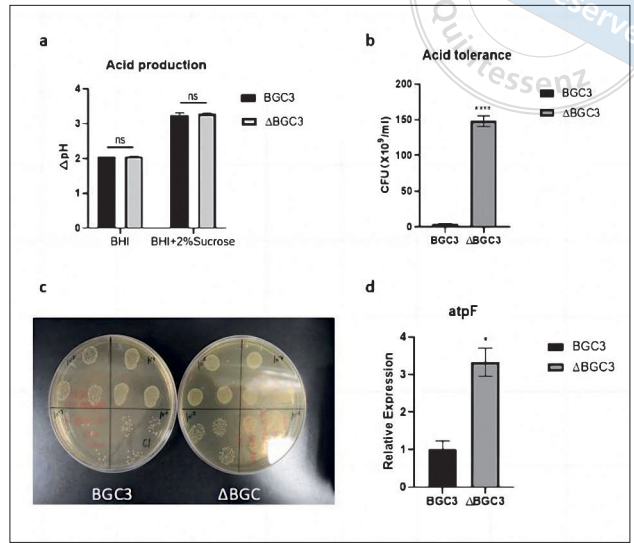

Fig 2a to d Acid production and tolerance comparison between BGC3 and ΔBGC3. Difference in pH values of BGC3 and ΔBGC3 over 16 hours in both BHI and BHI supplemented with 2% sucrose **(a)**. Colony-forming units per millilitre for ΔBGC3 and BGC3 after treatment with acidic solution (pH 3.0) **(b)**. Growth of ΔBGC3 and BGC3 on the culture medium after treatment with acidic solution (pH 3.0). The dilution times for the upper right, upper left, lower right and lower left quadrants are 10^4,10^5,10^6 and 10^7 respectively **(c)**. Expression level of *atpF* in BGC3 and ΔBGC3 **(d)**. Data are expressed as mean ± standard deviation (SD). NS, not significant. **P* < 0.05, ***P* < 0.01, ****P* < 0.001 and *****P* < 0.0001.

Virulence assessment of BGC3 and ΔBGC3 strains

Bacterial virulence was evaluated in both the BGC3 and ΔBGC3 strains. No significant difference in acid production was revealed between the two strains (Fig 2a); however, a marked increase in acid tolerance was noted in the absence of BGC3 (Fig 2b). This increase was evidenced by the higher number of bacterial colonies formed by the ΔBGC3 group in an acidic environment compared to the control group (Fig 2c). Additionally, the expression of the acid resistance gene atpF was upregulated in the ΔBGC3 group relative to the wild type (Fig 2d).

Further investigation into gene regulation potentially influenced by BGC3 was conducted using reverse transcription-qPCR. This analysis showed significant upregulation of key biofilm formation-associated genes such as *gtfC*, *gtfD*, *spaP*, *vicR* and *ftf* in the ΔBGC3

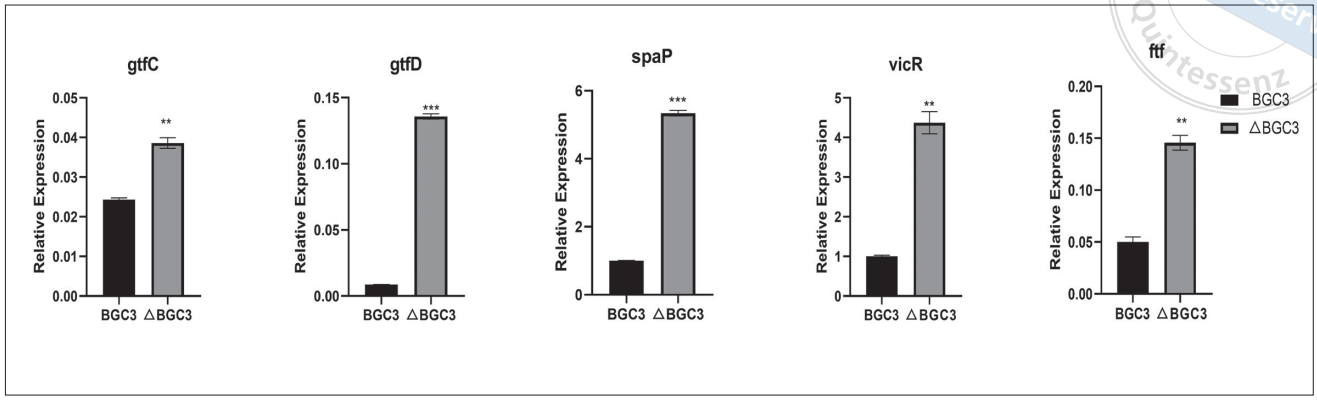

Fig 3 Expression of adhesion-related genes by reverse transcription-quantitative PCR. Effects of BGC3 on *gtfC/D*, *spaP*, *vicR* and *ftf* gene expression levels in *S. mutans*. Data are expressed as mean ± SD. $^{**}P < 0.01$, $^{***}P < 0.001$.

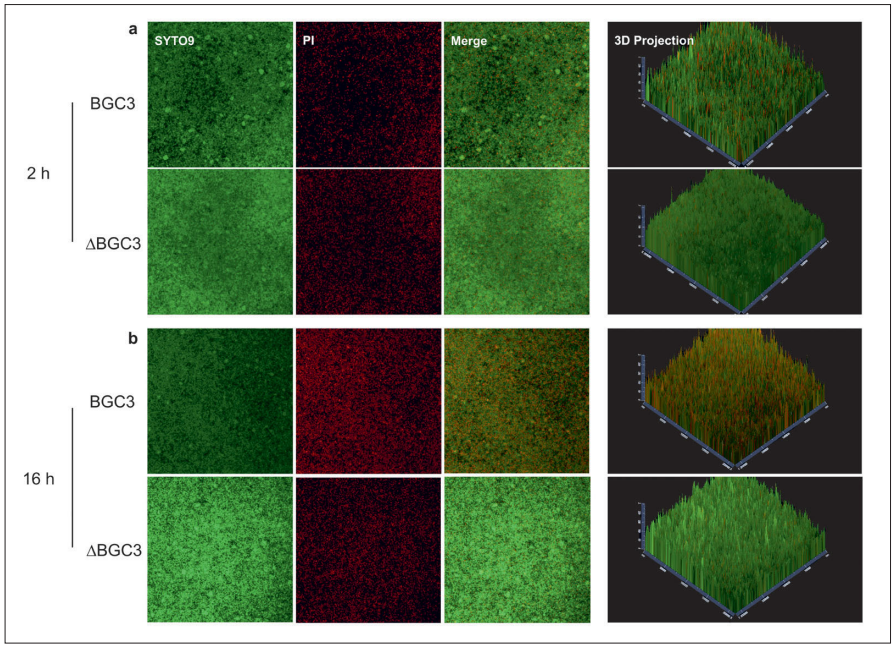

Fig 4a and b Confocal microscope images of biofilms at 2 and 16 hours. Green indicates living/active cells (SYTO9) and red shows inactive/dead cells (PI). Confocal microscope images of biofilms cultured for 2 hours **(a)**. Confocal microscope images of biofilms cultured for 16 hours **(b)**.

mutant compared to the BGC3 strain ($P < 0.05$), as indicated in Fig 3.

Bacterial viability and dominance of ΔBGC3 in co-culture

SYTO9-PI live/dead staining enabled clear differentiation between viable (green) and dead (red) bacteria. At 2 hours (Fig 4a) and particularly at 16 hours (Fig 4b), the BGC3 group exhibited more dead bacteria.

In co-culture assays, BGC3 displayed significantly lower viability when competing with ΔBGC3. A growth competition assay was conducted to assess any potential growth benefits of BGC3. This process involved mixing the two bacterial cultures in a ratio of approximately 50:50 and culturing them together in fresh medium. This assay, conducted over various hours, indicated superior growth in ΔBGC3 compared to the wild-type strain, as shown in Fig 5.

Discussion

Six types of hybrid PKS/NRPS gene clusters have been identified in *S. mutans*. BGC1, with the highest detection rate, has been shown to confer protection against oxygen and H_2O_2 stress, thereby enabling *S. mutans* to counteract the defence mechanisms of pioneer colonisers.[8] Our analysis of 413 *S. mutans* genomes revealed that the frequency of BGC3, the focus of this study, ranked second. Notably, *S. mutans* strains both with and without

the BGC3 gene clusters exist naturally.[8] However, the specific functions of BGC3 have not been explored previously.

S. mutans, as the primary pathogen in human dental caries, manifests its cariogenic toxicity predominantly in three aspects: strong adhesion ability, generation of substantial amounts of organic acids leading to the corrosion of dental hard tissues, and the ability to withstand environmental stress, particularly under low pH conditions.[1,15] Therefore, we sought to compare the impacts of BGC3 and ΔBGC3 on the virulence of *S. mutans* in these respects. Considering that the adhesion of *S. mutans* to teeth surface relies on sucrose-dependent and independent mechanisms, we measured the expression levels of five related genes in total. Among them, the sucrose-independent adhesin gene *SpaP* represents adhesion in a sucrose free environment.[16] In the sucrose-dependent mechanism, *gtfC*, *gtfD* can synthesise glucans, while *ftf* is related to fructans synthesis.[17,18] The response regulator *VicR* positively regulated the expression of exopolysaccharide synthesis and adhesion related genes *gtfC*, *gtfD* and *ftf*.[19] The glucosyltransferase genes (*gtfC*, *gtfD*) and a single fructosyltransferase gene (*ftf*) encode enzymes which are important in formation of exopolysaccharides, and these genes are also more frequently detected in research. The expressions of gtf and *ftf* genes were crucial for the initial adhesion of *S. mutans* to the tooth surfaces.[20] However, the sucrose-independent mechanism cannot be ignored, and in order to be as comprehensive as possible, we have selected these genes. In this study, compared to the wild type, the knockout strain showed significantly higher expression of the aforementioned genes, indicating that the impact of BGC3 on the two adhesion mechanisms of *S. mutans* is consistent. *VicRK* is a signalling system of *S. mutans* in response to environmental changes. The response regulator *VicR* positively regulated the expression of exopolysaccharide synthesis and adhesion related genes *gtfC*, D and *ftf*.[19,21] The trend of the expression of these genes was the same in this study. By measuring the expression of these genes, we found that the presence of BGC3 reduced the expression of virulence genes related to adhesion of *S. mutans*; however, the mechanisms require further study.

The ΔBGC3 strain exhibits greater acid tolerance and significantly higher expression of the acid tolerance-related gene *atpF* than the wild-type strain. The *atpF* gene encodes the H^+-translocating ATPase on the cell membrane. It hydrolyses ATP and expels protons to maintain a transmembrane pH gradient, making a relatively alkaline environment inside the cell.[22] The presence of BGC3 may affect bacterial tolerance to acidic environments by downregulating the expression of atpF. We found no significant difference in acid production between the BGC3 and ΔBGC3 *S. mutans* strains. An article reported that the presence of BL-BGCs significantly reduced the biofilm pH in *S. mutans*, while other virulence and fitness properties remained unchanged compared to the knockout strain.[9] Thus it can be seen that different BGC gene clusters may have different effects on the acid production and acid resistance of *S. mutans*.

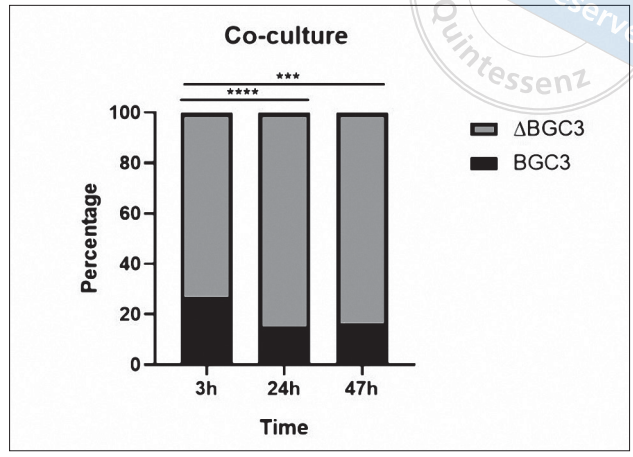

Fig 5 Co-culture of BGC3 and ΔBGC3 in a 50:50 ratio over different durations. The vertical axis represents the percentages of BGC3 and ΔBGC3 strains. ***$P < 0.001$, ****$P < 0.0001$.

In this study, the ΔBGC3 strain exhibited lower mortality and dominated in co-culture experiments compared to the wild type, while the BGC3 strain presented worse adaptability to harsh environments, which indicates the presence of BGC3 negatively affected the expression of certain virulence genes. This outcome is understandable, secondary metabolite synthesis demanded substantial energy which imposes an additional metabolic burden on *S. mutans*. Therefore, gene deletion may reduce the energy consumption associated, offering a survival advantage.[23] In addition, *S. mutans* has also been detected in a caries-free group,[24] which provides evidence to suggest that the cariogenic ability of different *S. mutans* strains varies. Moreover, previous studies suggest that the numerous BGCs identified in *S. mutans* may affect its cariogenic virulence from different perspectives, raising questions about potential interactions among them.[6,9,10]

For *S. mutans* strains that do not carry BGC3, it is easier to withstand the screening of acidic environment and survive, which may be conducive to the expression of other cariogenic gene clusters and provide a good basis for cariogenesis. However, it is necessary to con-

sider the limitations of in vitro experiments. Further studies should examine the effect of BGC3 on plaque biofilms containing a variety of bacteria. Furthermore, given the complex bacteria-host interactions, animal models could reflect the role of BGC3 more intuitively.

Conclusion

Overall, the BGC3 gene cluster in *S. mutans* was associated with bacterial acid tolerance and expression of adhesion-related genes, and the knockout strain exhibited greater adaptability, highlighting the potential influence of this gene cluster on bacterial survival and virulence characteristics.

Conflicts of interest

The authors declare no conflicts of interest related to this study.

Author contribution

Drs Jing Yi YANG, Yi Xin ZHANG and Yu Wei ZHANG contributed to the acquisition and analysis of data and the drafting, revision and editing of the manuscript; Drs Ying CHEN, Min Di XU and Dan Dan WANG contributed to the acquisition and analysis of data; Drs Yi Hua CHEN, Bin XIA and Yi Xiang WANG contributed to the conception and study design; Drs Bin XIA and Yi Xiang WANG also contributed to the critical revision of the manuscript.

(Received Apr 16, 2024; accepted Dec 06, 2024)

References

1. Lemos JA, Abranches J, Burne RA. Responses of cariogenic streptococci to environmental stresses. Curr Issues Mol Biol 2005;7:95–107.
2. Abranches J, Zeng L, Kajfasz JK, et al. Biology of oral streptococci. Microbiol Spectr 2018;6:10.
3. Loesche WJ. Role of *Streptococcus mutans* in human dental decay. Microbiol Rev 1986;50: 353–380.
4. Baker JL, Faustoferri RC, Quivey RG Jr. Acid-adaptive mechanisms of Streptococcus mutans-The more we know, the more we don't. Mol Oral Microbiol 2017;32:107–117.
5. Baker JL, Abranches J, Faustoferri RC, et al. Transcriptional profile of glucose-shocked and acid-adapted strains of Streptococcus mutans. Mol Oral Microbiol 2015;30:496–517.
6. Liu L, Hao T, Xie Z, Horsman GP, Chen Y. Genome mining unveils widespread natural product biosynthetic capacity in human oral microbe Streptococcus mutans. Sci Rep 2016;6:37479.
7. Bérdy J. Thoughts and facts about antibiotics: Where we are now and where we are heading. J Antibiot (Tokyo) 2012;65:385–395.
8. Wu C, Cichewicz R, Li Y, et al. Genomic island TnSmu2 of Streptococcus mutans harbors a nonribosomal peptide synthetase-polyketide synthase gene cluster responsible for the biosynthesis of pigments involved in oxygen and H2O2 tolerance. Appl Environ Microbiol 2010;76:5815–5826.
9. Momeni SS, Beno SM, Baker JL, et al. Caries-associated biosynthetic gene clusters in Streptococcus mutans. J Dent Res 2020;99:969–976.
10. Li ZR, Sun J, Du Y, et al. Mutanofactin promotes adhesion and biofilm formation of cariogenic Streptococcus mutans. Nat Chem Biol 2021;17:576–584.
11. Engler C, Gruetzner R, Kandzia R, Marillonnet S. Golden gate shuffling: A one-pot DNA shuffling method based on type IIs restriction enzymes. PLoS One 2009;4:e5553.
12. Hao T, Xie Z, Wang M, et al. An anaerobic bacterium host system for heterologous expression of natural product biosynthetic gene clusters. Nat Commun 2019;10:3665.
13. Xie Z, Qi F, Merritt J. Cloning-independent plasmid construction for genetic studies in streptococci. J Microbiol Methods 2013;94:77–82.
14. Shailaja A, Bruce TF, Gerard P, Powell RR, Pettigrew CA, Kerrigan JL. Comparison of cell viability assessment and visualization of Aspergillus niger biofilm with two fluorescent probe staining methods. Biofilm 2022;4:100090.
15. Krzyściak W, Jurczak A, Kościelniak D, Bystrowska B, Skalniak A. The virulence of Streptococcus mutans and the ability to form biofilms. Eur J Clin Microbiol Infect Dis 2014;33: 499–515.
16. Yang J, Deng D, Brandt BW, et al. Diversity of SpaP in genetic and salivary agglutinin mediated adherence among Streptococcus mutans strains. Sci Rep 2019;9:19943.
17. Durso SC, Vieira LM, Cruz JN, Azevedo CS, Rodrigues PH, Simionato MR. Sucrose substitutes affect the cariogenic potential of Streptococcus mutans biofilms. Caries Res 2014;48:214–222.
18. Guan C, Che F, Zhou H, Li Y, Li Y, Chu J. Effect of rubusoside, a natural sucrose substitute, on Streptococcus mutans biofilm cariogenic potential and virulence gene expression in vitro. Appl Environ Microbiol 2020;86:e01012–e01020.
19. Lei L, Long L, Yang X, et al. The VicRK two-component system regulates Streptococcus mutans virulence. Curr Issues Mol Biol 2019;32:167–200.
20. Salehi R, Savabi O, Kazemi M, et al. Effects of Lactobacillus reuteri-derived biosurfactant on the gene expression profile of essential adhesion genes (gtfB, gtfC and ftf) of Streptococcus mutans. Adv Biomed Res 2014;3:169.
21. Senadheera MD, Guggenheim B, Spatafora GA, et al. A VicRK signal transduction system in Streptococcus mutans affects gtfBCD, gbpB, and ftf expression, biofilm formation, and genetic competence development. J Bacteriol 2005;187: 4064–4076.
22. Sturr MG, Marquis RE. Comparative acid tolerances and inhibitor sensitivities of isolated F-ATPases of oral lactic acid bacteria. Appl Environ Microbiol 1992;58:2287–2291.
23. Xie Z, Zhang Z, Liu L, Liu X, Chen Y. Secondary metabolites from Streptococcus mutans and their ecological roles in dental biofilm [in Chinese]. Sheng Wu Gong Cheng Xue Bao 2017;33:1547–1554.
24. Zhang Y, Fang J, Yang J, et al. Streptococcus mutans-associated bacteria in dental plaque of severe early childhood caries. J Oral Microbiol 2022;14:2046309.

Oral Microbiota Profiling by CLIN-MALDI-TOF-MS: Distinct Representative Species Across Sites

Yang Jia LIU[1], Cai Ping MA[2], Feng CHEN[1]

Objective: *To establish a rapid and high-throughput clinical matrix-assisted laser desorption ionisation-time of flight mass spectrometry (CLIN-MALDI-TOF-MS) method for identifying oral microorganisms and to determine the distinct representative species across various oral sites.*
Methods: *Samples were collected from 54 volunteers from four oral sites: saliva, supragingival plaque, oral mucosa and dorsum of the tongue. Microorganisms were cultured on brain heart infusion (BHI) plates and identified using CLIN-MALDI-TOF-MS after processing with specific reagents for mass spectrometry.*
Results: *The method identified 15 species and 12 genera of microorganisms, revealing significant differences in microbial composition among the oral sites, and different oral cavity sites harboured distinct relatively representative species.*
Conclusion: *The CLIN-MALDI-TOF-MS method offers a rapid and efficient approach for large-scale microbial identification in the oral cavity, providing a suitable approach for future experimental teaching and highlighting the importance of site-specific microbial communities in oral health research.*
Keywords: *CLIN-MALDI-TOF-MS, oral microbe identification, rapid and high-throughput identification, representative species differences*
Chin J Dent Res 2025;28(1):63–71; doi: 10.3290/j.cjdr.b6097814

The oral cavity is home to various microorganisms, making the oral microbiome the second largest microbial community in the human body after the gut microbiome.[1] The oral microbiota consists of bacteria, fungi, viruses and protozoa, with bacteria being the most significant component. Bacterial species alone amount to more than 40 genera and 700 species. The Human Microbiome Project (HMP) examined the microbial composition of nine parts of the oral cavity (buccal mucosa, hard palate, keratinised gingiva, palatine tonsils, saliva, supra- and subgingival plaque, larynx and dorsum of the tongue) in samples from around 200 individuals and found 185 to 355 genera of bacteria in 13 to 19 phyla.[2] Microorganisms vary from person to person and change dynamically under different clinical conditions and microenvironments and due to other influences. Several studies have confirmed that microorganisms are the aetiological agents of various oral diseases (such as periodontitis,[3] caries,[4] oral candidiasis[5] and mucositis[6]), and they have also been suggested to be potentially linked to several systemic diseases, such as diabetes,[7] cardiovascular diseases,[8] cancers[9] and Alzheimer's disease.[10] Studies have shown that the pathogenesis and progression of dental caries, an oral disease, may be associated with *Streptococci*, *Porphyromonas*, *Prevotella* spp. and *Lactobacillus* spp. in the oral cavity.[11,12] Individuals with periodontal disease or tooth loss are at an increased risk of gastrointestinal cancers caused by oral bacteria.[13,14] Carrying the oral

1 Central Laboratory, Peking University School and Hospital of Stomatology & National Center for Stomatology & National Clinical Research Center for Oral Diseases & National Engineering Research Center of Oral Biomaterials and Digital Medical Devices, Beijing, P.R. China.
2 Experimental Teaching Center of Modern Life Science, School of Life Sciences, Tsinghua University, Beijing, P.R. China.

Corresponding authors: Dr Cai Ping MA, Experimental Teaching Center of Modern Life Science, School of Life Science, Tsinghua University, Haidian District, Beijing 100084, P.R. China. Email: mcp@tsinghua.edu.cn.

Dr Feng CHEN, Central Laboratory, Peking University School and Hospital of Stomatology, #22 Zhongguancun South Avenue, Haidian District, Beijing 100081, P.R. China. Email: chenfeng2011@hsc.pku.edu.cn.

This study was supported by grants from the 6th Laboratory Innovation Fund of Tsinghua University, the China Postdoctoral Science Foundation (grant number 2023M740139), the National Key Research and Development Program of China (grant number 2022YFA1206103 and 2022YFE0118300), and the National Natural Science Foundation of China (grant number 81991501).

pathogens *Porphyromonas gingivalis* and *Porphyromonas actinomycetemcomitans* is associated with an increased risk of pancreatic cancer.[15] *Klebsiella* spp. strains from the salivary microbiota colonise the gut and effectively induce chronic intestinal inflammation.[16]

Furthermore, Chen et al[17] found that hypertensive patients had increased oral-gut microbiota exchanges, and in particular, the proportion of microorganisms of salivary origin in the gut microbiota was increased significantly, with the most significant increase seen in the relative abundance of *Veillonella*. This suggests that the oral microbiome plays a vital role in the microbial community and human health.[18] Moreover, investigating characteristics such as the composition and proportion of oral microbiota can reveal the relationship between the occurrence of diseases and microbial communities, providing a rational theoretical basis for their prevention and treatment.

Traditional microbial diversity research relies on isolation and culture techniques to identify microorganisms through morphological observation, physiological and biochemical characteristics and immunoserotyping.[19] This method is well-established but has significant drawbacks: it is time-consuming and laborious with poor accuracy; there are several bacteria in the oral cavity that are difficult to culture under the current technological conditions; and it cannot accurately reflect the actual composition of the microbial species and numbers in the oral cavity. Using molecular biology and other related techniques has provided new tools for studying microbial diversity, allowing for the direct detection of microorganisms in the oral cavity. It can provide a truer reflection of the distribution and composition of these microorganisms. Until now, the most widely used techniques have been fingerprinting based on PCR amplification, macro-genomic technology based on DNA libraries, metabolomic and proteomic technology based on high-sensitivity chemical analysis, and high-throughput sequencing technology.[20] The application and combination of these technological approaches makes it possible to explore the characteristics of oral microbial communities better.

CLIN-TOF-MS microbial identification is established based on MALDI-TOF-MS (matrix-assisted laser desorption ionisation-time of flight mass spectrometry) technology.[21] MALDI-TOF-MS contributes to diagnosing tumours, rheumatoid arthritis, Alzheimer's disease and allergies by identifying specific biochemical markers.[22] Thanks to its rapid and high-throughput characterisation, it can solve various problems in the identification of microorganisms in the clinic and laboratory, and it is a standard method that can be used for rapid and accurate identification of microorganisms. CLIN-TOF-MS fits the peak plots of mass spectra based on the mass-to-charge ratio (m/z ratio) of flying atoms through thousands of excitations of the charged microbial lysate at the target site and is, therefore, a plausible result with a high repetition rate.[23] To complete the identification of microorganisms, CLIN-MALDI-TOF-MS can collect the unique fingerprints of specific biochemical markers of the microorganisms to be tested, process these fingerprints through the software and compare them with the standard fingerprints of various known microorganisms in the database. To verify whether this method is quick and effective at identifying microbial species, the present authors recruited volunteers, and four sites, namely saliva, mucosal tissues, tooth surface and dorsum of the tongue, were selected for microbial sampling, culture and identification, and the obtained oral microorganisms were characterised after culturing using CLIN-TOF-MS methods. Our study found suitable applications for this method and different microbial-dominant strains in various oral cavity sites.

Materials and methods

Ethical approval

All studies conformed to the research ethics guidelines of Peking University School and Hospital of Stomatology and all experimental works were approved by the Ethics Committee of Peking University School and Hospital of Stomatology (2023-55). All the participants gave written informed consent.

Sampling of oral microflora

A total of 54 volunteers with no obvious oral diseases were recruited to participate in this research. To mitigate potential variations in microbial composition due to different time points, sampling was conducted at 9:00 a.m. The volunteers were from two classes in the same college grade, shared relatively uniform daily routines and were instructed to rinse their mouths after breakfast to remove any food debris. The samples were collected from four locations inside the oral cavity: saliva, supragingival plaque on the surface of the teeth, dorsum of the tongue and oral mucosa.

Collection of saliva

There are four ways to collect unstimulated saliva. The first is to have the volunteer hold a sterile container; sit

still with their head down, mouth slightly open, eyes open and head slightly forward; avoid swallowing and allow the saliva to flow naturally into the container. The second is to have the volunteer sit still with their head up, avoiding swallowing, keep the saliva in the mouth and spit it into the container. The third is to sample the saliva by placing a sterile absorbent pad in the mouth, then squeeze the saliva into a container. Collecting saliva with absorbent material should avoid removing plaque from the mucosal surface. Collecting 1 ml unstimulated saliva usually takes 5 to 10 minutes. The fourth method involves having the volunteer sit in a dental chair with their mouth open. A sterile syringe is then used to aspirate the accumulated saliva from the mouth.

Collection of supragingival plaque on the tooth surface

The volunteers opened their mouths and the sampling site was isolated from saliva with sterile cotton before sampling. Plaque samples were scraped from the surface of the target teeth using a sterile swab. Dental plaque was later collected by scrubbing in prepared phosphate-buffered saline (PBS) buffer (1×) for around 1 minute.

Sampling of plaque on the surface of the oral mucosa

The sampling sites on the oral mucosa mainly included the buccal mucosa and palate. Volunteers rinsed their mouths with purified water before sampling to remove food residue, then scraped the plaque on the surface of the mucosa with a sterile swab, put it in a sterile 1.5 ml tube and wash it repeatedly in the tube with PBS buffer.

Sampling of microorganisms on the dorsum of the tongue

Volunteers rinsed their mouths with purified water before sampling to remove any food residue. They opened their mouth, stuck out their tongue slightly and brushed from one side to the other with a sterile swab before placing it in a sterile 1.5 ml tube and rinsing it repeatedly with PBS buffer.

Sample processing and culture of oral microflora

The collected oral microbiological samples were centrifuged at 14,000 rpm for 15 minutes at 4°, after which the supernatant was discarded, and the sediment was left as the microbiological sample for subsequent testing. The precipitated colonies were resuspended with 1× PBS to create a microbial suspension, which was plated onto the brain heart infusion (BHI) medium plates and incubated overnight at 37° in a thermostatic incubator. To pick out the single clones, the microbial suspension was plated using a non-uniform plating method, i.e., two-thirds of the plate was spread evenly with the suspension and the remaining one-third was scraped in one direction with a small amount of suspension left on the applicator stick. All plates grew colonies, and then the following steps were performed.

Identification of oral microflora

After incubation, a single clone of microorganisms was picked up using a sterile cotton swab from the BHI plates and applied to the stainless-steel target plate supplied with the instrument, spreading it evenly to form a thin film. According to the manufacturer's instructions, 1 μl component I (bacterial processing reagents for time-of-flight mass spectrometry systems, Bioyong, Beijing, China) was pipetted over the above bacterial membrane and dried at room temperature to lyse the bacteria. Then, to charge the lysate, 1 ul component II was taken with a pipette to cover the exact position of the previous step and dried at room temperature, and the target plate was put into the time-of-flight mass spectrometry system (CLIN-TOF-II, Bioyong) for detection. Vacuuming began after the target plate was placed and the hatch was closed. Mass spectrometry can be performed when the pressure value is less than $5\times e^{-6}$ mbar. The parameters of energy, spectrum, null and optimal pulse extraction (Da) were set to 20 to 200 mv, 100, 1,000 and 8,330 Da, respectively. The curve was first calibrated by using *Escherichia coli* as a standard sample and setting the tolerance to 700 ppm. Afterwards, profile spectra were obtained by averaging 400 laser shots per sample, with a defined peak intensity mass range (measured in m/z) of 1,000 to 10,000.

Results

Establishment of an experimental process for microbial identification based on culture and CLIN-TOF-MS

We identified microbial species through a series of processes. The specific experimental process, as depicted in Fig 1, included sample collection, microbial culture, selection of single colonies, pretreatment of bacteria, identification by CLIN-TOF-MS and data analysis.

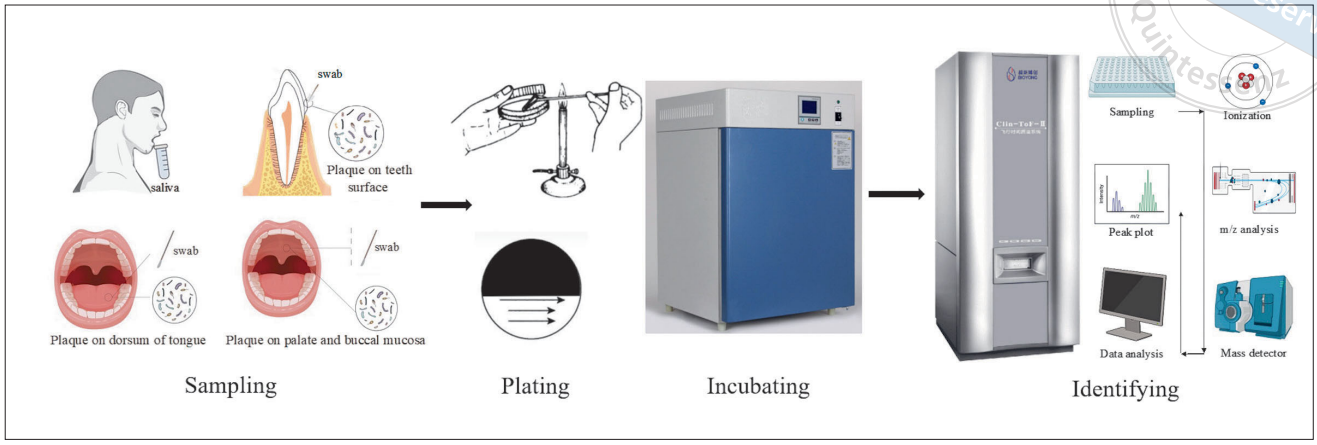

Fig 1a to c Schematic diagram of the experimental flow. The flowchart represents a simple process from sampling, incubation and sample processing to CLIN-TOF mass spectrometry identification. Some cartoons in this figure were from BioRender.com.

Rapidly available mass spectrometry profiles for microbial identification

The selected single colonies were plated on the wells of the target plate, and after treatment with the reagents, they were placed into the mass spectrometer to obtain the data. A total of 54 samples were identified in the CLIN-TOF mass spectrometry. As a result, 15 microorganisms were identified, and they belonged to 12 genera of bacteria (Table 1 and Fig S1 [provided on request]). Among them, the peak plots of the typical eight strains of bacteria identified are shown in Fig 2.

E. coli and *Staphylococcus aureus* were used as positive controls to verify the reliability of the experiment, and normal saline as a negative control. We also performed CLIN-TOF-MS under the same conditions and reagent treatments. Both *E. coli* and *S. aureus* controls were successfully recognised with a reasonably high confidence level. At the same time, normal saline did not match any of the bacteria, i.e., the confidence level for none of the bacteria was 0. These findings indicate that the experimental results are credible.

Relatively representative species vary from different oral locations

Statistical analysis of the results of CLIN-TOF identification showed that we obtained different numbers of strains identified at various sampling sites. The tooth surface had the highest number of strains detected at 15, compared to the mucosal tissue, the dorsum of the tongue and the saliva, where 13 strains each were detected.

The composition of the species obtained from the identification of the different sampling sites is shown in Fig 3. The results show that the relatively representative species differ in different oral locations. In the saliva samples, the most significant percentage was *Streptococcus salivarius*, at 46%. As for tooth surface, the largest proportion was *S. aureus*, at 40%. In contrast, in mucosal tissues, although *S. aureus* was the most abundant, there were no typical species with a higher percentage, as in the microbial composition of the dorsum of the tongue.

Discussion

There are a variety of habitats in the oral cavity that, together, form the oral micro-ecosystem, and each microenvironment houses a specific microbial community, with the amounts of colonising bacteria varying widely depending on the site. The bacterial community of different oral sites has different characteristics and can provide various information. Saliva comes from a variety of sources and soaks into almost all surfaces of hard and soft tissues, and can be used to study a wide range of oral diseases, as well as some systemic diseases.[24] In the present study, the most representative species in the saliva samples was *S. salivarius*, a genus of *Streptococcus* that belongs to the normal flora of the oral cavity. The known possible functions of *S. salivarius* include promoting oral health and improving intestinal function and anti-inflammatory bioactivity of specific subspecies (such as K12).[25] On the surfaces of hard and soft tissues of the oral cavity, microorganisms are present as biofilms that form the so-called plaque on the surface, which is a complex structure. Plaque from the oral mucosa may facilitate the understanding of oral mucosal diseases and the development of therapeutic options. Unlike the

Table 1 Strains identified by CLIN-TOF-MS.

Number	Sampling site	Species identified	Genus
1	Surface of teeth	*Acinetobacter calcoaceticus-baumannii* complex	*Acinetobacter*
2	Surface of teeth	*Bacillus cereus*	*Bacillus*
3	Surface of teeth	*Neisseria macacae*	*Neisseria*
4	Surface of teeth	*Rothia mucilaginosa*	*Rothia*
5	Surface of teeth	*Schizosaccharomyces pombe*	*Schizosaccharomyces*
6	Surface of teeth	*Staphylococcus aureus*	*Staphylococcus*
7	Surface of teeth	*Staphylococcus aureus*	*Staphylococcus*
8	Surface of teeth	*Staphylococcus aureus*	*Staphylococcus*
9	Surface of teeth	*Staphylococcus aureus*	*Staphylococcus*
10	Surface of teeth	*Staphylococcus aureus*	*Staphylococcus*
11	Surface of teeth	*Staphylococcus aureus*	*Staphylococcus*
12	Surface of teeth	*Staphylococcus epidermidis*	*Staphylococcus*
13	Surface of teeth	*Staphylococcus epidermidis*	*Staphylococcus*
14	Surface of teeth	*Staphylococcus epidermidis*	*Staphylococcus*
15	Surface of teeth	*Staphylococcus epidermidis*	*Staphylococcus*
16	Oral mucosa-Palate	*Rothia mucilaginosa*	*Rothia*
17	Oral mucosa-Palate	*Staphylococcus aureus*	*Staphylococcus*
18	Oral mucosa-Palate	*Streptococcus salivarius*	*Streptococcus*
19	Oral mucosa-Palate	*Streptococcus salivarius*	*Streptococcus*
20	Oral mucosa-Buccal mucosa	*Cronobacter sakazakii*	*Cronobacter*
21	Oral mucosa-Buccal mucosa	*Klebsiella oxytoca*	*Klebsiella*
22	Oral mucosa-Buccal mucosa	*Neisseria sicca*	*Neisseria*
23	Oral mucosa-Buccal mucosa	*Rothia mucilaginosa*	*Rothia*
24	Oral mucosa-Buccal mucosa	*Rothia mucilaginosa*	*Rothia*
25	Oral mucosa-Buccal mucosa	*Staphylococcus aureus*	*Staphylococcus*
26	Oral mucosa-Buccal mucosa	*Staphylococcus aureus*	*Staphylococcus*
27	Oral mucosa-Buccal mucosa	*Staphylococcus aureus*	*Staphylococcus*
28	Oral mucosa-Buccal mucosa	*Streptococcus salivarius*	*Streptococcus*
29	Dorsum of the tongue	*Acinetobacter calcoaceticus-baumannii complex*	*Acinetobacter*
30	Dorsum of the tongue	*Bacillus cereus*	*Bacillus*
31	Dorsum of the tongue	*Bacillus cereus*	*Bacillus*
32	Dorsum of the tongue	*Bacillus cereus*	*Bacillus*
33	Dorsum of the tongue	*Bacteroides helcogenes*	*Bacteroides*
34	Dorsum of the tongue	*Rothia mucilaginosa*	*Rothia*
35	Dorsum of the tongue	*Rothia mucilaginosa*	*Rothia*
36	Dorsum of the tongue	*Staphylococcus aureus*	*Staphylococcus*
37	Dorsum of the tongue	*Staphylococcus aureus*	*Staphylococcus*
38	Dorsum of the tongue	*Staphylococcus epidermidis*	*Staphylococcus*
39	Dorsum of the tongue	*Staphylococcus epidermidis*	*Staphylococcus*
40	Dorsum of the tongue	*Streptococcus salivarius*	*Streptococcus*
41	Dorsum of the tongue	*Bacillus cereus*	*Bacillus*
42	Saliva	*Agromyces bracchium*	*Agromyces*
43	Saliva	*Neisseria flavescens*	*Neisseria*
44	Saliva	*Neisseria flavescens*	*Neisseria*
45	Saliva	*Propionibacterium acnes*	*Propionibacterium*
46	Saliva	*Rothia mucilaginosa*	*Rothia*
47	Saliva	*Staphylococcus aureus*	*Staphylococcus*
48	Saliva	*Staphylococcus epidermidis*	*Staphylococcus*
49	Saliva	*Streptococcus salivarius*	*Streptococcus*
50	Saliva	*Streptococcus salivarius*	*Streptococcus*
51	Saliva	*Streptococcus salivarius*	*Streptococcus*
52	Saliva	*Streptococcus salivarius*	*Streptococcus*
53	Saliva	*Streptococcus salivarius*	*Streptococcus*
54	Saliva	*Streptococcus salivarius*	*Streptococcus*

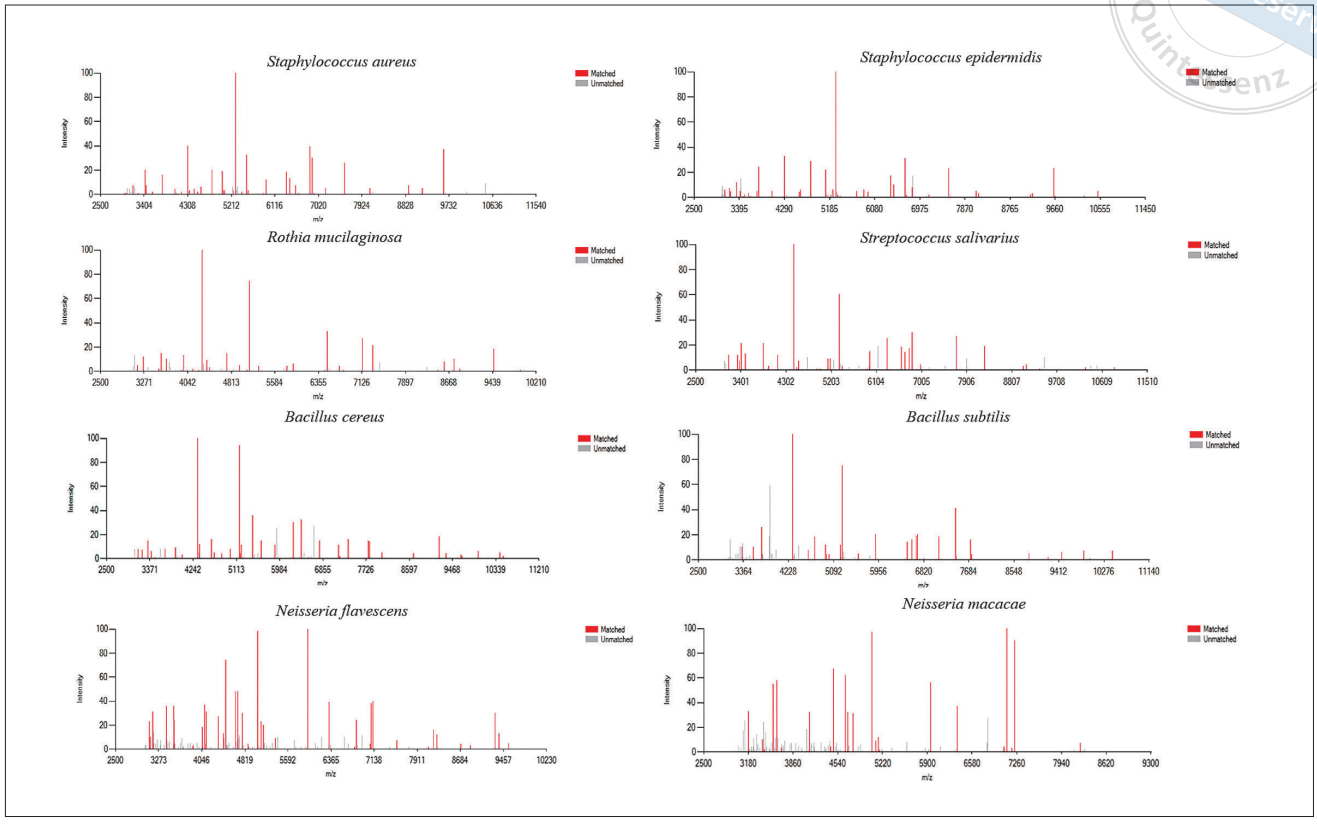

Fig 2 Summary of mass spectrometry profiles. The profiles of several typical strains of bacteria identified by mass spectrometry were selected for the figure. The horizontal coordinate m/z represents the mass-to-charge ratio, and the vertical coordinate represents the relative signal intensity. The red indicates the signals that match the species' standard mass spectral peak plots, and the grey colour shows the signals that failed to match the standard mass spectral peak plots.

exfoliated surfaces of the oral epithelium, the tooth surface is the only non-shedding surface in the oral cavity.[26] This non-shedding surface contributes to the stability of the location where biofilms develop over time.

Moreover, as the biofilm matures, the microbial community becomes more complex, which explains why the most significant number of species was found on the tooth surface (Table 1). Of these, *S. aureus* has the highest percentage on the tooth surface (Fig 3), a prominent human pathogen that colonises the nasal cavity, skin, intestines and oral cavity as commensal bacteria.[27] Under appropriate microenvironmental conditions, *S. aureus* forms part of the biofilm microbiota.[28] In addition to producing many virulence factors such as toxins and exoenzymes, *S. aureus* also produces factors that act on specific cellular receptors and the complement system, as well as innate immune antimicrobial peptides that prevent host derivation.[29,30] There is increasing experimental evidence of an association between *S. aureus* and endodontic infections,[31] peri-implantitis,[32] periodontitis[33] and angular cheilitis,[34] etc. Thus, the present findings reinforce the importance of studying *S. aureus*.

The oral cavity is a complex ecosystem where microbial interactions and network relationships play a crucial role in shaping microbial community dynamics. The present findings, which highlighted the distinct microbial populations at different oral sites, underscore the importance of these interactions in maintaining oral health and potentially influencing disease progression. In the context of these results, it is noteworthy that the interactions between bacteria, such as synergistic and competitive relationships, can significantly affect the overall composition and function of the oral microbiota. For instance, Nguyen et al[35] reported that certain species can promote the growth of others through the production of growth factors or by creating a favourable microenvironment. Conversely, competition for nutrients can lead to the suppression of some species, thus influencing the stability of the microbial community.[36] Our findings suggest that more species were detected on the surface of the teeth, which may reflect the complex interplay of these ecological processes. The biological significance of the distinct microbial signatures observed at different oral sites

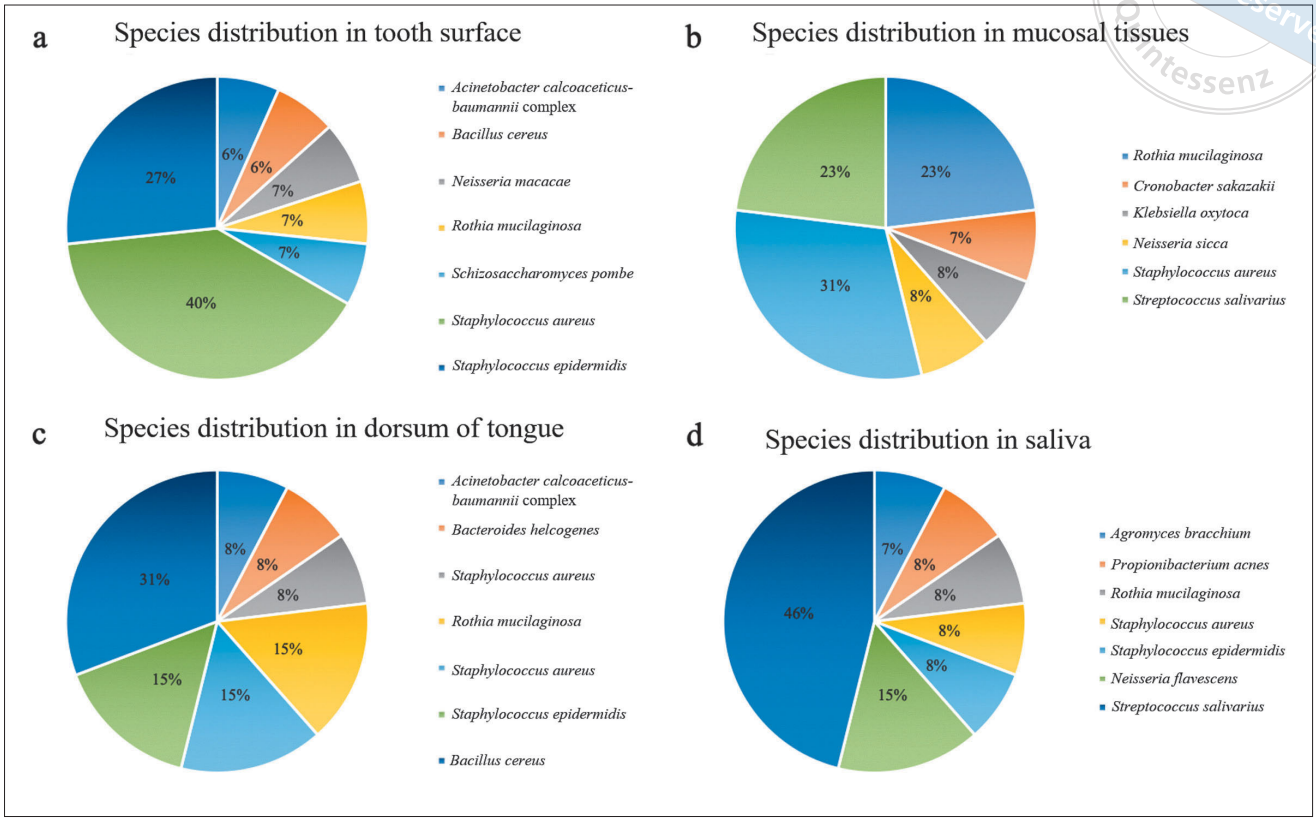

Fig 3a to d Colony abundance statistics. Each sector graph represents the species composition of one sampling site, with the sampling sites being the tooth surface **(a)**, oral mucosal tissue **(b)**, dorsum of the tongue **(c)** and saliva **(d)**.

could also relate to these locations' unique microenvironments and host factors. For example, the dorsum of the tongue, with its rough surface and variable moisture, may harbour a distinct set of species adapted to these conditions.[37] Similarly, the gingival crevice near the gingival epithelium may support a community enriched with species capable of interacting with host immune responses.[38] In conclusion, the present research provides a foundation for further exploration of the intricate relationships within the oral microbiota and their implications for oral health.

As technology advances and research into the microbiome increases, there is a need for reliable, feasible and practical sampling strategies for the oral microbiome to work towards sampling more microbial samples. In this paper, the present authors constructed a rapid method for identifying microbial species, where 54 microorganisms belonging to 15 species and 12 genera were cultured and identified from different oral sampling sites through a process of sampling, incubation and identification by mass spectrometry with CLIN-TOF (Fig 1). The time required in this set of processes is very short, with mass spectrometry identification taking less than 1 minute per sample. It is also more cost-effective with the main reagent components of acetonitrile, formic acid, trifluoroacetic acid and a-cyano-4-hydroxycinnamic acid. Compared to sequencing methods such as 16sRNA,[39] it saves nearly 2 hours of PCR time, half an hour of PCR purification and more, including a day of waiting for sequencing. In a clinical environment where microbial species urgently need to be identified, it is possible to apply the collected clinical samples directly to a metal target plate and, after lysis and charging, to quickly identify what species the sample belongs to using CLIN-TOF, so that a clinical treatment plan can be designed in time for the characterisation of this species. In addition, the requirement of high throughput can also be achieved by the 96-well target plate. Of course, the present study still poses specific problems, such as the fact that the number of samples was not large enough. In the future, we will continue to recruit volunteers and cultivate more colony samples using culturomics methods to increase our data volume. Still, the current results fully

support the conclusion that our experimental process is capable of rapid and high-throughput microbial species identification.

In addition to identifying microorganisms experimentally and clinically, the method constructed in this paper can be applied to the teaching of microbiology laboratory courses. In our new "Fun with Microorganisms" course, we dedicated 3 class hours to giving a lecture about microbial identification by CLIN-TOF-MS. Students mastered the method of rapid microbial species identification using mass spectrometry through sampling, culturing, target spotting, sample processing and mass spectrometry identification (Fig 1), and also gained a deeper appreciation and knowledge of the structure and diversity of oral microbial communities.

Conclusion and prospects

In this paper, a rapid and high-throughput method for the identification of microorganisms, i.e., sampling, incubation and CLIN-MALDI-TOF mass spectrometry, was successfully constructed. From 54 examples of samples, 15 microorganisms belonging to 12 genera were identified. They were classified and analysed according to different sampling sites, suggesting that the representative species varies across oral sites. The finding of significant differences in microbial communities across oral sites contributes to our understanding of how specific microbes function in different oral microenvironments. It lays the groundwork for future studies of how they are associated with oral health and disease states. This article also provides a foundation for rapidly identifying microorganisms and the future survey of microbe-disease relationships.

Conflicts of interest

The authors declare no conflicts of interest related to this study.

Author contribution

Dr Yang Jia LIU contributed to performing the experiments, analysing the data and drafting the manuscript; Drs Cai Ping MA and Feng CHEN contributed to the review and revision of the manuscript; Dr Feng CHEN provided the idea and created the conceptual framework.

(Received Apr 30, 2024; accepted Sep 20, 2024)

References

1. Caselli E, Fabbri C, D'Accolti M, et al. Defining the oral microbiome by whole-genome sequencing and resistome analysis: The complexity of the healthy picture. BMC Microbiol 2020;20:120.
2. Zaura E, Nicu EA, Krom BP, Keijser BJ. Acquiring and maintaining a normal oral microbiome: current perspective. Front Cell Infect Microbiol 2014;4:85.
3. How KY, Song KP, Chan KG. Porphyromonas gingivalis: An overview of periodontopathic pathogen below the gum line. Front Microbiol 2016;7:53.
4. Zhang Y, Wang X, Li H, Ni C, Du Z, Yan F. Human oral microbiota and its modulation for oral health. Biomed Pharmacother 2018;99:883–893.
5. Khoury ZH, Vila T, Puthran TR, et al. The role of Candida albicans secreted polysaccharides in augmenting Streptococcus mutans adherence and mixed biofilm formation: In vitro and in vivo studies. Front Microbiol 2020;11:307.
6. Min Z, Yang L, Hu Y, Huang R. Oral microbiota dysbiosis accelerates the development and onset of mucositis and oral ulcers. Front Microbiol 2023;14:1061032.
7. Wang RR, Xu YS, Ji MM, et al. Association of the oral microbiome with the progression of impaired fasting glucose in a Chinese elderly population. J Oral Microbiol 2019;11:1605789.
8. Aarabi G, Heydecke G, Seedorf U. Roles of oral infections in the pathomechanism of atherosclerosis. Int J Mol Sci 2018;19:1978.
9. Radaic A, Ganther S, Kamarajan P, Grandis J, Yom SS, Kapila YL. Paradigm shift in the pathogenesis and treatment of oral cancer and other cancers focused on the oralome and antimicrobial-based therapeutics. Periodontol 2000 2021;87:76–93.
10. Zhan X, Stamova B, Jin LW, DeCarli C, Phinney B, Sharp FR. Gram-negative bacterial molecules associate with Alzheimer disease pathology. Neurology 2016;87:2324–2332.
11. Ma C, Chen F, Zhang Y, et al. Comparison of oral microbial profiles between children with severe early childhood caries and caries-free children using the human oral microbe identification microarray. PLoS One 2015;10:e0122075.
12. Wang Y, Zhang J, Chen X, et al. Profiling of oral microbiota in early childhood caries using single-molecule real-time sequencing. Front Microbiol 2017;8:2244.
13. Meurman JH. Oral microbiota and cancer. J Oral Microbiol 2010;2:10.3402/jom.v2i0.5195.
14. Rogers AB, Fox JG. Inflammation and cancer. I. Rodent models of infectious gastrointestinal and liver cancer. Am J Physiol Gastrointest Liver Physiol 2004;286:G361–G366.
15. Fan X, Alekseyenko AV, Wu J, et al. Human oral microbiome and prospective risk for pancreatic cancer: A population-based nested case-control study. Gut 2018;67:120–127.
16. Atarashi K, Suda W, Luo C, et al. Ectopic colonization of oral bacteria in the intestine drives TH1 cell induction and inflammation. Science 2017;358:359–365.
17. Chen BY, Lin WZ, Li YL, et al. Roles of oral microbiota and oral-gut microbial transmission in hypertension. J Adv Res 2023;43:147–161.
18. Zarco MF, Vess TJ, Ginsburg GS. The oral microbiome in health and disease and the potential impact on personalized dental medicine. Oral Dis 2012;18:109–120.
19. Uvarova YE, Bryanskaya AV, Rozanov AS, et al. An integrated method for taxonomic identification of microorganisms. Vavilovskii Zhurnal Genet Selektsii 2020;24:376–382.

20. Zhou J, He Z, Yang Y, Deng Y, Tringe SG, Alvarez-Cohen L. High-throughput metagenomic technologies for complex microbial community analysis: open and closed formats. mBio 2015;6:e02288-14.
21. Tanaka K, Waki H, Ido Y, et al. Protein and polymer analyses up to m/z 100 000 by laser ionization time-of-flight mass spectrometry. Rapid Commun Mass Spectrom 1988;2:151–153.
22. Marvin LF, Roberts MA, Fay LB. Matrix-assisted laser desorption/ionization time-of-flight mass spectrometry in clinical chemistry. Clin Chim Acta 2003;337:11–21.
23. Ng EW, Wong MY, Poon TC. Advances in MALDI mass spectrometry in clinical diagnostic applications. Top Curr Chem 2014;336:139–175.
24. Cuevas-Córdoba B, Santiago-García J. Saliva: A fluid of study for OMICS. OMICS 2014;18:87–97.
25. Burton JP, Wescombe PA, Moore CJ, Chilcott CN, Tagg JR. Safety assessment of the oral cavity probiotic Streptococcus salivarius K12. Appl Environ Microbiol 2006;72:3050–3053.
26. Costalonga M, Herzberg MC. The oral microbiome and the immunobiology of periodontal disease and caries. Immunol Lett 2014;162(2 Pt A):22–38.
27. Kukita K, Kawada-Matsuo M, Oho T, et al. Staphylococcus aureus SasA is responsible for binding to the salivary agglutinin gp340, derived from human saliva. Infect Immun 2013;81:1870–1879.
28. Thurnheer T, Belibasakis GN. Integration of non-oral bacteria into in vitro oral biofilms. Virulence 2015;6:258–264.
29. Foster TJ. Immune evasion by staphylococci. Nat Rev Microbiol 2005;3:948–958.
30. Rooijakkers SH, van Kessel KP, van Strijp JA. Staphylococcal innate immune evasion. Trends Microbiol 2005;13:596–601.
31. Kaufman AY, Henig EF. The microbiologic approach in endodontics. Oral Surg Oral Med Oral Pathol. 1976;42:810–816.
32. Belibasakis GN. Microbiological and immuno-pathological aspects of peri-implant diseases. Arch Oral Biol 2014;59: 66–72.
33. Fritschi BZ, Albert-Kiszely A, Persson GR. Staphylococcus aureus and other bacteria in untreated periodontitis. J Dent Res 2008;87:589–593.
34. MacFarlane TW, Helnarska SJ. The microbiology of angular cheilitis. Br Dent J 1976;140:403–406.
35. Nguyen J, Fernandez V, Pontrelli S, Sauer U, Ackermann M, Stocker R. A distinct growth physiology enhances bacterial growth under rapid nutrient fluctuations. Nat Commun 2021;12:3662.
36. Lopes W, Amor DR, Gore J. Cooperative growth in microbial communities is a driver of multistability. Nat Commun 2024;15:4709.
37. Wilbert SA, Mark Welch JL, Borisy GG. Spatial ecology of the human tongue dorsum microbiome. Cell Rep 2020;30:4003–4015.e3.
38. Kilian M, Chapple IL, Hannig M, et al. The oral microbiome - An update for oral healthcare professionals. Br Dent J 2016;221:657–666.
39. Tringe SG, Hugenholtz P. A renaissance for the pioneering 16S rRNA gene. Curr Opin Microbiol 2008;11:442–446.

CURRENT BEST PRACTICE

NEW

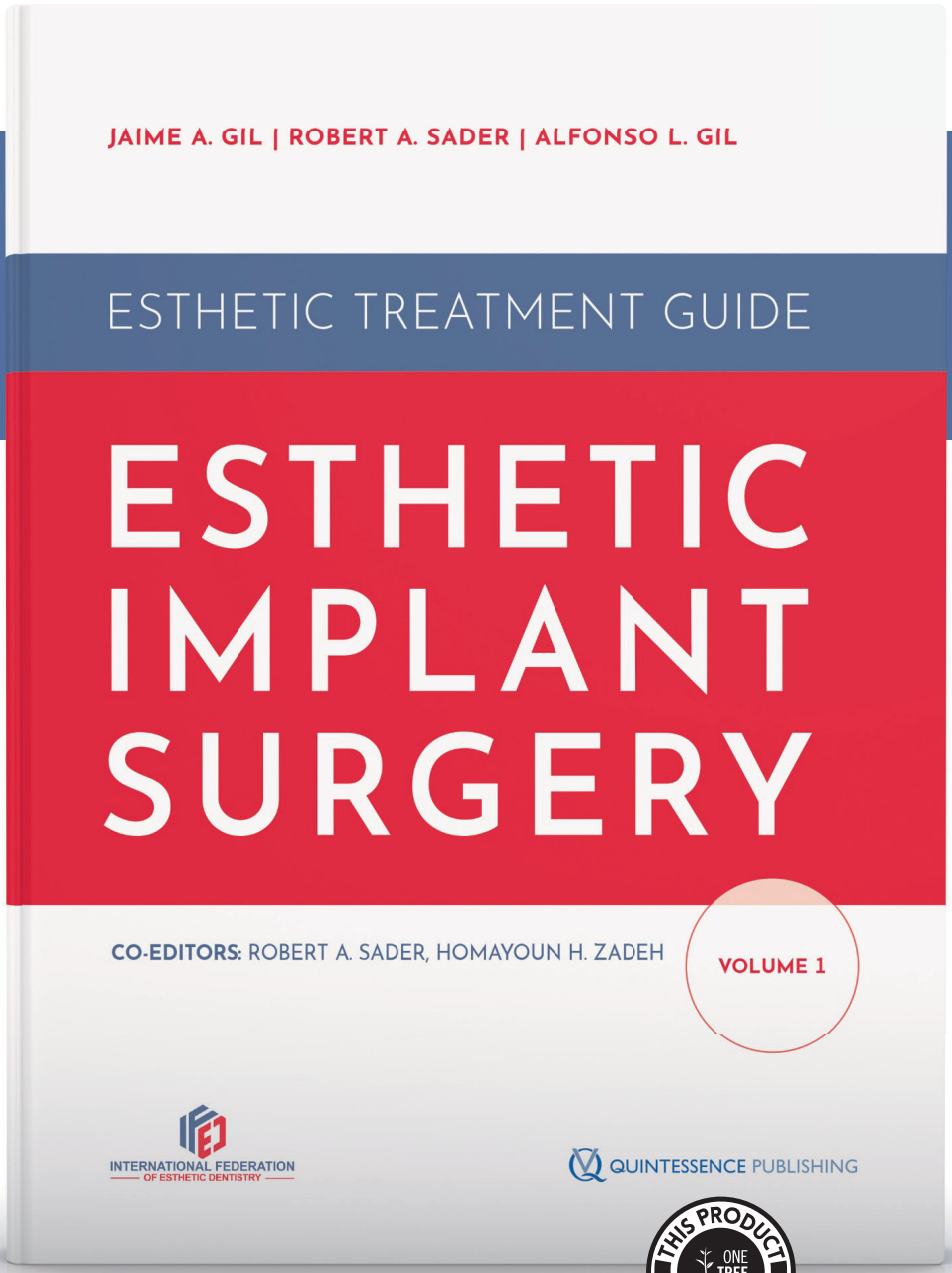

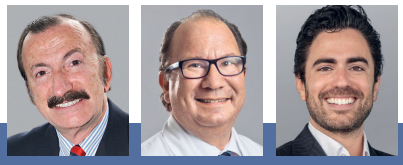

Jaime A. Gil | Robert A. Sader | Alfonso L. Gil

Esthetic Implant Surgery

Esthetic Treatment Guide Vol 1

208 pages, 900 illus
ISBN 978-1-78698-119-6, €128

This guide is a welcome and timely addition to current knowledge in the field of esthetic dentistry. In addition to chapters on esthetic implant site development, ridge augmentation, and managing esthetic complications in implant placement, the book also examines bone, soft tissue, and sinus augmentation, thus providing a comprehensive perspective and description of current techniques and approaches. Implant placement in the esthetic zone and anterior maxilla, which can be challenging for both clinician and patient, is also comprehensively covered. Beautiful illustrations and high-resolution photographs and images help the clinician to understand and apply the described techniques in everyday clinical practice. Case studies complement and further illustrate the issues and solutions highlighted in each chapter, thus grounding theory into real-world practice.

www.quint.link/
esthetic-treatment-vol1

books@quintessenz.de

+49 (0)30 761 80 667

QUINTESSENCE PUBLISHING

Eruption Status and Caries Condition of the First Permanent Molars in Chinese Children

Yang YANG[1], Xue Nan LIU[2], Chun Xiao WANG[1]

Objective: *To determine whether the targeting age should be adjusted for the National Children's Pit and Fissure Sealant (PFS) Programme.*

Methods: *Statistical analysis was conducted on the results of oral health examination results of school-aged children in regions covered by the National Children's Oral Disease Comprehensive Intervention Programme (NCODCIP) in 2018. We analysed the eruption status and dental caries condition of the children's four first permanent molars (FPMs) and performed statistical tests for the data.*

Results: *Data analysis from 811,855 children aged 6 to 9 years showed that the complete eruption rate (CER) of the FPMs in Chinese children aged 6 years was 67.2%, and reached 94.1% by age 9. Before the implementation of the PFS Programme, the prevalence of dental caries in 6-year-olds was 11.0%, and 23.2% by age 9. Caries prevalence was higher in girls than boys. The growth rate of caries prevalence slowed with age.*

Conclusion: *Our study indicated that the eruption time of FPMs in Chinese children has been earlier than predicted, and the caries prevalence was more severe than expected. Therefore, it is recommended that the targeting age for the National PFS Programme be lowered from 7 years old to 6 years old.*

Keywords: *caries prevalence, complete eruption rate, first permanent molars, pit and fissure sealant*

Chin J Dent Res 2025;28(1):73–78; doi: 10.3290/j.cjdr.b6097821

Dental caries is one of the most common chronic diseases worldwide.[1] Although its prevalence in 12-year-old children in China is still low,[2] there has been a significant increase over the past few decades, from 28.9% in 2005 to 38.6% in 2015.[3,4] Around 60% to 80% of dental caries occur in the first permanent molars (FPMs), making preventing caries lesions in these teeth extremely important.[5-7] In 2008, the Chinese government launched its first major public health programme related to oral health: a school-based free oral examination and Pit and Fissure Sealant (PFS) Programme aimed at reducing the prevalence of dental caries among children. By 2018, the programme had been in operation for 10 years. The programme consists of two steps: the first involves conducting free oral examinations for school-age children, and the second involves applying fissure sealants to children whose FPMs have fully erupted and meet the criteria for fissure sealing. Oral examinations are conducted annually, and children whose FPMs have not fully erupted at the time of examination will be re-examined a year later. Since it is generally believed that the FPMs of 6-year-olds rarely fully erupt, the programme has primarily targeted children aged 7 to 9 years (typically second to fourth graders in China) since its inception in 2008. Due to oral examinations being typically conducted at the class level, we also had the opportunity to record data from some additional age groups, mainly on the eruption and caries status of 6-year-old children.

1 Department of Oral Health, National Center for Chronic and Noncommunicable Disease Control and Prevention, Chinese Center for Disease Control and Prevention, Beijing, P.R. China.

2 Department of Preventive Dentistry, Perking University School and Hospital of Stomatology, Beijing, P.R. China

Corresponding author: Dr Chun Xiao WANG, Department of Oral Health, National Center for Chronic and Noncommunicable Disease Control and Prevention, Chinese Center for Disease Control and Prevention, #27 Nanwei Road, Xicheng District, Beijing 100050, P.R. China. Tel: 86-10-83136487. Email: wangchunxiao@ncncd.chinacdc.cn

This study aimed to analyse the eruption status and dental caries conditions of the FPMs of children aged 6 to 9 years in China in 2018, to understand the changes and trends in the caries of FPMs in Chinese children and to explore the appropriate age for conducting the PFS Programme among school-aged children in China, providing valuable information for caries prevention.

Materials and methods

Data resources

This study utilised oral examination data collected in 2018 from all 6 to 9-year-old children in areas covered by the National Children's Oral Disease Comprehensive Intervention Programme (NCODCIP). In 2008, the central government initially launched the Children's Oral Disease Comprehensive Intervention Project in the central and western regions of China. By 2014, the project had expanded to cover the entire country, and by the end of 2018, it had been in operation for 10 years. In 2018, the project covered 1,213 project counties (cities and districts) across 31 provincial-level administrative units nationwide, including the Xinjiang Production and Construction Corps, involving a total of 12,153 schools.

Clinical examinations

The study followed the Basic Method for Oral Health Survey (5th edition) recommended by the World Health Organization (WHO).[8] The parents of the participating children all signed informed consent forms. The oral examination included the eruption status and caries conditions of the four FPMs. Trained dental professionals conducted oral health examinations on the participating children under artificial light, using a combination of visual inspection and probing. The examination instruments included a plane mirror and a Community Periodontal Index (CPI) probe, and a cotton swab was used when necessary to remove soft deposits from the tooth surface. To ensure the quality of the project, all examiners involved were required to undergo rigorous standard training. After training, the examiners were assessed by the training institution using a consistency test between the reference examiner and the examiners themselves. Only those whose Kappa value exceeded 0.8 in the consistency test passed the assessment and were allowed to participate in oral examinations.

The overall caries status and experience was assessed by calculating the decayed, missing, and filled teeth (DMFT) index, including separate calculations of decayed teeth (DT), missing teeth (MT) and filled teeth (FT) for permanent teeth.

Indicator definition

The complete eruption rate (CER) for FPMs was the percentage of individuals in whom all four FPMs had fully erupted at the time of oral examination; caries prevalence for FPMs was the percentage of individuals with at least one decayed FPM among all examined individuals; and DMFT for FPMs was the mean number of FPMs that were decayed, missing due to caries and filled due to decay per person.

Statistical analysis

Data analysis was performed using SAS 9.4 software (SAS Institute, Cary, NC, USA). Categorical variables were presented as numbers (percentages), and continuous variables were expressed as mean ± standard deviation (SD). The mean DMFT of the FPMs showed a skewed distribution, and a Mann-Whitney U test (Wilcoxon Rank-Sum Test) was used for group comparisons. The complete eruption rate and caries prevalence of the FPMs were compared between groups using a chi-square test. A P value of less than 0.05 was considered statistically significant.

Results

Demographic characteristics

A total of 811,855 children were examined in this study. The age distribution was as follows: 40,967 children (5.0%) were 6 years old, 274,950 (33.9%) were 7 years old, 350,190 (43.1%) were 8 years old and 145,748 (18.0%) were 9 years old. In terms of sex distribution, there were 427,247 boys (52.6%) and 384,608 girls (47.4%) (Table 1).

Eruption status of FPMs

The CER of the FPMs was 67.2% (95% confidence interval [CI] 66.7% to 67.7%) at the age of 6, 78.7% (95% CI 78.5% to 78.8%) at the age of 7, 89.2% (95% CI 89.1% to 89.3%) at the age of 8 and 94.1% (95% CI 94.0% to 94.3%) at the age of 9. With the exception of the age 9 group, the CER of the FPMs was higher in girls than boys across other age groups, with statistically significant differences ($P < 0.0001$) (Table 2).

Table 1 Demographic information for children aged 6 to 9 years by sex and age group.

Variable		n	%
Total		811,855	100.0
Sex	Male	427,247	52.6
	Female	384,608	47.4
Age group (y)	6	40,967	5.0
	7	274,950	33.9
	8	350,190	43.1
	9	145,748	18.0

Table 2 CERs of the FPMs in children aged 6 to 9 years by sex and age group (%).

Age (y)	6	7	8	9
Total	67.2 (66.7, 67.7)	78.7 (78.5, 78.8)	89.2 (89.1, 89.3)	94.1 (94.0, 94.3)
Male	65.8 (65.2, 66.5)	77.5 (77.3, 77.7)	88.7 (88.6, 88.9)	94.1 (94.0, 94.3)
Female	68.4 (67.8, 69.1)	80.0 (79.8, 80.2)	89.8 (89.7, 90.0)	94.1 (94.0, 94.3)
P value	< 0.0001	< 0.0001	< 0.0001	0.7931

Table 3 Caries prevalence in the FPMs of children aged 6 to 9 years by sex and age group.

Age (y)	6	7	8	9
Total	11.1 (10.7, 11.4)	17.7 (17.6, 17.9)	21.6 (21.5, 21.8)	23.2 (23.0, 23.5)
Male	10.1 (9.7, 10.6)	15.9 (15.7, 16.0)	19.3 (19.1, 19.5)	21.1 (20.9, 21.4)
Female	11.9 (11.5, 12.4)	19.7 (19.5, 19.9)	24.3 (24.1, 24.5)	25.7 (25.4, 26.1)
P value	< 0.0001	< 0.0001	< 0.0001	< 0.0001

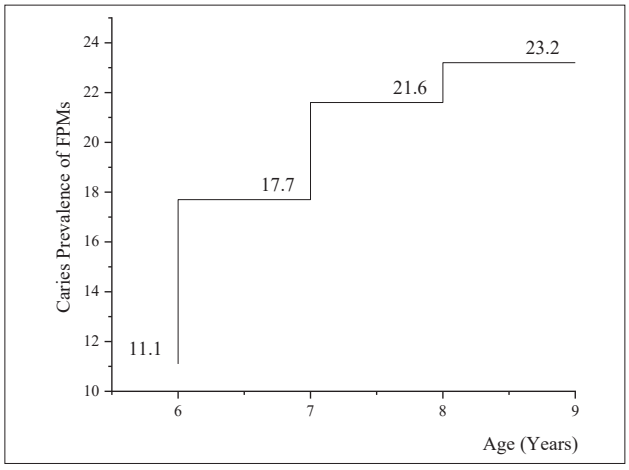

Fig 1 Trend for caries prevalence in the FPMs of children aged 6 to 9 years (%).

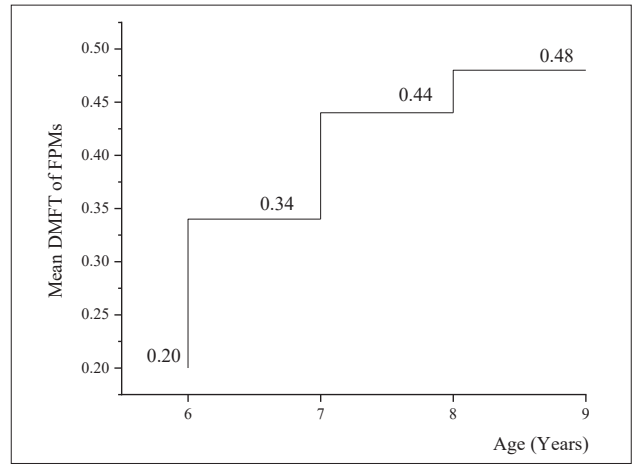

Fig 2 Trend for mean DMFT in the FPMs of Chinese children aged 6 to 9 years.

Caries condition of FPMs

The caries prevalence in the FPMs of children aged 6, 7, 8 and 9 years was 11.1% (95% CI 10.7% to 11.4%), 17.7% (95% CI 17.5% to 17.9%), 21.6% (95% CI 21.5% to 21.8%) and 23.2% (95% CI 23.0% to 23.5%), respectively. In all age groups, the prevalence of dental caries in the FPMs was higher in girls than in boys, with statistically significant differences (Table 3). The caries prevalence increased significantly between the ages of 6 and 7 years and 7 and 8 years, while the increases were smaller between ages 8 and 9 years (Fig 1).

The mean DMFT of the FPMs gradually increased with age; for children aged 6, 7, 8 and 9 years, it was 0.20 ± 0.65, 0.34 ± 0.85, 0.44 ± 0.97 and 0.48 ± 1.01, respectively. The mean DMFT of the FPMs in girls was significantly higher than in boys across all age groups ($P < 0.05$) (Table 4). The trend in the increase of the mean DMFT was similar to that of the caries prevalence; that was, the growth rate slowed with age (Fig 2).

Table 4 Mean DMFT of the FPMs in children aged 6 to 9 years by sex and age group.

Age (y)	6		7		8		9	
	Mean	SD	Mean	SD	Mean	SD	Mean	SD
Total	0.20	0.65	0.34	0.85	0.44	0.97	0.48	1.01
Male	0.19	0.63	0.30	0.80	0.38	0.91	0.43	0.96
Female	0.22	0.66	0.39	0.90	0.51	1.04	0.54	1.07
P value	< 0.0001		< 0.0001		< 0.0001		< 0.0001	

Discussion

Permanent tooth decay has always been one of the most common chronic diseases in the world, affecting hundreds of millions of people and imposing a heavy economic burden on governments and society.[9,10] Compared to data from a previous study[11] conducted in 2014, the present study showed that the caries prevalence of FPMs increased from 12.2% to 17.7% in 7-year-old children, from 16.8% to 21.6% in 8-year-old children, and from 19.6% to 23.2% in 9-year-old children. The present authors also found that the caries prevalence in the FPMs in 6-year-old children had reached approximately 11.1%, indicating that some permanent teeth develop caries soon (within a year) after eruption. Therefore, it is crucial to closely monitor the crucial period from FPM eruption to caries occurrence and to implement appropriate preventive and intervention measures during this stage.

Our findings indicated that the eruption time of permanent molars was associated with their caries incidence, which was consistent with previous studies.[12,13] The caries prevalence and mean DMFT in girls were significantly higher than in boys, aligning with the trend of earlier eruption of permanent teeth in girls. Additionally, differences in dietary habits and oral hygiene practices between sexes may also contribute to this disparity. The eruption characteristics and caries prevalence of the FPMs observed in our study were consistent with recent findings in other regions, such as African areas.[6] Thus, it is important to monitor the eruption patterns of FPMs and identify factors that influence them.

Although most permanent teeth develop caries 2 to 4 years after eruption, the onset of caries begins when the teeth first erupt. Monitoring changes in eruption time is crucial for implementing effective public health programmes. Previous studies have indicated that children's FPMs begin to erupt at around the age of 6 years. One study reported the mean eruption time of FPMs to be 6.3 years.[14] In 2008, the eruption rate of the FPMs in 6-year-old children in China was only 22.09%.[15] Based on these findings, China launched a free school-based oral examination and PFS programme in 2008 targeting children aged 7 to 9 years, excluding 6-year-olds. However, the eruption time of FPMs is not fixed and is influenced by various factors, including genetics, sex, oral and nutritional status, and external environment.[13] Previous reports have suggested obesity is related to tooth eruption, including the eruption times of the first and second permanent molars.[12] Other studies have pointed out that socioeconomic status, body composition and other factors could affect tooth eruption times.[16]

Our study showed that the eruption time of permanent teeth in Chinese children has become earlier, with 67.2% of 6-year-olds having all four FPMs fully erupted. This change indicates that the risk period for dental caries in children has also become earlier, necessitating adjustments in preventive measures and strategies.

School-based PFS programmes have proven effective and cost-efficient in preventing dental caries.[17-19] Applying sealants when FPMs have just fully erupted is most effective. With the development of China's economy and the increasing health demands of its citizens, the Chinese government has implemented a series of public health projects to promote health. In 2008, the central government began to invest annually in a national comprehensive oral health intervention programme for children that aimed to promote oral health, control oral diseases and explore and establish mechanisms for the construction of regional oral health teams. This was the first national oral health project supported by the Chinese government, marking a significant milestone. The project provides free dental examinations for children aged 7 to 9 years and offers free pit-and-fissure sealing for the FPMs for those who meet the indications. Although the coverage of the pit-and-fissure sealing programme is not as high as in some other developing countries, the incidence of caries in areas covered by the programme is significantly lower than in areas not covered, fully demonstrating its effectiveness.[20] Applying pit-and-fissure sealing measures when the FPM has just fully erupted is most effective; however, the existing programme targets children aged 7 to 9 years, which means that many

6-year-old children miss the optimal timing for intervention. By the time they reach the eligible age, some children have already developed caries. Given that most 6-year-olds now have erupted FPMs, it is necessary to adjust the target age range of the programme to include younger children.

In response to these findings, similar policy recommendations have been made in other countries,[21,22] and the central government has now adopted this suggestion, expanding the target age range of the school-based PFS programme to include children aged 6 to 9 years. This adjustment aims to enhance the effectiveness of the programme by providing timely interventions during the critical period of FPM eruption.

Despite the proven effectiveness of the programme, challenges remain. School-based oral public health programmes are usually conducted once a year, and parents often do not pay sufficient attention to their children's oral health or are not in the habit of taking them for regular dental check-ups. This situation makes it difficult to accurately and promptly determine the eruption time of children's FPMs, limiting the timeliness of pit-and-fissure sealing. To address this issue, we suggest increasing the frequency of oral examinations from once a year to once a quarter. This change would allow children to receive pit-and-fissure sealant within a short period (within 3 months) after the FPMs have fully erupted. Additionally, with advancements in artificial intelligence technology, digital and intelligent oral health screening methods can be adopted to promptly remind parents to take their children for dental check-ups and pit-and-fissure sealing immediately after FPM eruption.

Moreover, the prevention and treatment of FPM caries cannot rely solely on school-based PFS interventions. Comprehensive measures should be strengthened, such as actively preventing and treating primary tooth caries before FPM eruption and maintaining good oral hygiene during the tooth replacement period.[23,24] Strengthening oral health education for parents is crucial; by encouraging them to value, supervise and monitor their children's oral hygiene, preventive interventions can become more routine and family orientated.

Considering that girls' teeth usually erupt earlier and our study found higher caries rates in girls, oral health education should focus more on them. Parents of girls should closely monitor the eruption of the FPMs. Providing targeted oral health education to parents and utilising digital technology to inform them promptly about relevant information can encourage them to pay more attention to their daughters' tooth eruption and caries status. Cultivating good dietary and oral hygiene habits in children and ensuring timely PFS can significantly reduce the risk of caries.

Our study emphasised the need for earlier and more comprehensive preventive measures to address the rising caries prevalence in FPMs in children. By adjusting existing programmes to include younger children, increasing examination frequency, leveraging technological advancements and strengthening parental education, we can better protect children's oral health and reduce the burden of dental caries on society.

Conclusion

This study showed that 67.2% of 6-year-old children had fully erupted FPMs, and the caries prevalence in FPMs in 6-year-olds had reached 11.0%. Given that the eruption time of the FPMs among Chinese children has advanced compared to previous years, including 6-year-old children (mainly first graders in China) in the school-based PFS programme and increasing the frequency of oral examinations would be of great importance for preventing caries in children's FPMs.

Acknowledgements

The authors express their sincere gratitude to all the participants in this study.

Conflicts of interest

The authors declare no conflicts of interest related to this study.

Author contribution

Dr Yang YANG conducted the statistical analysis and drafted the manuscript; Dr Xue Nan LIU supervised the research and provided valuable guidance; Dr Chun Xiao WANG designed the study, drafted and revised the manuscript. All the authors read and approved the final version.

(Received Apr 08, 2024; accepted Aug 12, 2024)

References

1. GBD 2017 Disease and Injury Incidence and Prevalence Collaborators. Global, regional, and national incidence, prevalence, and years lived with disability for 354 diseases and injuries for 195 countries and territories, 1990-2017: a systematic analysis for the Global Burden of Disease Study 2017. Lancet 2018;392:1789–1858 [erratum 2019;393:e44].

2. Quan JK, Wang XZ, Sun XY, et al. Permanent teeth caries status of 12-to 15-year-olds in China: Findings from the 4th National Oral Health Survey. Chin J Dent Res 2018;21:181–193.
3. Qi XL. Report of the Third National Oral Health Survey of China [in Chinese]. Beijing: People's Medical Publishing House, 2008.
4. Wang X. Report of the Fourth National Oral Health Survey of China [in Chinese]. Beijing: People's Medical Publishing House, 2018.
5. Que L, Jia M, You Z, et al. Prevalence of dental caries in the first permanent molar and associated risk factors among sixth-grade students in São Tomé Island. BMC Oral Health 2021;21:483.
6. Abuaffan AH, Hayder S, Hussen AA, Ibrahim TA. Prevalence of dental caries of the first permanent molars among 6-14 years old Sudanese children. Indian J Dent Educ 2018;11: 14–16.
7. Sadeghi M. Prevalence and bilateral occurrence of first permanent molar caries in 12-year-old students. J Dent Res Dent Clin Dent Prospects 2007;1:86–92.
8. World Health Organization (ed). Oral Health Surveys: Basic Methods, ed 5. Geneva: World Health Organization, 2013.
9. Peres MA, Macpherson LMD, Weyant RJ, et al. Oral diseases: A global public health challenge. Lancet 2019;394:249–260.
10. Kassebaum NJ, Bernabé E, Dahiya M, Bhandari B, Murray CJ, Marcenes W. Global burden of untreated caries: A systematic review and metaregression. J Dent Res 2015;94:650–658.
11. Wang CX, Yang Y, Zhang Q, Liu XN. Eruption and caries prevalence of first permanent molar in Chinese children aged 7-9 years [in Chinese]. Zhongguo Gong Gong Wei Sheng 2016;32:599–601.
12. Rastogi V, Sharma B, Sengupta S, Singh S, Sabharwal R. Correlation of body mass index with eruption time of permanent first molars and incisors and caries occurrence: A cross-sectional study in school children in Uttar Pardesh, India. Eur J Gen Dent 2013;2:114–118.
13. Zenkner JEA, Alves LS, de Oliveira RS, Bica RH, Wagner MB, Maltz M. Influence of eruption stage and biofilm accumulation on occlusal caries in permanent molars: A generalized estimating equations logistic approach. Caries Res 2012;47:177–182.
14. Ekstrand KR, Christiansen J, Christiansen MEC. Time and duration of eruption of first and second permanent molars: A longitudinal investigation. Community Dent Oral Epidemiol 2003;31:344–350.
15. Liang L, Li X, Xiao R, Wu J, Fan XH. The survey of eruption time and caries degree of the first permanent molars of the children of 6–9 years old in Haidian district of Beijing [in Chinese]. Beijing Yi Xue 2008;30:421–423.
16. Rossete Melo R, Rezende JS, Gomes VE, Ferreira E Ferreira E, Oliveira AC. Sociodemographic, biological and behavioural risk factors associated with incidence of dental caries in schoolchildren's first permanent molars: A 3-year follow-up study. Eur J Paediatr Dent 2013;14:8–12.
17. Zhou L, Liu B, Li Y, et al. Cost-effectiveness of pit and fissure sealing at schools for caries prevention in China: A Markov modeling analysis. Caries Res 2023;57:516–523.
18. Bertrand É, Mallis M, Bui NM, Reinharz D. Cost-effectiveness simulation of a universal publicly funded sealants application program. J Public Health Dent 2011;71:38–45.
19. Liu W, Xiong L, Li J, Guo C, Fan W, Huang S. The anticaries effects of pit and fissure sealant in the first permanent molars of school-age children from Guangzhou: A population-based cohort study. BMC Oral Health 2019;19:156.
20. Yuan C, Wang XZ, Sun XY, et al. Oral health status of 12-year-olds from regions with and without coverage of the National Oral Health Comprehensive Intervention Program for children in China. Chin J Dent Res 2018;21:299–306.
21. Nazir MA, Bakhurji E, Gaffar BO, Al-Ansari A, Al-Khalifa KS. First permanent molar caries and its association with carious lesions in other permanent teeth. J Clin Diagn Res 2019;13: ZC36–ZC39.
22. Wright JT, Crall JJ, Fontana M, et al. Evidence-based clinical practice guideline for the use of pit-and-fissure sealants: A report of the American Dental Association and the American Academy of Pediatric Dentistry. J Am Dent Assoc 2016;147:672–682.e12.
23. Emmanuelli B, Knorst JK, Menegazzo GR, Mendes FM, Ardenghi TM. The impact of early childhood factors on dental caries incidence in first permanent molars: A 7-year follow-up study. Caries Res 2021;55:167–173.
24. Songur F, Simsek Derelioglu S, Yilmaz S, Koşan Z. Assessing the impact of early childhood caries on the development of first permanent molar decays. Front Public Health 2019;7:186.

THE WHOLE PICTURE

NEW

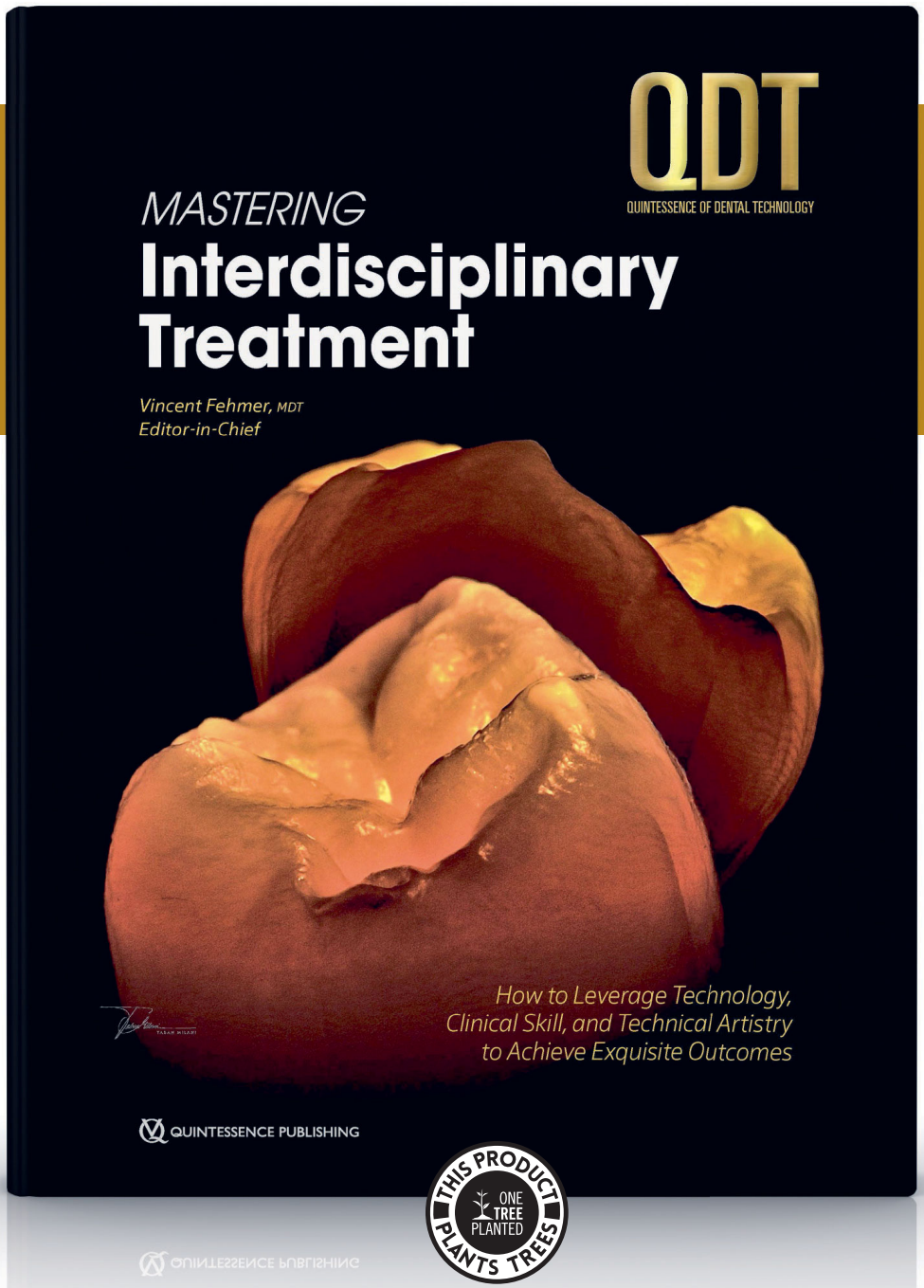

Vincent Fehmer (Ed)

Mastering Interdisciplinary Treatment

How to Leverage Technology, Clinical Skill, and Technical Artistry to Achieve Exquisite Outcomes

276 pages, 742 illus
ISBN 978-1-64724-201-5, €168

QDT has always served dental technicians with the best of the best work being done in the field. But technical artistry is only half of the equation, which is why QDT 2025 focuses on the whole picture of interdisciplinary dentistry, highlighting how clinician and technician work together to achieve predictable and esthetic outcomes. This year's issue is stacked with several articles on FP1 prostheses and the digital workflows and procedures required for their planning and delivery, as well as multiple articles on minimally invasive laminate veneers and other topics relevant to daily practice, such as the fabrication of digital complete dentures, shade matching zirconia crowns, and managing the single central incisor. Throughout the issue, the latest technologies and their capabilities are emphasized, truly reflecting this era of digital dentistry while always relying on the foundation of manual skills and artistry, which can never fully be replaced by digital tools. With such a stellar group of contributing authors, this may just be the best issue of QDT yet.

www.quint.link/qdt25
books@quintessenz.de
+49 (0)30 761 80 667
QUINTESSENCE PUBLISHING